University of Colorado
Department of Aerospace Engineering Sciences
ASEN 4018

Fall Final Report
HERMES

Hazard **E**xamination and **R**econnaissance **M**essenger for **E**xtended **S**urveillance

Monday 17th December, 2018

1. Project Information

1.1. Team Members

Name: Marcos Mejia Email: mame9430@colorado.edu Phone: (979) 436-3821 Position: Project Manager	Name: Quinter Nyland Email: quny6969@colorado.edu Phone: (505) 506-6160 Position: Integration Engineer
Name: Alexis Sotomayor Email: also3761@colorado.edu Phone: (719) 360-6322 Position: Chief Financial Officer	Name: Katelyn Griego Email: kagr9537@colorado.edu Phone: (303) 330-9050 Position: Safety Officer
Name: Colin Chen Email: coch6258@colorado.edu Phone: (801) 643-9082 Position: Mechanical Engineer	Name: Ashley Montalvo Email: asmo4361@colorado.edu Phone: (719) 424-5397 Position: Testing Engineer
Name: Brandon Santori Email: brsa7220@colorado.edu Phone: (512) 434-9234 Position: Software Engineer	Name: Chase Pellazar Email: chpe5771@colorado.edu Phone: (949) 344-3519 Position: Systems Engineer
Name: Michely Tenardi Email: mite0831@colorado.edu Phone: (720) 487-0962 Position: Manufacturing Engineer	Name: Alexander Sandoval Email: alsa3744@colorado.edu Phone: (303) 882-7443 Position: Communications, Software and Electrical Engineer
Name: Junzhe He Email: juhe9842@colorado.edu Phone: (720) 900-9484 Position: Structural Engineer	Name: Brindan Adhikari Email: brad6459@colorado.edu Phone:(720) 917-6911 Position: Electrical Engineer

1.2. Project Customer, Advisor, and Course Coordinator

Role	**Name**	**Affiliation**
Customer	Barbara Streiffert	JPL
Faculty Advisor	Kathyrn Anne Wingate	CU/AES
Course Coordinator	Jelliffe Jackson	CU/AES

Table of Contents

1 Project Information **2**
1.1 Team Members . . . 2
1.2 Project Customer, Advisor, and Course Coordinator . . . 2

Acronyms and Nomenclature **9**

2 Project Purpose **10**
2.1 Field of Application . . . 10
2.2 Problems Addressed . . . 10
2.3 Benefits of a successful Project . . . 10

3 Project Objectives and Functional Requirements **12**
3.1 Levels of Success . . . 12
3.2 Terrain Definition . . . 12
3.3 Concept of Operations . . . 13
3.4 Functional Block Diagram . . . 16

4 Concept Design **17**
4.1 Conceptual Design Alternatives Considered . . . 17
4.1.1 Mobility System . . . 17
4.1.1.1 Rocker Bogie system . . . 17
4.1.1.2 Tank Track System . . . 18
4.1.1.3 Four Wheel Drive, Four Wheels . . . 19
4.1.1.4 Six Wheel Chassis . . . 20
4.1.2 Communication System . . . 21
4.1.2.1 Point-to-Point Wi-Fi . . . 22
4.1.2.2 Point-to-Multipoint Wi-Fi . . . 23
4.1.2.3 Zigbee . . . 23
4.1.2.4 Global System for Mobile Communications . . . 24
4.1.3 Guidance, Navigation, and Control System . . . 25
4.1.3.1 Imaging System . . . 25
4.1.3.1.1 Wide FOV Fixed Camera . . . 25
4.1.3.1.2 Actuated Camera with 360^o FOV . . . 26
4.1.3.1.3 360^o 3 DOF Camera . . . 27
4.1.4 Environmental Sensing System . . . 28
4.1.4.1 LiDAR Sensor . . . 29
4.1.4.2 Ultrasonic Sensor . . . 30
4.1.4.3 Infrared Sensors . . . 30
4.1.4.4 Image Processing . . . 31
4.2 Trade Studies Process and Results . . . 32
4.2.1 Mobility System . . . 32
4.2.1.1 Trade Criteria Selection for Mobility . . . 32
4.2.1.2 Weighting Assignment for Mobility . . . 33
4.2.1.3 Scale Assignment for Mobility . . . 34
4.2.1.4 Trade Matrix for Mobility . . . 35
4.2.2 Communications System . . . 35
4.2.2.1 Trade Criteria Selection for Communications . . . 35
4.2.2.2 Weighting Assignment for Communications . . . 36
4.2.2.3 Scale Assignment for Communication . . . 37
4.2.2.4 Trade Matrix for Communications . . . 37
4.2.3 Guidance, Navigation, and Control System . . . 37
4.2.3.1 Trade Criteria Selection for Guidance, Navigation, and Control . . . 38
4.2.3.2 Weighting Assignment for Guidance, Navigation, and Control . . . 38
4.2.3.3 Scale Assignment for Guidance, Navigation, and Control . . . 39

4.2.3.4 Trade Matrix for Guidance, Navigation, and Control . . . 39
4.2.4 Environmental Sensing System . . . 39
4.2.4.1 Trade Criteria Selection for In-Plane Object Detection . . . 39
4.2.4.2 Weighting Assignment for In-Plane Object Detection . . . 40
4.2.4.3 Scale Assignment for In-Plane Object Detection . . . 41
4.2.4.4 Trade Matrix for Environmental Sensing for In-Plane Object Detection . . . 41
4.2.4.5 Trade Criteria Selection for Discontinuity Detection . . . 41
4.2.4.6 Weighting Assignment for Discontinuity Detection . . . 42
4.2.4.7 Scale Assignment for Discontinuity Detection . . . 42
4.2.4.8 Trade Matrix for Discontinuity Detection . . . 43
4.3 Baseline Design . . . 43
4.3.1 Mobility System . . . 43
4.3.2 Communications System . . . 43
4.3.3 Guidance, Navigation, and Control System . . . 44
4.3.4 Environmental Sensing System . . . 45

5 Requirements Development **46**
5.1 Functional Requirement 1: CSR.1 . . . 46
5.2 Functional Requirement 2: CSR.2 . . . 46
5.3 Functional Requirement 3: CSR.3 . . . 47
5.4 Functional Requirement 4: CSR.4 . . . 49
5.5 Functional Requirement 5: CSR.5 . . . 49

6 Detailed Design **51**
6.1 Mobility System Detailed Design . . . 51
6.1.1 Powertrain Analysis and Selection . . . 51
6.1.2 Linear Mass Stage Analysis and Selection . . . 62
6.1.3 Power Analysis and Selection . . . 63
6.1.4 Chassis Material Analysis and Selection . . . 65
6.1.5 Mobility Control . . . 68
6.2 Communications Detailed Design . . . 68
6.2.1 Hardware Integration and Setup . . . 69
6.2.1.1 Hardware Integration . . . 69
6.2.1.2 Setup . . . 71
6.2.2 Link Budget Analysis . . . 72
6.2.3 Data Budget Analysis . . . 75
6.3 Guidance, Navigation, and Control Detailed Design . . . 76
6.3.1 Hardware Selection . . . 76
6.3.1.1 Guidance and Navigation . . . 77
6.3.1.1.1 Global Positioning System . . . 77
6.3.1.1.2 Magnetometer . . . 78
6.3.1.1.3 Imaging System . . . 79
6.3.1.2 Control . . . 80
6.3.1.3 Power . . . 80
6.3.2 CSR Robot Operating System Utilization . . . 81
6.3.3 CSR Control Software Design . . . 81
6.3.4 CSR ROS Node Software Architecture . . . 86
6.4 Environment Sensing Detailed Design . . . 87
6.4.1 In-Plane Object Detection Sensing System . . . 88
6.4.2 Discontinuity Detection Sensing System . . . 92
6.4.3 Depth Sensing for Discontinuity Traversal Mode System . . . 95
6.4.4 Environment Sensing Control . . . 97

7 Verification and Validation **97**
7.1 Object Detection Component Testing . . . 99
7.2 Camera Operations Testing . . . 99
7.3 Communications Testing . . . 100
7.4 C&DH Testing and Integration . . . 101
7.5 Sensing Integration (Object Detection & Discontinuity Testing) . . . 102
7.6 CSR Functional Testing . . . 103
7.7 Environmental Maneuverability Testing . . . 104
7.8 Obstacle Maneuverability Testing . . . 105
7.9 Path Determination Test . . . 106

8 Risk Assessment and Mitigation **108**

9 Project Planning **113**
9.1 Work Breakdown Structure . . . 113
9.2 Organizational Chart . . . 113
9.3 Work Plan . . . 114
9.4 Cost Plan . . . 116

10 Individual Report Contributions **117**

11 Appendix **120**

List of Figures

1 Concept of Operations for arriving to the Location of Interest . . . 14
2 Concept of Operations for arriving to Other Terrain . . . 15
3 Concept of Operations for arriving to loss of communications . . . 15
4 System Functional Block Diagram . . . 16
5 Rocker Bogie Configuration . . . 17
6 Rocker Bogie Differential Suspension . . . 18
7 Tank Track System Configuration . . . 19
8 Tank Track System Tipping Risk . . . 19
9 4WD System Configuration . . . 20
10 Six Wheel Chassis Configuration, fulfilling MOB.3.2 requirement . . . 21
11 Wi-Fi method showing a Point-to-Point approach by using long-range radios. . . . 22
12 Wi-Fi method showing a Point-to-Multipoint approach by using long-range radios. . . . 23
13 Zigbee method using a mesh network which incorporates utilizing last year's Xbee radio modules. . . . 24
14 Global System for Mobile Communications method using a Point-to-Multipoint approach by communicating through a cell tower. . . . 24
15 Curvilinear vs Rectilinear Images . . . 25
16 Wide FOV Fixed Camera Configuration . . . 26
17 Actuated Camera with 360^o FOV Configuration . . . 27
18 360^o 3 DOF Configuration . . . 28
19 LiDAR operation . . . 29
20 Ultrasonic detection operation[18] . . . 30
21 Infrared sensor operation . . . 30
22 Vision processing flow chart . . . 31
23 The baseline design of our communications system with a radio, power over ethernet (POE) injector, and controller per system. . . . 44
24 The CSR Final Design . . . 51
25 CSR Powertrain CAD Model . . . 52
26 Mechanical Wheel Interface . . . 52
27 Conceptual Diagram of Slope Model . . . 53
28 Free Body Diagram of Slope Model . . . 53
29 Obstacle Free Body Diagram - Case A . . . 55
30 Obstacle Free Body Diagram - Case C . . . 55

31 Obstacle Free Body Diagram - Case B 55
32 AndyMark Redline 775 Motor - Photo Source: AndyMark Website 58
33 4” Radius (8” OD) Rubber Treaded Wheel 59
34 Gearbox Drive Sprocket FEM Analysis 59
35 Axial Load from Skid Steer Free Body Diagram 60
36 Effect of Linear Mass Stage on CSR Center of Mass 62
37 Conceptual Diagram of the Discontinuity Traversal 63
38 AndyMark 775 Redline Motor Torque Datasheet - Torque in mNm 64
39 CSR Simulated Mission - Projected Current Consumption 65
40 Projected Current Consumption Calculations 65
41 Power Distribution Block Diagram (Mobility) 65
42 Aluminum Base Plate FEM Model 66
43 Middle Acrylic Plate FEM Model 67
44 Top Acrylic Plate FEM Model - Stress 67
45 Top Acrylic Plate FEM Model - Strain 68
46 The hardware interface diagram for mobility control. 68
47 CSR communication hardware interface diagram. 70
48 GS communication hardware interface diagram. 70
49 MR communication hardware interface diagram. 71
50 Power distribution block diagram (communications). 71
51 The communications setup between all our systems that creates a Local Area Network. 72
52 Tree depth visualization. 73
53 Vegetation scenarios. 73
54 Attenuation due to trees in different scenarios at various tree depths. 74
55 Link budget calculation. 75
56 The hardware interface diagram for guidance and navigation which comprises of a GPS, Magnetometer/Accelerometer, and Camera. 77
57 GPS Interface 78
58 Magnetometer Diagrams 79
59 Imaging System 80
60 The hardware interface diagram for the main controller comprising of a ASUS Tinker Board and Arduino Due. 80
61 Power Distribution Block Diagram (C&DH) 81
62 CSR Main Loop 82
63 CSR Initialization Mode 82
64 CSR Manual Mode 83
65 CSR Semi-Autonomous Mode 84
66 CSR Discontinuity Traversal Mode 85
67 CSR Loss of Communications Mode 86
68 CSR LOI Arrival Mode 86
69 CSR ROS Map 87
70 Slamtec RPLIDAR A2M8 88
71 Isometric View of CSR Showing Mounting Location and Diagram of Desired Sensing Area of the RPLIDAR 88
72 Diagram of the RPLIDAR’s Required Ability to Detect 1 in Obstacles 89
73 Required Angular Resolution for 1 inch Object Detection at range 90
74 Interface Diagram for RPLIDAR A2M8 and C&DH System 90
75 Data Flow Diagram for RPLIDAR A2M8 91
76 Speed Analysis for RPLIDAR A2M8 91
77 Lidar-Lite v3 and Front View of CSR showing Sensor Mounting Locations 92
78 Side View of the Moment of Discontinuity Detection 93
79 120 Seconds of Raw Lidar-Lite v3 Data Pointed at Cardboard Box 1 m Away 94
80 Residiuals of 1 m Cardboard Box Lidar-Lite v3 Test 94
81 Interface Diagram for Lidar-Lite v3 and C&DH System 95
82 Itead Studio HC-SR04 and Bottom View of CSR showing Sensor Mounting Locations 96
83 Interface Diagram for HC-SR04 and C&DH System 96

84 Timing Diagram for PWM Control on the HC-SR04 . . . 96
85 Hardware Interface Diagram for Environment Sensing that Comprises of Ultrasonic Sensors, Single Beam Lidars, and the 360^o Lidar Scanner . . . 97
86 Power Distribution Block Diagram (Sensing). . . . 97
87 Verification & Validation Phases . . . 98
88 Obstacle Detection Component Test Setup . . . 99
89 Camera Operations Test Setup . . . 100
90 Communications Test Setup . . . 101
91 Single Beam LiDAR Test . . . 102
92 Ultrasonic Sensor Test . . . 103
93 360 ° LiDAR Test . . . 103
94 CSR Functional Test Setup . . . 104
95 LabVIEW Command Interface . . . 104
96 Environmental Maneuverability Test Setup & CU Boulder South Terrain . . . 105
97 Obstacle Maneuverability Test Setup . . . 106
98 Path Determination Test . . . 107
99 Path Determination Test Continued . . . 107
100 Pre Mitigation Risk Matrix . . . 110
101 Post Mitigation Risk Matrix . . . 112
102 Work Break Down Structure . . . 113
103 Organizational Chart . . . 114
104 Work Plan . . . 115
105 Projected Expenditures by Subsystem . . . 116
106 Bill of Materials . . . 120
107 Bill of Materials . . . 120

List of Tables

1 Levels of Success for the HERMES Mission . . . 12
2 Terrain Definition and Classifications . . . 13
3 Pros and Cons of the Rocker Bogie Suspension System . . . 18
4 Pros and Cons of the Tank Track Suspension System . . . 19
5 Pros and Cons of the Four-Wheel-Drive System . . . 20
6 Pros and Cons of the 6WD Six Wheel Configuration . . . 21
7 Pros and Cons of the 2-Motor Six Wheel Configuration . . . 21
8 Pros and Cons of a Point-to-Point Wi-Fi communication system. . . . 22
9 Pros and Cons of a Point-to-Multipoint Wi-Fi communication system. . . . 23
10 Pros and Cons of a Zigbee communication system. . . . 24
11 Pros and Cons of a Global System for Mobile Communications approach. . . . 25
12 Pros and Cons for Wide FOV Fixed Camera . . . 26
13 Pros and Cons: Actuated Camera with 360° FOV . . . 27
14 Pros and Cons: 360° 3 DOF Camera . . . 28
15 Pros and Cons of LiDAR Sensor . . . 29
16 Pros and Cons of Ultrasonic Sensor . . . 30
17 Pros and Cons of Infrared Sensors . . . 31
18 Pros and Cons of Image Processing . . . 32
19 Translational System Weighting Criteria and Rationale . . . 33
20 Translational System Scale Assignment and Ranges . . . 34
21 Translational Trade Matrix . . . 35
22 Communication system weighting criteria and rationale. . . . 36
23 Communication scale assignment and ranges. . . . 37
24 Communication trade matrix. . . . 37
25 Imaging System Weighting Criteria and Rationale . . . 38
26 Imaging System Scale Assignment and Ranges . . . 39
27 Imaging System Trade Matrix . . . 39
28 In-Plane Object Detection Criteria and Rationale . . . 40
29 Object Detection Scale Assignment and Ranges . . . 41

30	In-Plane Object Detection Trade Matrix	41
31	Discontinuity Detection Weighting Criteria and Rationale	42
32	Discontinuity Detection Scale Assignment and Ranges	42
33	Discontinuity Detection Trade Matrix	43
34	Communication radio characteristics.	44
38	Torque and Coefficient of Friction Requirements	57
39	Universal communication setup hardware characteristics.	69
40	Required bandwidth for camera.	76
41	Data rate margin.	76
42	GNC Hardware Selection	77
43	The CSR controller characteristics for both the ASUS Tinker Board and Arduino Due.	80
44	CSR Software Modes	81
45	Major Tests	98
46	Severity	108
47	Likelihood	108
48	Risks	109
49	Mitigations	111

Nomenclature

Nomenclature

$2WD$	Two-Wheel Drive
$4WD$	Four-Wheel Drive
$6WD$	Six-Wheel Drive
AWD	All-Wheel Drive
CD	Child Drone
$CD\&H$	Command Data and Handling
$CHIMERA$	CHIld drone deployment MEchanism and Retrieval Apparatus
$COTS$	Commercial Off the Shelf
CSR	Child Scout Rover
$DRIFT$	Drone-Rover Integrated Fire Tracker
FPS	Frames per Second
GPS	Global Positioning System
GS	Ground Station
$HERMES$	Hazard Examination and Reconnaissance Messenger for Extended Surveillance
$INFERNO$	INtegrated Flight Enabled Rover for Natural disaster Observation
$Lidar$	Laser Imaging Detection and Ranging
LOI	Location of Interest
MR	Mother Rover
$PtMP$	Point-to-Multipoint
PtP	Point-to-Point
$V\&V$	Verification and Validation
DOF	Degree of Freedom
FOV	Field of View

2. Project Purpose

Author: Alexis Sotomayor, Quinter Nyland

2.1. Field of Application

The JPL Fire Tracker System's overall application is reconnaissance and sensing in forest fire prone areas, and to detect potential for wildfires in these areas; the goal is early detection and early containment. Currently, there are no systems in widespread private or public use that are documented to work like the JPL Fire Tracker system. The majority of early fire detection, and subsequent containment, is done through watch towers and camera systems.

JPL has developed firefighting artificial intelligence for use during the actual fire, primarily in residential areas. This system is called AUDREY (Assistant for Understanding Data through Reasoning, Extraction, and synthesis) and its objective is to provide mapping and guidance to firefighters in the presence of a blaze that obscures vision and decreases orientation[1]. Inspired by terrain mapping technology developed for the Europa moon mission, AUDREY begins with human input and learns how to identify different objects and various kinds of flames, creates a 3D map and then directs firefighters on the ground accordingly.

The Fire Tracker System is composed of four distinct projects, with HERMES, the project sponsored for the 2018-2019 academic year, being the most recent in the continuum. The prior projects have consisted of INFERNO, CHIMERA, and the most recent DRIFT. INFERNO, the first in the series, was responsible for an autonomous flying child drone (CD) that drops a sensor package in an area prone to wildfires. CHIMERA's objective was to build the landing platform for INFERNO's CD, with the capabilities to secure and recharge INFERNO's CD. The most recent of the prior projects, DRIFT, built the mother rover (MR) and attached the landing platform, while integrating data processing and communication among the ground station (GS), the MR and the CD[9]. The MR is launched from the GS and has the ability to carry and level INFERNO's CD and the CHIMERA platform.

2.2. Problems Addressed

The effects of climate change include steadily increasing global temperatures, permanent changes in precipitation patterns, more frequent droughts and heat waves[6]. Year after year, these effects have extended the duration of the wildfire season in geographical locations with a dry climate, especially the western United States[7]. The wildfire prevention, suppression, and rehabilitation budget of the United States Forest Service has increased with this trend. In 1995, fire suppression costs made up 16% of the US Forest Services annual budget and in 2015, 50% of the budget was devoted to forest fires. Scientific statisticians estimate that in 2025, this number could exceed 67%[8]. The current method of wildfire prediction, identification, and rehabilitation will clearly not be cost-effective in the future, which motivates the development of the Jet Propulsion Laboratory's Fire Tracker System. This system aims to be a low-cost, hands-off approach to forest fire identification that will lead to earlier containment and elimination of forest fires.

HERMES aims to improve the Fire Tracker System by assisting the MR to avoid potential risk of damage by large obstacles and uneven terrain while traversing the forested environment. The HERMES team will design and build a child scout rover (CSR) that will deploy on command, take images/video of its surroundings using an image capturing system, determine a viable path to a location of interest (LOI), send the LOI to the MR. The CSR will investigate these forested areas within a 250 meter (820 ft) radius from its deployment point from the MR, detect obstructions, and determine a viable path for the MR to travel to a location of interest (LOI), defined by an operator at the GS. It must perform these operations while navigating the dense environment with mobility and maneuverability. The specific actions it must perform are driving forward and reverse, executing a 360° turn, driving up and down slopes of 20°, and driving over discontinuities of 1 ft (0.30 m). With the success and integration of this mission, the full system can perform more effectively with less risk.

The MR is large and bulky, which is not ideal given that the desired, searchable wildfire environment is characterized by dense forest, underbrush, and uneven terrain. This situation prevents the system from reaching critical areas of forests where the most scientific data can be accrued. Additionally, operating the large system in these tight spaces is a risk to the system's health and safety. Moreover, the lack of maneuverability and low speed of the MR limits the efficiency of the mission.

2.3. Benefits of a successful Project

The overall aim of the JPL Firetracker is to integrate a child drone (INFERNO), a landing platform (CHIMERA), a mother rover (DRIFT), and a child scout rover (HERMES) into a cohesive system operated from a ground station.

This year's iteration of the project will primarily prevent the DRIFT's mother rover from damage and reduce time of the mission. The HERMES CSR is more agile than the MR and will find a viable path through a forest for the mother rover, thereby removing potential paths where the Mother Rover could become damaged or get stuck. The time of the mission is reduced because this project eliminates the need for the slower mother rover to find its own path, which would be cumbersome and essentially becomes a trial-and-error method.

The addition of this year's CSR lends to a more efficient mission, as the Mother Rover can get to its intended LOI to deploy the child scout drone more efficiently and faster. The total cost of the project will be hovering around $20,000$ after the completion of HERMES.

3. Project Objectives and Functional Requirements

Author: Marcos Mejia and Chase Pellazar

3.1. Levels of Success

Criteria	Level 1	Level 2	Level 3
Control	• The CSR shall navigate by received control commands from the GS. • The CSR shall perform a 360° turn. • The CSR shall travel forward and reverse.	• The CSR shall navigate to a LOI and shall detect obstacles en route to the LOI, but manual control is needed to circumvent the obstacles.	• The CSR shall autonomously return to the last known GPS location if connection to the GS and MR is lost. • The CSR shall be able to verify its location from the LOI within ± 5 meters.
Communications	• The CSR shall verify connection to the MR/GS. • The CSR shall send at least one GPS data packet to MR/GS upon command. • The CSR shall have functional communication up to a 250 meter radius from the deployment point in an open area. • The CSR shall be able receive control commands from MR/GS.	• The CSR shall be able to record and send pathpoint locations after encountering obstacles	• The CSR shall transmit continuous video feed. • The CSR shall have functional communications through type D terrain up to a 250 meter radius from the deployment point.
Range	• The CSR shall be able to drive up to a 250 meter radius from the deployment point on flat terrain.	• The CSR shall be able to drive up to a 250 meter radius from the deployment point on flat terrain with obstacles present.	• The CSR shall be able to drive in a 250 meter radius from the deployment point at a 20° inclined slope.
Environment	• The CSR shall be able to traverse the following: 1) Open areas 2) 20° incline slopes	• The CSR shall be able to traverse the following: 1) Type A underbrush 2) Roots and obstacles up to a 2.4 inch (6 cm diameter)	• The CSR shall be able to traverse the following: 1) Type D underbrush 2) Up to a 9 inch wide discontinuities with depths greater than a 2.4 inches (6 cm)
Video/Image	• The camera on the CSR shall capture a FOV greater than 100°. • The image processing system shall send time-stamped images to the MR/GS.	• The CSR shall send videos to the MR/GS. • The MR shall toggle on/off the video capture from the CSR on or off	• The CSR shall be able to send and receive continuous video feed to MR and GS

Table 1: Levels of Success for the HERMES Mission

3.2. Terrain Definition

To clarify what kind of terrain the CSR shall be able to operate in, various categories for forest, ground, and underbrush have been defined. These definitions are shown in the table below, Table 2. The CSR's operating conditions are constrained by the terrain that the MR can travel in, and by the MR's dimensions (60 in (1.524 m) wide and 35 in

(0.889 m) high). Due to this, the CSR will travel in the terrain defined in the table below, through areas the size of the MR, and in inclined slopes of 20 ^{o} or less. The forest and ground classifications are based on existing classification metrics. Specifically, the forest was based off a classification found in an article on Basal Area on ThoughtCo.[10], while the ground classification is based on the Wentworth Scale, which is a scale for classifying and describing sediments by grain size[11]. There was not an existing metric for underbrush, however the classification was based on the CSR's estimated capabilities. It should be noted that an acre is equivalent to 43,560 ft^2 and 4046.86 m^2, and that the average tree diameter will be around 11 in (roughly 28 cm). The height of the trees will not be considered in this classification because the average tree height of a tree is over 6 m tall (around 20 ft)[12]. The root diameter classification is based on average root diameters measured at a distance 2-3 m from the tree base[13].

Terrain	**Forest**	**Ground**	**Underbrush**
Type A	Open: 0 trees per acre	Mud: Grain size: 0.00006 - 0.0039 mm (< .0002 in)	Dirt with no vegetation: - Refer only to ground classification - Scattered leaves
Type B	Understocked: ~100 trees per acre	Silt: Grain Size: 0.0039 - 0.0625 mm (< .003 inch)	Grass and Fallen Leaves - Full ground coverage by leaves - Grass between 2cm - 10cm height (.8 - 4 inches) - Small roots 1-2 cm (.4 - .8 inches) in diameter
Type C	Fully Stocked: ~170 trees per acre	Sand: Grain Size: 0.0625 - 2.00 mm (< .08 inch)	Grass and Fallen Leaves - Includes type A and B underbrush - Medium roots: 3-4 cm (1.2 - 1.6 inches) in diameter
Type D	Overstocked: ~200 trees per acre	Gravel: Grain Size: 2.00 - 4.096 mm (< .2 inch)	Grass and Fallen Leaves - Includes type A, B, and C underbrush - Large Roots: 5-6 cm (2 - 2.4 inches) in diameter

Table 2: Terrain Definition and Classifications

It should be noted that the terrain types (rows) and categories (columns) are not mutually exclusive. An example would be that the CSR could travel through a Type A forest, Type B ground, and Type C Underbrush at the same time. The categories can be combined depending on the test.

3.3. Concept of Operations

The goal of the project is to find a viable path to a location of interest for the mother rover. This first concept of operations displays how the CSR would arrive to the location of interest if the terrain was a flat obstacle free environment. In this ConOps, the CSR is deployed from the GS, then it receives a LOI from the GS, and is then commanded to point towards the LOI. Afterwards, the CSR will be commanded into a semi- autonomous mode by the GS, where this semi-autonomous mode consists of object detection, discontinuity detection, slope detection, checking to determine if the LOI has been reached, and checking to make sure the CSR still has connection to the GS. Once the CSR arrives at the LOI, it notifies the GS, stops, and requests human intervention.

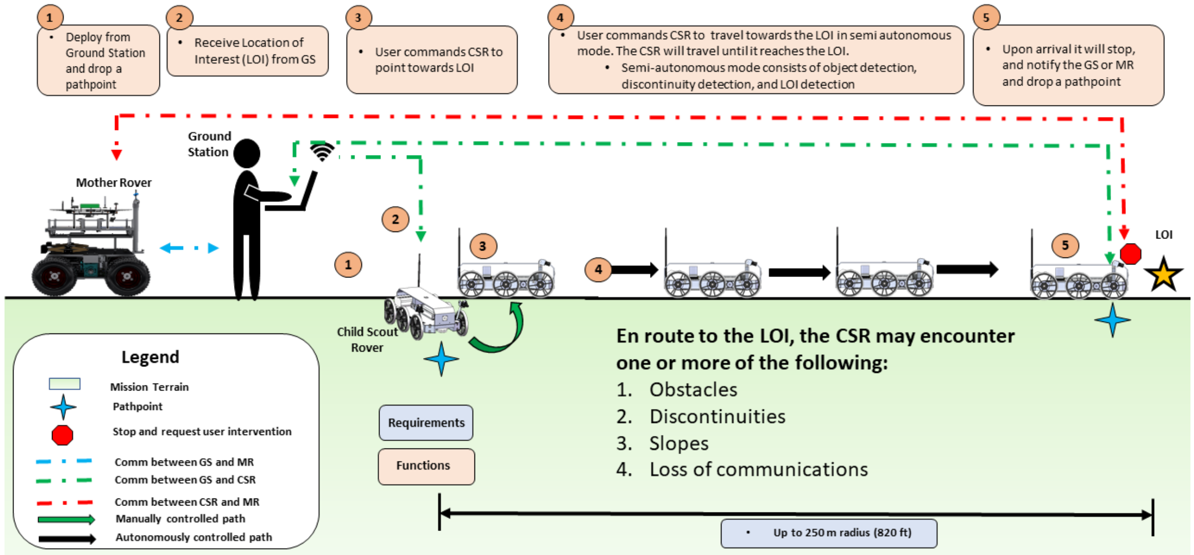

Figure 1: Concept of Operations for arriving to the Location of Interest

As stated previously, the CSR might encounter non- traversable obstacles, discontinuities, and slopes. This next ConOps displays what would happen in these situations. In all three situations the CSR would detect the non-traversable obstacle, discontinuity, and slope and then stop. At this moment the CSR would request human intervention, and afterwards, the user at the ground station would take manual control of the CSR. In the case of non traversable obstacles, the user would manually control the CSR around the obstacle using mobility commands. After every mobility command is received and executed a pathpoint would be recorded on the CSR's onboard memory and sent to the GS as a GPS coordinate. After maneuvering the CSR around an obstacle, the user would command the CSR to point towards the LOI again, and then return the CSR into a semi-autonomous mode. In the case of discontinuities, once the user takes control of the CSR, they would send a command to the CSR for it to enter a discontinuity traversal mode. This mode is an autonomous mode that the CSR uses to cross discontinuities. This mode includes moving the linear mass stage to move the center of mass of the CSR, and proceed over the discontinuity in a consistent coordinated manner. After the CSR crosses the discontinuity it will stop, deploy a pathpoint, and request user intervention. After detecting slopes, the user will manually control the CSR up the slope from flat ground, and then return the CSR into a semi-automous mode again. If the CSR is going from a sloped ground to a flat ground, then the CSR would still detect flat ground as an obstacle, in which case the user would intervene to navigate the CSR onto flat ground again. Afterwards they would have full control of the CSR.

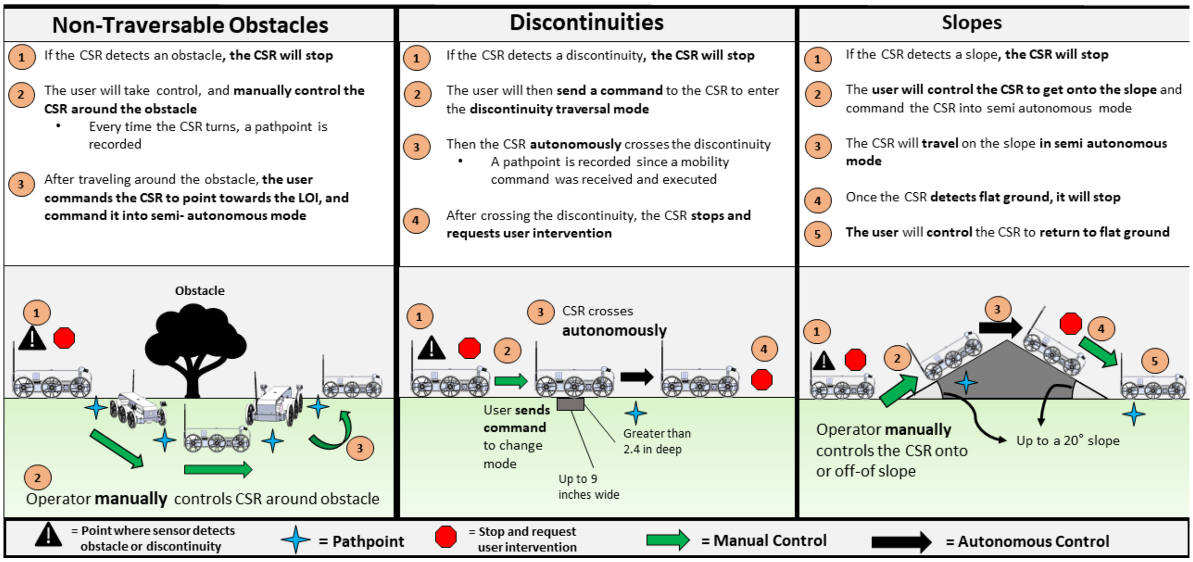

Figure 2: Concept of Operations for arriving to Other Terrain

Another situation the CSR may encounter is a loss of communication or signal from the Ground Station. This concept of operations would resolve functional requirement CSR.4, that states "The CSR shall travel back to the last recorded pathpoint upon loss of communications with the GS". In this concept of operations, the CSR would lose connection to the ground station, establish the last recorded pathpoint as a temporary location of interest, perform a 360^o turn, and then proceed to that pathpoint. Once it arrives within 5 m of the last recorded pathpoint, it will stop and wait until it recieves communications again.

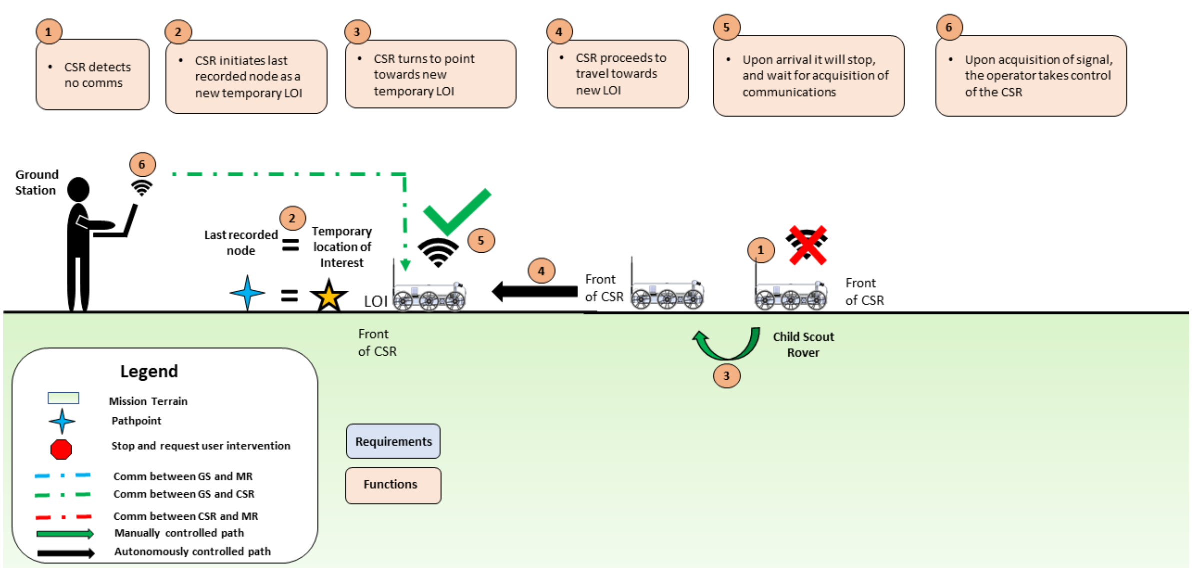

Figure 3: Concept of Operations for arriving to loss of communications

3.4. Functional Block Diagram

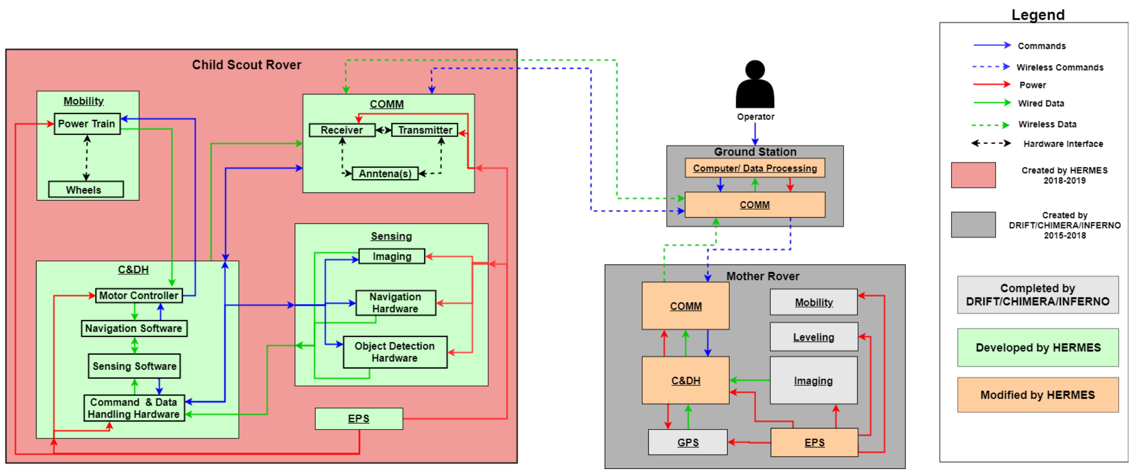

Figure 4: System Functional Block Diagram

Provided above is the system block diagram for the HERMES project which illustrates at a high level how the CSR's subystems interface with each other as well as how the CSR itself interfaces with heritage projects. As is indicated by the chart, an operator will be the primary controller for the CSR, sending commands to the CSR via a wireless communications link between the two communications systems. These commands are transmitted as signals through wires to the C&DH subsystem on the CSR which, utilizing team developed software, distributes signals to either the motor controller and thus the mobility subsystem, the sensing subsystem, the power subsystem, or a combination of the three based on the operation.

Moreover, in order for the project to be successful the team will modify the communications, C&DH, and power subsystem on the mother rover as well as the CDH and communications subsystems on the ground station to account for the design choices made for the CSR.

4. Concept Design

4.1. Conceptual Design Alternatives Considered

4.1.1. Mobility System

Author: Junzhe He, Colin Chen, Michely Tenardi

The translational system was chosen to be a key design parameter to be considered because of how critical its function is to the mission. The translational system relates directly to the mobility capabilities of the CSR, which in turn relate to the functional requirements MOB.3.2, MOB.3.2, MOB.3.3, MOB.3.4.1, and POW.3.1. The CSR must be able to travel forward and backwards in forest fire prone areas and perform 360° turns. Otherwise it cannot navigate and would be unable to reach a LOI.

4.1.1.1 Rocker Bogie system

The Rocker Bogie system is a suspension system consisting two links on each side connected with six wheels with no springs used. On each side, there is a large link called a 'rocker' and a smaller link called a 'bogie'. The rockers on each side are connected by a differential for leveling purpose. Namely, when one side goes up relative to the main body, the other side goes down to help level the main body and avoid tipping. The 'bogies' are commonly used in the tank track as loading wheels. In the rocker bogie system, 'bogie' refers to the wheels on the small link which can distribute weights. However, in order to drive over 9 in (0.23 m) discontinuity required by MOB.3.2., the stiffness of the axles must be increased, possibly through the use of torsion springs, such that the system does not fall into the gap. This required stiffness decreases the effectiveness of the rocker bogie suspension. Additionally, the moving linkages of the system add mechanical and manufacturing complexity to the system. An image of rocker-bogie system is shown below:

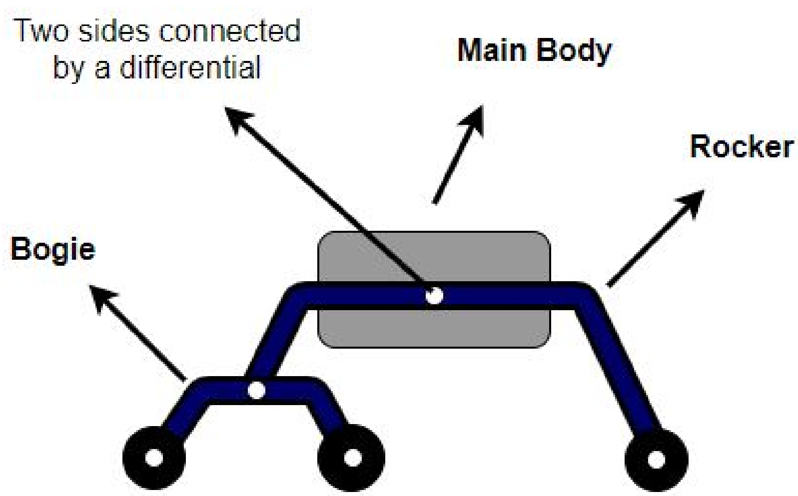

Figure 5: Rocker Bogie Configuration

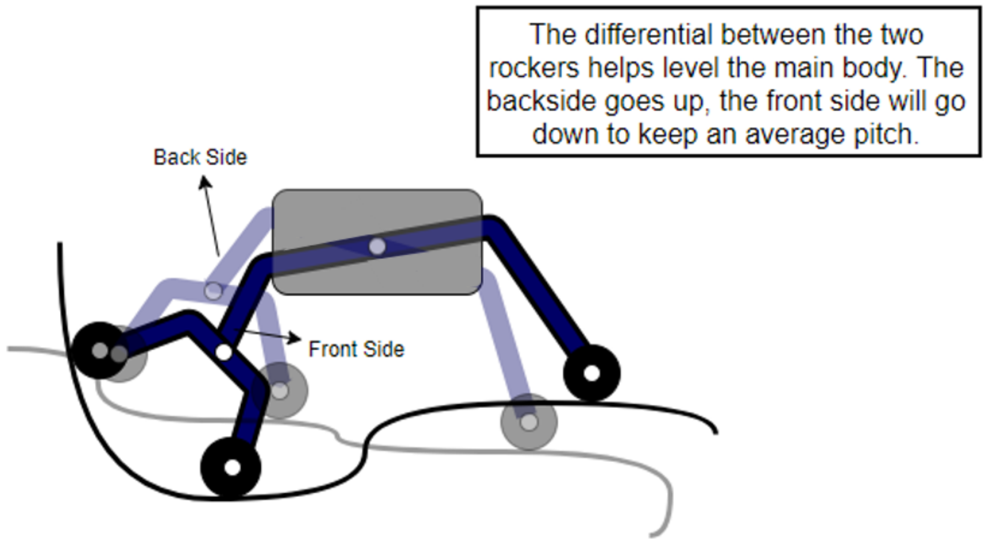

Figure 6: Rocker Bogie Differential Suspension

Description	Pro	Con
Can climb over obstacles up to twice its wheel size	**X**	
Reduces the motion of the main body	**X**	
Low potential of flipping over	**X**	
Gear damage caused by single differential		**X**
Unstable at high speed		**X**
Mechanically complex		**X**
Required axle stiffness reduces suspension effectiveness.		**X**

Table 3: Pros and Cons of the Rocker Bogie Suspension System

4.1.1.2 Tank Track System

The tank track system contains several wheels and a continuous track link on each side of the vehicle body. The continuous track link keeps the wheels from the potentially getting stuck and increases the traction. However, since the continuous track link is long and not flexible, there is a potential of tipping if the vehicle is trying to go over large obstacles as shown in the figure below. This system is mechanically complex and would be extremely difficult to manufacture without COTS parts, which are extremely expensive for treads longer than 18 in (0.46 m), which is needed to meet the 9 in (0.23 m) discontinuity requirement, MOB.3.2.

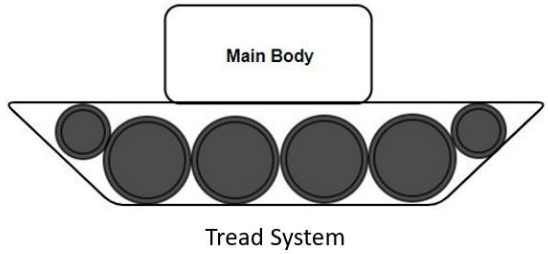

Figure 7: Tank Track System Configuration

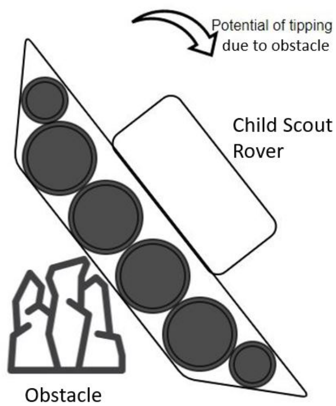

Figure 8: Tank Track System Tipping Risk

Description	Pro	Con
Mechanically complex		**X**
Significant traction	**X**	
Low contact pressure	**X**	
Capable of crossing 1 ft (0.30 m) discontinuity with a smaller profile.	**X**	
High potential of tipping		**X**
Expensive (>$1000) COTS parts required.		**X**

Table 4: Pros and Cons of the Tank Track Suspension System

4.1.1.3 Four Wheel Drive, Four Wheels

This system has four wheels fixed on the vehicle body, each being supplied power. This system is easier to design and manufacture while still meeting the design requirements. The main drawback with this design is that in order to cross the 9 in (0.23 m) discontinuity, the wheel diameters must be greater than 9 in (0.23 m). This results in a physically large, expensive system. The benefit of the large wheels is it provides more traction and suspension than smaller wheels. An all wheel drive design using two motors was considered; however, due to the added mechanical and manufacturing complexity it would require, it was deemed not worthy to be a key design consideration. Additionally, trading for system with an active suspension system was considered; however, due to the low travel speeds of the CSR, the existing suspension provided by the large wheels, and the mechanical and manufacturing complexity required to design active suspension, it was not considered for trading.

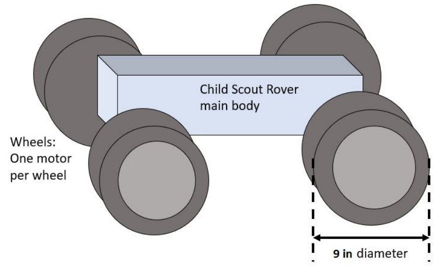

Figure 9: 4WD System Configuration

Description	Pro	Con
Mechanically Simple	**X**	
Relatively Simple to Manufacture	**X**	
Greater traction and suspension than small wheels	**X**	
Large required size of CSR		**X**
Expensive		**X**

Table 5: Pros and Cons of the Four-Wheel-Drive System

4.1.1.4 Six Wheel Chassis

Six wheel chassis is designed to go over 9 in (0.23 m) discontinuity with minimal mechanical complexity. With the additional wheels at center as supports of center of mass, the vehicle could go over 9 in (0.23 m) discontinuity with smaller wheels, as demonstrated by Figure 10. However, this design requires a moving mass stage to vary the center of mass which may increase manufacturing complexity. Additionally, the smaller wheels result in even less suspension and traction than the four wheeled system. There are several potential configurations for a six-wheeled translational system.

The first is implementing active suspension versus having fixed wheels. Due to the mechanical and manufacturing complexity required to design a suspension system, and the low benefit it would have due to the low travel speeds and stiffness required to cross a 9 in (0.23 m) discontinuity, it was decided that implementing an active suspension system would not be worth it, and is not considered in the trade study.

The next potential configuration is whether to drive the wheels directly through the motor, or to design an all wheel drive system, where there are less motors than wheels such as two motors with a drive train. For the trade study, both the design configurations using 6 motors driving 6 wheels and using two motors with a drive train to drive 6 wheels will be considered for the six-wheeled translational system. Their pro's and con's are tabulated in Tables 6 and 7, respectively.

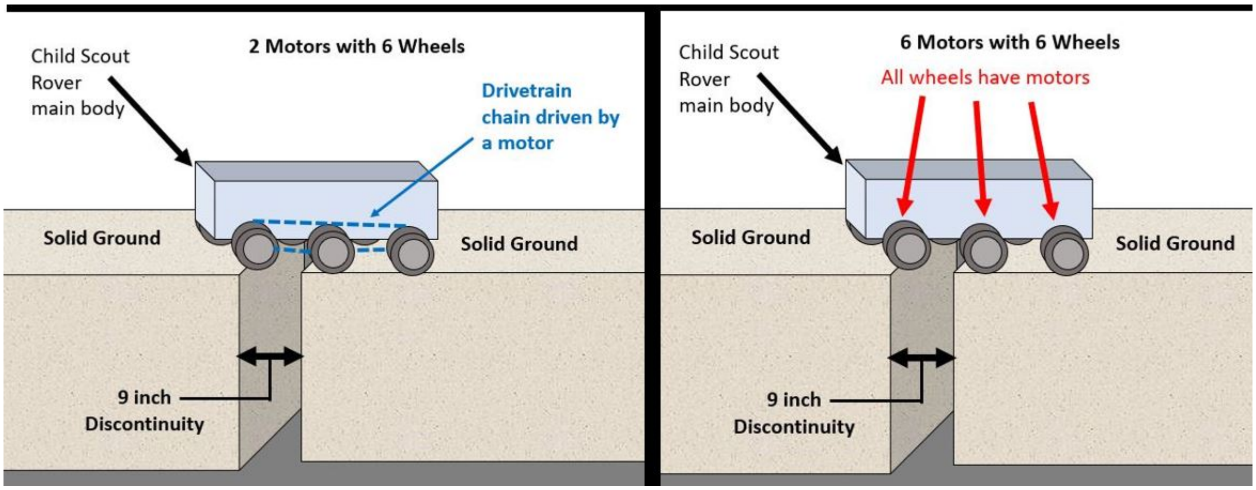

Figure 10: Six Wheel Chassis Configuration, fulfilling MOB.3.2 requirement

Description	Pro	Con
Mechanically simple	**X**	
Relatively simple to manufacture.	**X**	
Capable of crossing 9 in (0.23 m) discontinuity with a smaller profile.	**X**	
Minimal suspension capability		**X**
Minimal traction		**X**
Requires a moving mass stage to gain a variable center of mass		**X**
Each wheel is powered	**X**	
Increased control complexity		**X**

Table 6: Pros and Cons of the 6WD Six Wheel Configuration

Description	Pro	Con
Mechanically simple	**X**	
Relatively simple to manufacture.	**X**	
Capable of crossing 9 in (0.23 m) discontinuity with a smaller profile.	**X**	
Minimal suspension capability		**X**
Minimal traction		**X**
Requires a moving mass stage to gain a variable center of mass		**X**
Drive train may increase mechanical complexity		**X**
Simpler control complexity	**X**	

Table 7: Pros and Cons of the 2-Motor Six Wheel Configuration

4.1.2. Communication System

Author: Alexander Sandoval and Brindan Adhikari

A critical element of the project is to have the CSR communicate to the MR and the GS. These pieces of equipment will need to establish strong connection links with each other to satisfy the functional requirements demanded being CSR.1, CSR.2, and CSR.4. To meet these requirements, the CSR needs to be able to send and receive data from both the MR and GS. The max range needed across all these pieces of equipment needs to be 250 m (820 ft). On top of the range, obstructions may be present including trees, brushes, boulders, and hills. The data that is being sent and received will consist of videos, pictures, GPS locations, and guidance, navigation, and control (GNC) commands. This amount of complex data demands high transmission rates and low latency to preserve data integrity. Our design options will all be compared to each other for best performance in both a point-to-point (PtP) and point-to-multipoint (PtMP) network. PtP networks allows for only two devices to be communicating by having a transmitter and receiver whereas a PtMP network allows for multiple devices to be communicating by having a transmitter and multiple receivers. It is also important to point out that the prior year's work on communication led to minimal functionality between the MR and GS, however last year's approach will still be considered. Final decision will be based on the most optimal method that creates the strongest data link between all pieces of equipment. Thus, the options of consideration consist of PtP Wi-Fi, PtMP Wi-Fi, Zigbee, and Global System for Mobile Communications (GSM).

4.1.2.1 Point-to-Point Wi-Fi

Wi-Fi being one of the most common communication protocols available, creates ease of usability and efficiency for incorporation into our communication system. This technology is based on the IEEE 802.11 standard which is the broadband reserved for wireless technology using the Industrial, Scientific, and Medical Radio (ISM) band. This band use has been widely incorporated into vast number of devices and modules that are readily available to ensure maximum compatibility across off the shelf devices. Wi-Fi also allows for large amounts of data transfer, but with the drawback of higher power consumption and low transmission range without external amplification. According to Intel, data rates or throughput range from 2 to 450 Mbps[22]. For our implementation we need to design our Wi-Fi network with video transmission requirements in mind which require data rates from 600 to 800 Kbps for low quality streams and a minimum of 1.5 Mbps for medium quality streams[23]. A PtP setup would rely on having two independent radios for each system being the GS, CSR, and MR to allow for two way communication. Data rates are achievable with this approach as well as range. The benefits from this approach is that the system can reach higher throughput and create redundancy if one system was to fail. The drawbacks of this approach result from having additional hardware which creates the need for more integration. A schematic of implementation is shown in Figure 11.

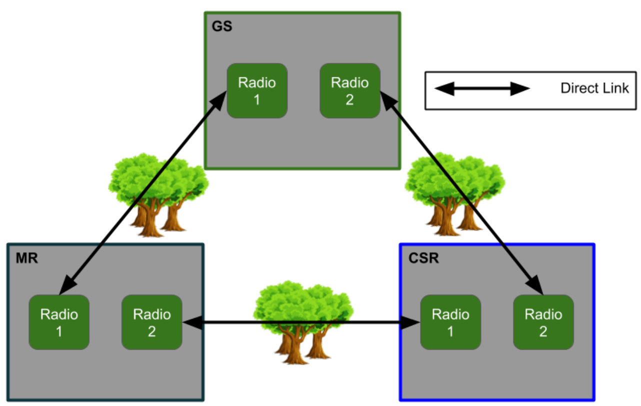

Figure 11: Wi-Fi method showing a Point-to-Point approach by using long-range radios.

Description	Pro	Con
Large data bandwidth	**X**	
Long range communication	**X**	
Direct communication w/out relay	**X**	
High power consumption		**X**
Hardware and software complexity		**X**

Table 8: Pros and Cons of a Point-to-Point Wi-Fi communication system.

4.1.2.2 *Point-to-Multipoint Wi-Fi*

Unlike the uncommon setup of a PtP approach using Wi-Fi, a more typical setup with Wi-Fi would consist of a wireless access point representing a simple PtMP implementation in which the GS will act as the wireless access point and thus relay messages between the CSR and MR indirectly. This creates a centralized form of communication which is much similar to a typical router configuration. Data rates with this approach are also achievable as well as the range of communication. The benefits from this approach is that the system will require less hardware and thus less integration. The drawbacks of this approach result from the possibility of having a single point failure if the main transmitter was to shutdown as well as having reduced throughput from competing connections to the transmitter. A schematic of implementation is shown in Figure 12.

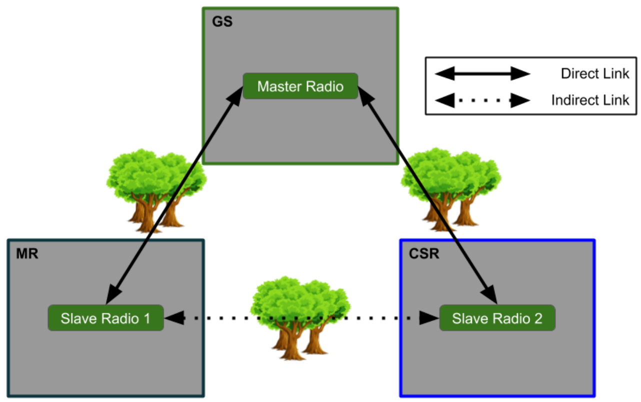

Figure 12: Wi-Fi method showing a Point-to-Multipoint approach by using long-range radios.

Description	Pro	Con
Large data bandwidth	**X**	
Long range communication	**X**	
Indirect communication with relay		**X**
High power consumption		**X**
Prone to single point failure		**X**

Table 9: Pros and Cons of a Point-to-Multipoint Wi-Fi communication system.

4.1.2.3 *Zigbee*

Zigbee is very similar to Wi-Fi in that it uses an IEEE standard with specifications defined under the 802.15.4 standard. This standard differs in that it specializes in low data rate, low power consumption, and low range wireless applications. According to Zigbee Alliance, data rates of 250 Kbps, 40 Kbps, and 20 Kbps can be achieved[24]. Video transmission will be unlikely to achieve with these rates; however, the data rates can be highly consistent for constant communication of sensor readings and signals being sent and received. This form of communication also allows ease of integration among off the shelf components and has been used in last years project. Last years project, DRIFT, used Xbee radio modules, which incorporate Zigbee's based protocol, for their form of communication between the MR and the GS. These tested Xbee modules can transmit over long ranges, but only with clear line of sight and direction for the path of transmission to the target. The benefits from this approach is that the system can communicate through a mesh network which allows for PtP communicaton with only one radio. The drawbacks from this approach result from the Zigbee protocol having low data rates of transmission as well as line of sight issues. Using this Zigbee approach will most likely incorporate last year's Xbee radios with modifications. The schematic of implementation is shown in Figure 13.

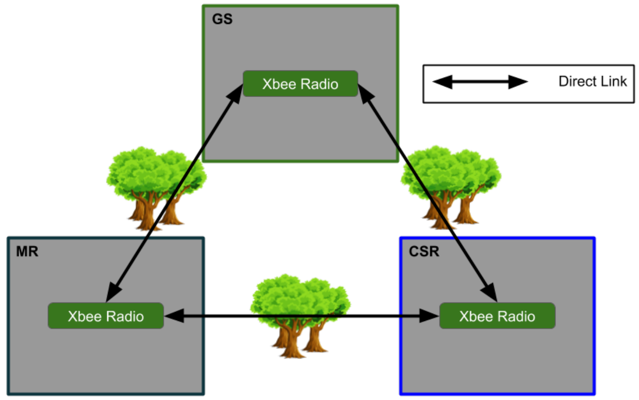

Figure 13: Zigbee method using a mesh network which incorporates utilizing last year's Xbee radio modules.

Description	Pro	Con
Inexpensive	**X**	
Low power consumption	**X**	
Long range communication	**X**	
Low data bandwidth		**X**
Prone to loss of reception from attenuation		**X**

Table 10: Pros and Cons of a Zigbee communication system.

4.1.2.4 Global System for Mobile Communications

GSM is more of a unique method to consider because it requires the use of cellular networks. The idea behind this method is to overcome the line of sight issues by utilizing cell towers near deployment. This method will allow each piece of equipment to have better path of transmission to the access point, being the cellular towers. According to Verizon, data rates of 5 to 12 Mbps can be achieved[25]. This method would require the MR, GS, and CSR to have their own cellular module which ultimately requires a Subscriber Identification Module (SIM) card that further brings along a paid service to the provider on top of the device itself. Speed and range can be easily achieved given the area of deployment has the right coverage, however the drawback to using cellular modules is the fact that they are complicated to setup and integrate given the lack of experience throughout the team. Nonetheless, a schematic of this approach is shown in Figure 14.

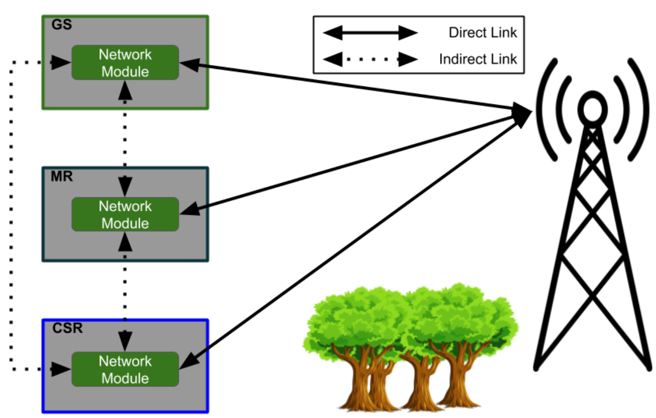

Figure 14: Global System for Mobile Communications method using a Point-to-Multipoint approach by communicating through a cell tower.

Description	Pro	Con
Large data bandwidth	**X**	
Long range communication (dependent on provider)	**X**	
Indirect communication with tower		**X**
Hardware and software complexity		**X**

Table 11: Pros and Cons of a Global System for Mobile Communications approach.

4.1.3. Guidance, Navigation, and Control System

Author: Chase Pellazar, Marcos Mejia, Katelyn Griego, and Alexis Sotomayor

4.1.3.1 Imaging System

The imaging system is a key component in the functionality of the CSR, and therefore a trade study is performed. The imaging system is the primary system for carrying out the functional requirement of sending data in the form of images and video to the GS and MR, specifically requirements CSR.2, CSR.5, and CSR.6. Moreover, this will be the primary system used for obstacle avoidance by the user at the ground station. These images and video will relay important information about the environment back to the GS to get the CSR and MR to the LOI. With these criteria in mind, four imaging system configurations were considered.

4.1.3.1.1. Wide FOV Fixed Camera

The option considered here is a wide FOV fixed camera with the capabilities of capturing a 100^o FOV. Due to a wide FOV required, distortion may be present. A rectilinear vs curvilinear lens in shown in Figure 15. A rectilinear lens is therefore ideal. To capture the full 100^o FOV; this would require a 15mm lens[29]. In this design option, there would only be one camera source from which to send images and video, which makes this option reliable, fast, and simple. In order to capture images and film video of other viewpoints outside the immediate FOV, the CSR must move the camera by moving the entire CSR in the desired direction. Pros and cons to this design option are shown in table 12.

Figure 15: Curvilinear vs Rectilinear Images

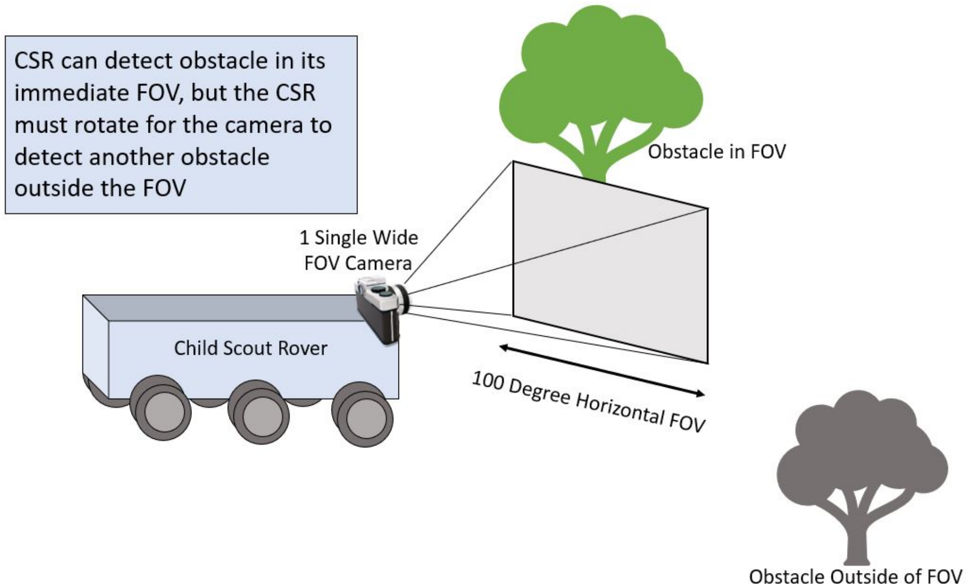

Figure 16: Wide FOV Fixed Camera Configuration

Condition	Pro	Con
The camera is able to capture the full required FOV	**X**	
Single imaging source to communicate with the GS and MR	**X**	
Limited image distortion	**X**	
Repositioning of the CSR required for expanded FOV		**X**

Table 12: Pros and Cons for Wide FOV Fixed Camera

4.1.3.1.2. Actuated Camera with 360^o FOV

This design concept is a single camera on a servo to rotate the camera 360^o. The actuated camera would have one degree-of-freedom (DOF) in yaw, rotating 360^o and giving full FOV. This would allow the GS to view the surrounding environment without moving the CSR, however additional commands would be required to turn the camera in the direction of interest. Additionally, this design requires mechanical implementation that increase the complexity and moving parts decrease reliability of the system. This mechanical implementation however is very popular and feasible for this case.

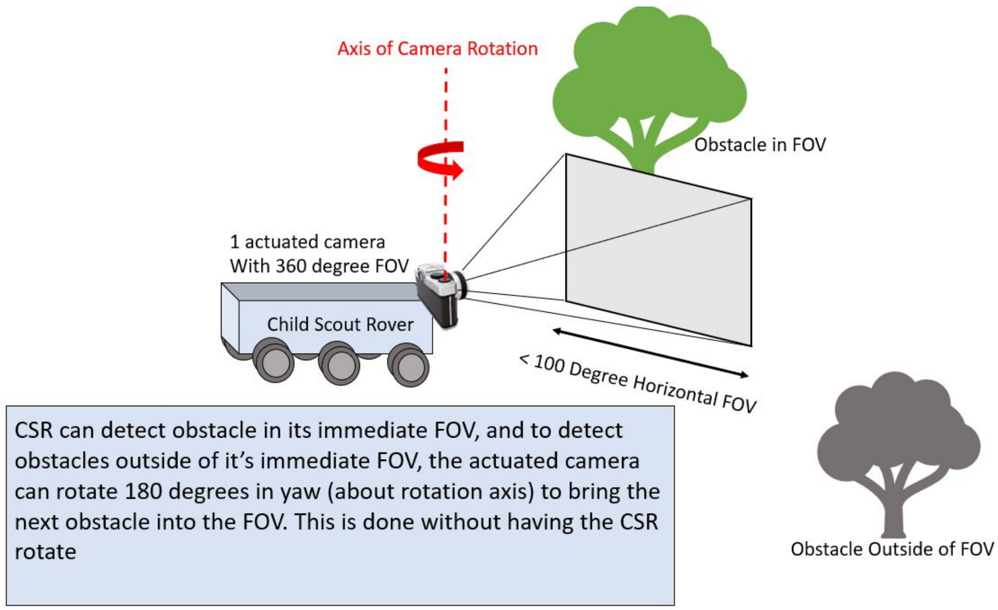

Figure 17: Actuated Camera with 360^o FOV Configuration

Condition	Pro	Con
The camera is able to capture the full required FOV	**X**	
Single imaging source to communicate with the GS and MR	**X**	
Limited image distortion	**X**	
Repositioning of the CSR is not needed for expanded FOV	**X**	
Complexity of mechanical integration for actuation of camera		**X**
Complexity of software integration for pointing control		**X**

Table 13: Pros and Cons: Actuated Camera with 360° FOV

4.1.3.1.3. 360^o 3 DOF Camera

The 360^o camera is a single camera with two lenses to capture images and video in all directions with its 3 DOF. This would potentially give an unlimited FOV; however with this distortion will arise. Image processing will again be needed for both distortion and to stitch images together. Depending on the camera chosen, the stitching can either happen instantaneously or is done in a post-processor. This can add difficulty as documentation to integrate and implement this software is sparse. Transmission rates would be significantly slower due to the expansive data collected by this camera, however there is again only one camera source sending data. A table of pros and cons can be seen in the table below.

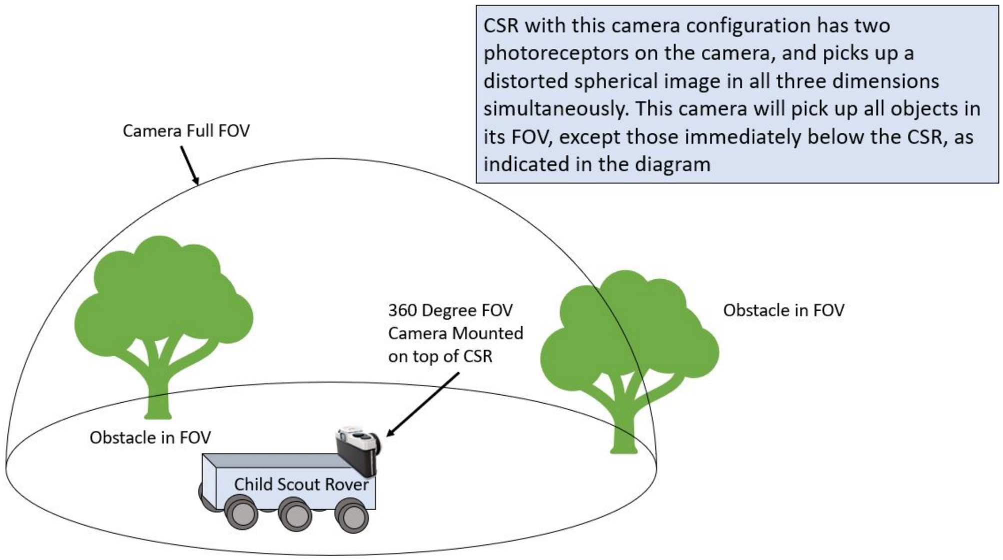

Figure 18: 360^o 3 DOF Configuration

Condition	Pro	Con
The camera is able to capture the full required FOV	**X**	
Single imaging source to communicate with the GS and MR	**X**	
No image distortion	**X**	
Repositioning of the CSR is not needed for expanded FOV	**X**	
Significantly more data to be transmitted to GS and MR, long transmission times		**X**
Image stitching required		**X**

Table 14: Pros and Cons: 360° 3 DOF Camera

4.1.4. Environmental Sensing System

Author: Katelyn Griego and Quinter Nyland

In order for the CSR to navigate to a particular LOI (Requirement CSR.3), the CSR must be able to navigate through an outdoor area containing a number of obstacles, such as trees and rocks (See Terrain Definition). The key design option that enables this process to occur is object detection within this environment, or the ability for the CSR to sense obstacles in the terrain that lie in between the CSR and the LOI. This system can be two fold: manually and semi-autonomously. Here, we consider a semi-autonomous mode, where the fundamental function of the CSR is purely detection of obstacles that would be potentially in the path of the MR. In order to do this, the sensing system on the CSR must act as the size of the MR for detection of such obstacles. Because of this, the following design alternatives have been considered as they all have the ability to detect the existence of an object. The alternatives considered for this design option are LiDAR sensors, ultrasonic sensors, collision sensors, and image processing. It should be noted that the image capturing system for image processing is entirely separate and independent from the image capturing system that will fulfill requirements CSR.5 and CSR.6. In particular, the image processing alternative directly fulfills the SENS.3.1 derived requirement, along with the other object detection methods.

4.1.4.1 LiDAR Sensor

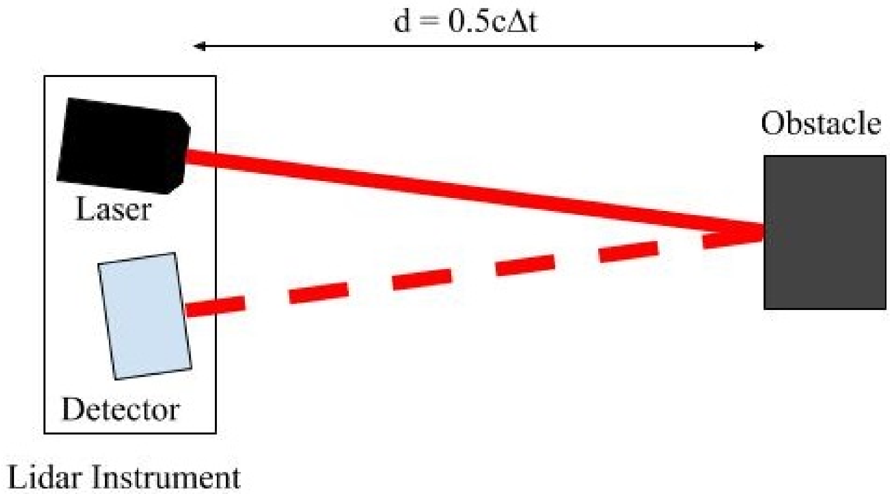

Figure 19: LiDAR operation

LiDAR (Light Detection and Ranging) sensors are used for remote sensing, creating environmental maps, and are able to accurately measure distances to objects within a given range. To measure distances, the LiDAR sensor emits quick consecutive laser pulses and makes calculations based on how fast those pulses reflect back to the sensor.[17] This process is depicted in Figure 19 along with the distance formula the instrument utilizes. LiDAR would serve as a useful object detection method due to its high accuracy and large amounts of available software, making the system easier to integrate. It must be taken into account, however, that the system must be precisely calibrated and have a stable mounting system to limit measurement uncertainty.

Description	Pro	Con
Many software libraries available in a variety of common microprocessor languages	**X**	
Produce accurate environmental maps to clearly show where landscape objects lie	**X**	
Wide range of applications (can operate as a simple distance finder or a terrain map builder)	**X**	
Some LiDAR systems do not function outdoors (light-sensitive)		**X**
Must have stable mounting to limit pointing uncertainty		**X**

Table 15: Pros and Cons of LiDAR Sensor

4.1.4.2 Ultrasonic Sensor

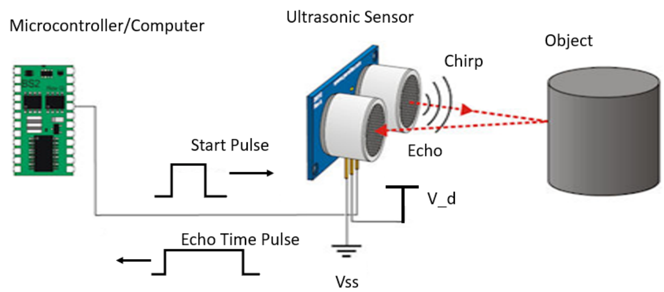

Figure 20: Ultrasonic detection operation [18]

Ultrasonic sensors are based off the use of sound for remote sensing. Typically these types of sensors are used for distance measurements and object detection. The method can be used to collect both types of data, however, boards are typically configured by the manufacturer to process either the distance or object detection data. To measure distances, the sensor emits a sound wave at a specific frequency. When the sound wave returns after colliding with an object, the distance can be computed since the sound wave travels at the speed of sound. Similarly, to detect objects an ultrasonic sensor sends out a sound wave and when the wave encounters an object it reflects (certain objects can absorb the sound wave). If the ultrasonic sensor receives a sound wave back then an object is in the direction of the source.

Description	Pro	Con
Available at different price ranges and fidelity levels	**X**	
Simple distance calculations	**X**	
Software is typically available for the ultrasonic sensor selected	**X**	
Material-dependent (some ultrasonic sensors give faulty data when sensing materials like wood)		**X**
Mapping can be difficult with lower fidelity hardware		**X**

Table 16: Pros and Cons of Ultrasonic Sensor

4.1.4.3 Infrared Sensors

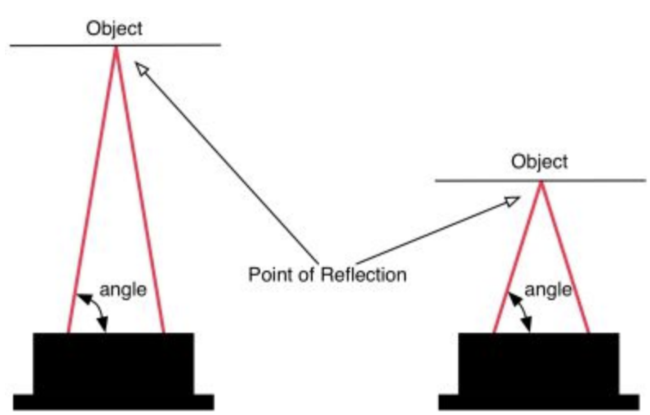

Figure 21: Infrared sensor operation

Infrared sensors are used to sense certain characteristics of its surroundings. This sensor accomplishes this by either emitting or detecting infrared radiation. Infrared sensors have the ability to detect the distance from an obstacle by utilizing triangulation. This is done by a pulse of light being emitted and traveling out into the FOV before it hits an object. The light is then reflected off of an object. It returns to the detector and creates a triangle between the emitter, the point of reflection, and the detector. From the incident angle of the reflected light the distance to an object can be found. An image of this is shown in Figure 21. This sensor would serve as a useful object detection method due to its relatively low cost and simple integration.

Description	Pro	Con
Simple distance calculations	**X**	
Software is typically available for the infrared sensor selected	**X**	
Material-dependent (give faulty data when sensing materials like wood)		**X**
Cannot function in shaded areas		**X**

Table 17: Pros and Cons of Infrared Sensors

4.1.4.4 Image Processing

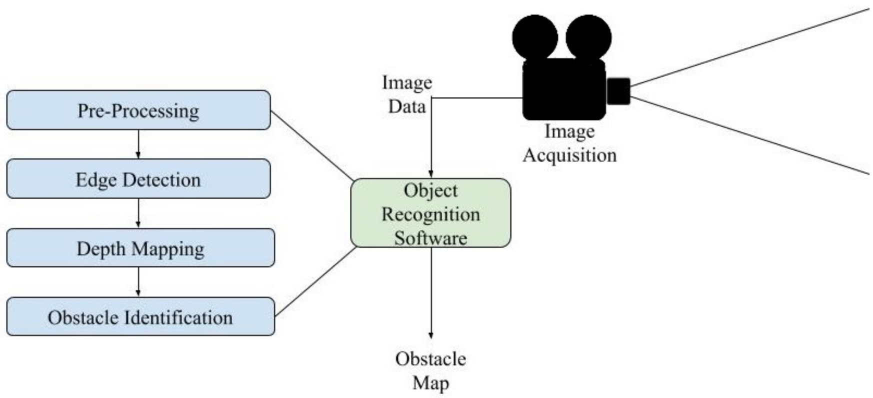

Figure 22: Vision processing flow chart

Image processing is the act of capturing an image and using computer-based algorithms to filter and enhance that image to extract useful data. Image processing techniques for object detection, for this study, refer to the hardware and software required to capture an image and gather relative distance information between a camera module and an obstacle. The two primary forms of image processing considered for this design alternative are traditional digital vision processing using a camera module with direct integration to a microcontroller and accurate depth map processing using an RGB-D camera.

Typically, microcontroller camera modules are capable of capturing images in several common formats including JPEG, PNG, Windows bitmap, RGB, and RGBA[20]. Many computer vision techniques exist in the industry today to perform the above procedure (Figure 22) to convert the images from raw image data to object maps that contain locations of determined objects in an environment. RGB-D camera modules are used in a stereo format and utilize an IR projected light pattern and an IR sensor to calculate and record relative depths[21]. These cameras are locked into the RGB format of images, but each pixel contains depth information, which is useful in determining relative distances between the camera module and an object.

Description	Pro	Con
Many software libraries available in a variety of common microprocessor languages	**X**	
Computationally heavy so may need an additional microprocessor		**X**
May struggle to determine accurate distances without multiple images or cameras		**X**
Large amounts of data must be processed per image		**X**

Table 18: Pros and Cons of Image Processing

4.2. Trade Studies Process and Results

4.2.1. Mobility System

4.2.1.1 Trade Criteria Selection for Mobility

There are many factors to consider when choosing a translational system that is capable of meeting the terrain capability requirements. The criteria chosen for the translational system's trade study are Suspension Capability, Cost, Traction, Size, Control Complexity, Manufacturing Complexity, and Mechanical Complexity. The suspension capability was selected as a trade criterion, as the CSR will travel over rough terrain that could cause the CSR to get stuck or tipped over. The systems cost was considered due to the fact that the entire project should not exceed the provided budget of $5000, and the translational system will command a significant percentage of the total budget. The traction of the CSR is important to consider, as it must be able to travel through dirt, underbrush, and slopes without slipping. The size of the system will be a driving design parameter, hence its selection as a trade criterion. The goal should be to minimize the size of the CSR, while still allowing it to meet the terrain requirements, namely the ability to cross a 9 in (0.23 m) discontinuity. The complexity of controlling the motors must also be considered such that the CSR can be successfully maneuvered. The manufacturing complexity must also be considered, as the translational system will require significant manufacturing. The system must be designed for manufacturability to minimize the time and financial cost required. The last trade criterion selected is the mechanical complexity of the design. In order to simplify the analysis required and to reduce the risk of mechanical failure, the system should aim to be as mechanically simple as possible. Another important criterion that was taken to consideration is the required power output of the translational system. However, all of the translational system will have approximately the same power output depending on the power input. While each individual motor may draw more or less power depending on the system, the overall power draw will be approximately the same, assuming similar efficiencies. The desired speed, mass, and range of the CSR will drive the power requirements much more than the translational system configuration. Further rationale behind the weight selection of the criteria is explained in Table 19 below.

4.2.1.2 *Weighting Assignment for Mobility*

Criteria	Weight (%)	Rationale
Suspension Capability	5	Suspension helps improve the performance of the CSR on rough terrains and reduces the risk of tipping. However, as the CSR must be stiff enough to cross a 9 in (0.23 m) discontinuity and will travel relatively slow, suspension will not be the a significant trade factor.
Cost	10	Ensuring the financial scope of the design lies within our given budget of $5000 is critical, as there are many other subsystems that will require part of this funding. However, while it will not likely command over $600 dollars, it is possible to purchase expensive COTS chassis. While significant, this is not the most significant trade criterion, at 10%.
Traction	10	The wheels of the CSR must have sufficient traction in order to travel through the rough terrain of the operating environment, such as slopes and underbrush. Although traction is important, the operating environment is mainly dry, thus traction is not the most significant design driver.
Size	10	The size of the CSR drives the design of the other subsystems, and because the CSR should ideally be smaller than the MR to gain better mobility, this criteria earns a weight of 10%.
Manufacturing Complexity	20	In order to be a successful project, the manufacturing process has to be done thoroughly with limited time, money and resources available. Due to the mission critical aspect of this criteria, it was given a higher weight at 20%.
Mechanical Complexity	20	Mechanical complexity can be defined by several different aspects such as the drive train, suspension, moving wheel linkages, etc. Increasing the mechanical complexity of the system increases the difficulty of modelling and analyzing the system, and introduces increased risk of CSR failure. Due to the critical nature of this criteria, it is weighted at 20%.
Control Complexity	25	The more motors the CSR contains, the more complex the CSR will be to control. By increasing the number of motors, thus control complexity, the risk of failure increases. Therefore, this criterion has 25% of the weight.

Table 19: Translational System Weighting Criteria and Rationale

4.2.1.3 Scale Assignment for Mobility

Criteria	1	2	3	4	5
Suspension Capability	No suspension and high potential of tipping	N/A	No suspension	N/A	With suspension
Cost	> \$900	\$700 - \$900	\$500 - \$700	\$300 - \$500	< \$300
Traction	Minimal contact with the ground	N/A	Medium contact with the ground	N/A	Significant contact with the ground
Size (length x width x height)	>3ft x >3ft x >3ft	(2.5ft - 3ft) x (1ft - 2ft) x (1ft - 2ft)	(2.5ft - 3ft) x ≤1ft x ≤1ft	(2ft - 2.5ft) x ≤1ft x ≤1ft	≤2ft x ≤1ft x ≤1 ft
Manufacturing Complexity	Too hard to manufacture. Component manufacturing must be outsourced	All in-house manufactured	Primarily in-house manufactured with some parts COTS	Significant COTS and in-house manufactured	Primarily COTS
Mechanical Complexity	• Complex Tread System	• No Tread System • Moving wheel linkages	• No Tread System • Fixed wheel linkages • Suspension	• No Tread System • Fixed wheel linkages • No Suspension • Power Train	• No Tread System • Fixed wheel linkages • No Suspension • Simple Wheels
Control Complexity	6 motors to control	N/A	4 motors to control	N/A	2 motors to control

Table 20: Translational System Scale Assignment and Ranges

4.2.1.4 Trade Matrix for Mobility

Criteria	**Weight(%)**	**Options**				
		Rocker Bogie	Tank Track	4WD 4 wheels	6 motors driving 6 wheels	2 motors driving 6 wheels with a drive train
Suspension Capability	5	5	1	1	3	3
Cost	10	4	1	4	4	4
Traction	10	3	5	3	1	1
Size	10	4	3	2	3	3
Manufacturing Complexity	20	2	3	3	3	3
Mechanical Complexity	20	2	1	5	5	4
Control Complexity	25	1	5	3	1	5
Weighted Total	100	2.4	2.5	3.3	2.8	3.6

Table 21: Translational Trade Matrix

4.2.2. Communications System

Author: Alexander Sandoval and Brindan Adhikari

4.2.2.1 Trade Criteria Selection for Communications

The trade criteria chosen for the communication system are data bandwidth, transmission power, receiver sensitivity, integration complexity, power consumption, and cost. The rationale for choosing these criteria are shown in Table 22. The most crucial criteria in choosing a communication system are data bandwidth, transmission power, and receiver sensitivity. Knowing a communication system's data bandwidth is vital as this mission requires different types of data that will be transferred between the GS, MR, and the CSR. This data includes video, GPS data, and user commands. Examining a communication system's range is also crucial to ensure successful communication between the GS, MR, and the CSR. The signal needs to travel at least 250m (820 ft) to meet the requirements while dealing with signal loss from obstructions and from the path of transmission. So, the range is ultimately determined by having a strong transmission power as well as receiver sensitivity to detect faint powers. The other criteria are integration complexity, power consumption, and cost. Since this project must be completed within a year, it is important to examine the complexity of each system to ensure that the system can be integrated on time. The factors considered were the amount of Detailed Design - Mobilitydocumentation available and hardware complexity as well as software complexity. The amount of power that the communications system draw is also important because it needs to be able to operate within an hour duration of operation. Finally, since this project must be completed on a limited budget, it is critical to examine the cost of each system.

4.2.2.2 *Weighting Assignment for Communications*

Criteria	Weight (%)	Rationale
Cost	5	Communication systems are more of a time requirement and a software challenge to establish. However, communication systems can be expensive therefore cost must be taken into account to maintain a reasonable project budget.
Power Consumption	10	Power consumption of the CSR needs to be minimal, but at the same time be able to support large transmission powers. If the power consumption of the communication system is too large, this will cause the need for a bigger battery.
Integration Complexity	15	Integration includes hardware/software complexity and the documentation available for the communication system.These factors will directly affect the time (man hour) needed to make a working communication system. Since this project has a time-limit of one year, it is critical to analyze the integration complexity of the system. These hours will be based on a per week basis for the duration of spring semester.
Receiver Sensitivity	20	The need for a high receiver sensitivity is critical to be able to detect small levels of transmission power that can be caused from signal attenuation.
Transmission Power	20	The communication range needs to be at least 250 meters (820 ft) for the functional requirement to be met. For this to occur, the communications system needs to have high transmission power to account for path loss and signal attenuation. This power will be represented in terms of achievable range for simplicity.
Data Bandwidth	30	During the mission numerous types of data (images, video, gps, etc) will be transmitted and received between GS, MR, and the CSR. Thus, it is essential that the communication system in place has enough bandwidth for the communication to function smoothly.

Table 22: Communication system weighting criteria and rationale.

4.2.2.3 Scale Assignment for Communication

Criteria	1	2	3	4	5
Cost	> $500	$250 - $500	$100 - $250	< $100	Free
Power Consumption (Watts)	> 24 W	12-24 W	6-12 W	1-6 W	< 1 W
Integration Complexity (Hours Till Completion)	> 60 hours	48 hours	36 hours	24 hours	< 24 hours
Receiver Sensitivity (dBm Threshold)	>-30 dBm	-30dBm	-60dBm	-90dBm	< -90dBm
Transmission Power (Achievable Range)	< 250 m (820 ft)	250-275 m (820-902 ft)	275-300 m (902-984 ft)	300-325 m (984-1066 ft)	> 325 m (1066 ft)
Data Bandwidth (Bits per second)	< 250 Kbps	250 Kpbs-1 Mbps	1 Mbps-10 Mbps	10-50 Mbps	> 50 Mbps

Table 23: Communication scale assignment and ranges.

4.2.2.4 Trade Matrix for Communications

Criteria	Weight(%)	Options			
		Wi-Fi point to point	Wi-Fi Point to Multipoint	Zigbee	GSM
Cost	5	1	3	5	2
Power Consumption	10	2	3	5	3
Integration Complexity	15	2	4	3	3
Receiver Sensitivity	20	4	4	5	4
Transmission Power	20	5	5	5	5
Data Bandwidth	30	5	5	1	3
Weighted Total	100	3.85	4.35	3.5	3.55

Table 24: Communication trade matrix.

4.2.3. Guidance, Navigation, and Control System

Author: Chase Pellazar, Marcos Mejia

4.2.3.1 Trade Criteria Selection for Guidance, Navigation, and Control

When looking at approaches to guidance, navigation, and control, particularly imaging the team focused in on five areas to judge potential solutions. These five areas are cost, image processing, effect of actuation, hardware/mechanical integration, and speed. As can be seen in the weighting matrix below the highest weighted criteria is speed. The reason for such a high weight is that the communications subsystem will be transmitting video continuously while the CSR is in operation. So, if the size of the video packets are large there will be a higher chance of a data budget deficit which will impact important quantities such as heading from being sent to the ground station. Another heavily weighted quantity is Hardware Integration. The reason for a heavy weight in this area is because if the imaging system is hard to integrate with the rest of the CSR it introduces complexities the team may not be able to address with respect to the other systems on board. In addition to the aforementioned heaviest criteria, the team also assessed solutions on effect of actuation, image processing, and cost. Effect of actuation addresses the team's concern with the camera being able to actuate when the CSR is being manually driven by the GS. If the operator cannot have visualization of the surroundings they may damage the CSR. For image processing, if the images provided by the camera need to be processed in any manner it will add unwanted complexity that's out of the scope for HERMES' mission. Finally, the lowest weighted criteria is cost which defines the impact the system will have on the team's budget.

4.2.3.2 Weighting Assignment for Guidance, Navigation, and Control

Criteria	**Weight** (%)	**Rationale**
Cost	10	Cost includes any cost for the cameras, wires, rotation devices, and software integration. The higher the cost, the lower the score for the category due to the projects maximum budget of $5,000. Cost was rated as the lowest weighted category because the maximum amount the team will spend on a camera system is approximately $1,000, which is only 20% of the overall budget.
Image Processing	15	Image processing required by image distortion (from wide FOV) and stitching of images is required for accurate environment, but will hinder performance by taking time. This category is weighted quite high due to the missions dependency on the data received concerning the CSR's surroundings.
Effect of Actuation	20	Effect of Actuation is defined as the effect of the camera's actuating abilities on the CSR's performance. The CSR's performance will increase with the ability of the camera to actuate independently of the CSR, gaining viewpoints outside of the immediate FOV. This is essential, as it would be much easier to rotate the camera to scan the environment than to have the CSR maneuver, resulting in faster determination of objects and waypoints. This is especially the case when obstacles are close in proximity.
Hardware/ Mechanical Integration	25	Hardware Integration can be difficult if the device does not have detailed documentation to be able to integrate the camera with the CSR. This criteria is important if the device requires uniquely designed mechanical parts as this integration process can become time consuming. With the complexity of other systems as a whole, it is important to try and keep this as simple as possible.
Speed	30	Speed is a percentage approximation of the total communications bandwidth required to send images/video to the GS and MR. This category is weighted heavily because a key functional requirement is to send data in the form of images and video to the GS and MR. The design options considered vary on the amount of data that needs to be sent, and therefore the bandwidth that would be required to do so.

Table 25: Imaging System Weighting Criteria and Rationale

4.2.3.3 Scale Assignment for Guidance, Navigation, and Control

Criteria	1	2	3	4	5
Cost	>$600	$400-$600	$200-$400	$100-$200	<$100
Image Processing	Image processing required due to image distortion and stitching of images	Image processing required due to image distortion	Image processing required to stitch images together, no distortion in images	No image processing is needed, image distortion present but is not extreme	No image processing due to distortion is needed
Effect of Actuation	Motion of CSR needed to gain additional FOV's	N/A	N/A	N/A	No motion of CSR needed to gain additional FOV's
Hardware/ Mechanical Integration	Poor documentation, mechanical integration required including moving parts in > 1 DOF	Poor documentation, mechanical integration required including moving parts in 1 DOF	Poor documentation, mechanical integration relatively simple	Good documentation, mechanical integration required including moving parts in 1 DOF	Mechanical integration for moving parts not required
Speed	>50% Bandwidth	40%-50% Bandwidth	30%-40% Bandwidth	20%-30% Bandwidth	<20% Bandwidth

Table 26: Imaging System Scale Assignment and Ranges

4.2.3.4 Trade Matrix for Guidance, Navigation, and Control

Criteria	**Weight(%)**	**Options**		
		Single Fixed Wide FOV Camera	Single Actuated Camera	360°3 DOF Camera
Cost	10	5	4	1
Image Processing	15	5	5	1
Effect of Actuation	20	1	5	5
Hardware/ Mechanical Integration	25	5	4	3
Speed	30	5	3	2
Weighted Total	100	4.2	4.05	2.60

Table 27: Imaging System Trade Matrix

4.2.4. Environmental Sensing System

Author: Ashley Montalvo, Quinter Nyland, and Katelyn Griego

4.2.4.1 Trade Criteria Selection for In-Plane Object Detection

The trade criteria chosen for object detection include cost, range, FOV, complexity, and environmental vulnerability. The rationale for these choices are clearly explained in the table below. The most important criteria, however,include environmental vulnerability and complexity. The environmental vulnerability was deemed highly critical as theCSR must be able to traverse complex areas in which a large number of irregular obstacles may be encountered. The chosen object detection sensor must be able to remain accurate within these conditions or else the system will be unable to determine a viable path. Furthermore, some in-plane object detection methods may be rather complex which may require computationally intense programs leading to slower performance of theCSR and interference with alternative functions of the microprocessor. This may also lead to lengthy software development time which would limit the time the team has to develop additional subsystem functions.

A design factor not taken into account in the trade criteria is power. Although power plays an important role in this project, the chosen in-plane object detection system was found to consume little power in comparison to that of the translational system. Thus, with the criteria that has been chosen for this trade study, it has been determined all critical aspects for each system can be evaluated fairly.

4.2.4.2 Weighting Assignment for In-Plane Object Detection

Criteria	**Weight** (%)	**Rationale**
Cost	10	Accurate sensor systems can be expensive, therefore the cost must be taken into account in order to maintain a reasonable project budget.
Range	15	The range of the sensor dictates its maximum capabilities. A sensor with a shorter range will not be able to detect distant obstacles.
FOV	20	The FOV of the sensors will dictate how many sensors will be needed. If the FOV is below the minimum required FOV of 103 to detect obstacles in the line of sight of the MR, multiple sensors will be required.
Complexity	25	Some methods may be extremely computationally intense and thus may interrupt other programs within the software controlling the CSR. Furthermore, object detection software is very complex and difficult to write, so it will be optimal to have a variety of available software for the chosen system. These sensors can have outputs that can only be read by atypical processors, and may require uniquely designed mechanical and electrical interfaces.
Environmental Vulnerability	30	The CSR will be in complicated terrain with variable conditions such as changing lighting and complicated surface materials and geometries. If the sensors data is made erroneous due to environmental obstacles then the CSR will be unable to accurately navigate and determine a viable path.

Table 28: In-Plane Object Detection Criteria and Rationale

4.2.4.3 Scale Assignment for In-Plane Object Detection

Criteria	1	2	3	4	5
Cost	> $550	$350 - $550	$150 - $350	$50 - $150	< $50
Range	0 m - 5 m	5 m - 15 m	15 m - 25 m	25 m - 35 m	> 35 m
FOV	<10°	10°-45°	45°-100°	100°-180°	>180°
Complexity	Extremely slow on-board computations. Little to no available software making integration difficult.	Slow on-board computation time. Some available software but difficult to access or find	Moderate on-board computation time. An average amount of available software with average documentation	Moderate on-board computation time. Large amounts of software that is easy to access and has average documentation	Quick on-board computations. Many software libraries available that are easy to access and are well documented, or has product specific software tailored for the device.
Environmental Vulnerability	Extremely vulnerable to light, material types, surface geometry, or collisions	Highly vulnerable to light, material types, surface geometry, or collisions	Moderately vulnerable to light, material types, surface geometry, or collisions	Low vulnerability to light, material types, surface geometry, or collisions	Not vulnerable to environmental factors

Table 29: Object Detection Scale Assignment and Ranges

4.2.4.4 Trade Matrix for Environmental Sensing for In-Plane Object Detection

Criteria	**Weight(%)**	**Options**			
		LiDAR	Ultrasonic	RGB D Camera	IR Sensor
Cost	10	2	4	3	5
FOV	15	5	2	3	2
Range	20	5	1	5	1
Complexity	25	3	5	3	4
Environmental Vulnerability	30	4	3	3	3
Weighted Total	100	3.90	3.05	3.40	2.90

Table 30: In-Plane Object Detection Trade Matrix

4.2.4.5 Trade Criteria Selection for Discontinuity Detection

The chosen trade criteria for discontinuity detection include cost, range, accuracy, complexity, and environmental vulnerability. As discussed in the trade criteria selection for in-plane object detection, complexity and environmental vulnerability are large subsystem concerns. Accuracy, however, is especially important in detecting discontinuities as the sensor must be able to determine a sudden change in depth (2.4 in) from a distance of 1 m away. If the sensor is unable to immediately detect this depth change, a signal will not be sent to the mobility system to stop, which could damage the CSR.

4.2.4.6 Weighting Assignment for Discontinuity Detection

Criteria	**Weight** (%)	**Rationale**
Cost	10	Accurate sensor systems can be expensive, therefore the cost must be taken into account in order to maintain a reasonable project budget.
Range	15	The range of the sensor dictates its maximum capabilities. A sensor with a shorter range will not be able to detect distant obstacles.
Accuracy	25	The sensor must take point data in order to ensure it is collecting data only within the discontinuity. This requires a sensor to not have an FOV when detecting discontinuities less than 9 in.
Complexity	25	Some methods may be extremely computationally intense and thus may interrupt other programs within the software controlling the CSR. Furthermore, object detection software is very complex and difficult to write, so it will be optimal to have a variety of available software for the chosen system. These sensors can have outputs that can only be read by atypical processors, and may require uniquely designed mechanical and electrical interfaces.
Environmental Vulnerability	25	The CSR will be in complicated terrain with variable conditions such as changing lighting and complicated surface materials and geometries. If the sensors data is made erroneous due to environmental obstacles then the CSR will be unable to accurately navigate and determine a viable path.

Table 31: Discontinuity Detection Weighting Criteria and Rationale

4.2.4.7 Scale Assignment for Discontinuity Detection

Criteria	1	2	3	4	5
Cost	> \$550	\$350 - \$550	\$150 - \$350	\$50 - \$150	< \$50
Range	0 m - 5 m	5 m - 15 m	15 m - 25 m	25 m - 35 m	> 35 m
Accuracy	Uses a defined FOV to sense environment				Uses a point sensor to sense environment
Complexity	Extremely slow on-board computations. Little to no available software making integration difficult.	Slow on-board computation time. Some available software but difficult to access or find	Moderate on-board computation time. An average amount of available software with average documentation	Moderate on-board computation time. Large amounts of software that is easy to access and has average documentation	Quick on-board computations. Many software libraries available that are easy to access and are well documented, or has product specific software tailored for the device.
Environmental Vulnerability	Extremely vulnerable to light, material types, surface geometry, or collisions	Highly vulnerable to light, material types, surface geometry, or collisions	Moderately vulnerable to light, material types, surface geometry, or collisions	Low vulnerability to light, material types, surface geometry, or collisions	Not vulnerable to environmental factors

Table 32: Discontinuity Detection Scale Assignment and Ranges

4.2.4.8 Trade Matrix for Discontinuity Detection

Criteria	**Weight(%)**	**Options**			
		Single Beam LiDAR	Ultrasonic	RGB D Camera	IR Sensor
Cost	10	2	4	3	5
Range	15	5	5	5	1
Accuracy	20	5	1	5	1
Complexity	25	3	5	3	4
Environmental Vulnerability	30	4	3	3	3
Weighted Total	100	3.90	2.80	2.80	2.65

Table 33: Discontinuity Detection Trade Matrix

4.3. Baseline Design

4.3.1. Mobility System

Author: Michely Tenardi

The results of the trade study concludes that a six wheel chassis with 2 motors driving six wheels with drivetrains is the optimal design with a score of 3.6/5. The second best design is the 4WD with 4 wheels, scored at 3.3. The main disadvantages for the 4WD 4 wheels are in the suspension capability and size. It will likely be stuck when going over the 9 in (0.2286 m) discontinuities and requires larger size of the CSR. The design of six wheels chassis using 2 motors with drivetrains has the desired benefits compared to other options: better performance, able to retain a relatively low profile and use smaller wheels to cross the 9 in (0.2286 m) discontinuity, while remaining less complex to control compared to 6 motors driving 6 wheels. When one wheel is not contacting the ground (lifted in the air), the other wheels increase their effective torque as appropriate. Due to these benefits, the six wheels chassis with 2 motors and drivetrains is the optimal mobility system design option. Further details regarding the model analysis and chosen components for our mobility system will be discussed in the Mobility Detailed Design Section.

4.3.2. Communications System

Author: Alexander Sandoval and Brindan Adhikari

From the trade study conducted under Table 24, it was concluded that the PtMP Wi-Fi communication system was the best design option. This system meets all the functional requirements and can be easily integrated. For the Zigbee option, the main concern was its low data bandwidth. Since we needed to send video continuously this wasn't feasible. For the GSM option, the main concern was the integration factor that required utilizing a mobile provider network card and being able to send and receive video that is dependent on that provided network connection. For the PtP Wi-Fi system, the main concern was again the integration complexity due to the fact that this would require two radios per system to provide long-range communication directly. Although there is better functionality that can be achieved with a PtP Wi-Fi system since the CSR will be able to talk with the MR directly, the PtMP Wi-Fi will allow for less time in integration and still satisfy all the requirements needed. This system also had the highest data bandwidth, exceptional receiver sensitivity, and the highest transmission power. This enables the GS, MR, and the CSR to communicate successfully at the required range. Using this PtMP system however, poses the potential for a single point failure since the GS will be providing the main point of contact for communications. The reasoning behind this is the fact that the user operator will oversee all operations and thus if the communications is lost at all with the GS then the mission can't continue even if the MR and CSR still had communications. A schematic of our baseline design is shown in Figure 23.

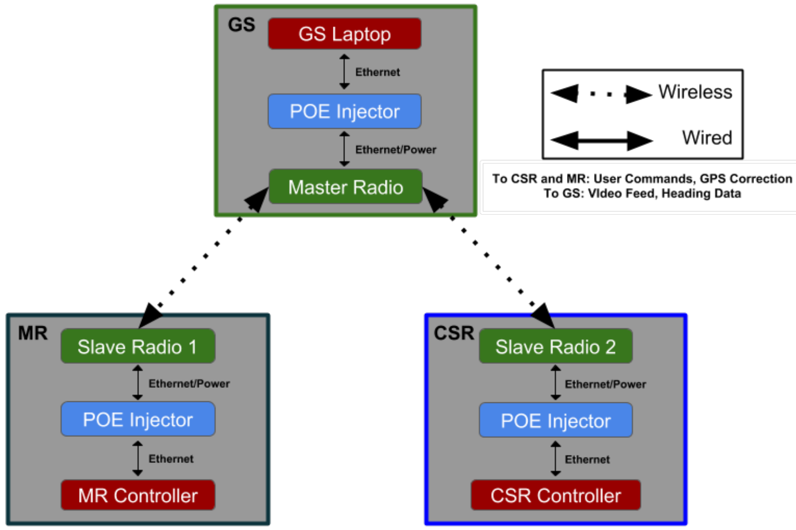

Figure 23: The baseline design of our communications system with a radio, power over ethernet (POE) injector, and controller per system.

The necessary hardware that makes our baseline design includes a radio that has large data bandwidth and long-range capability, a power over ethernet (POE) injector, and the controller/computer which connects to the radio. Essentially, this setup will exist for the CSR, MR, and GS. Doing so creates a Local Area Network (LAN) that allows the controller/computer to establish a static Internet Protocol (IP) address for its radio to be able to easily communicate to other static IP address radios within this network. It is important to note also that these radios communicate over a 900 MHz frequency which allows for better penetration around obstacles due to the larger wavelength of transmission. Since these radios act as the primary source for successful communications, their characteristics are shown in Table 34. Further discussion will be made in the detailed design for how exactly this LAN is setup among the radios and how exactly they are being integrated into the CSR, MR, and GS.

Voltage (V)	Amps (A)	Watts (W)	Data Bandwidth (Mbps)	Frequency (MHz)	Mass (kg)	Size (l x w x h mm)
24	0.3	7.2	+50	900	0.5	160 x 80 x 30

Table 34: Communication radio characteristics.

4.3.3. Guidance, Navigation, and Control System

Author: Marcos Mejia

The results of the trady study concluded that a Single Fixed Wide FOV Camera would be the best option for the imaging system in terms of Guidance, Navigation, and Control. Since the CSR would be able to skid steer in place there would be no need for an actuated camera, and since the FOV requirement is 100 ^{o}, the Wide FOV camera would meet this requirement without having to stitch images together, requiring additional software. The way this camera would work is that it would be connected to a controller, and continuously send video feed over the communication system to the ground station. This would allow the operator to sense the environment at all times.

In addition to the imaging system, other factor needed to be considered regarding GNC. Specifically these factors would be controllers used, software used, and navigation sensors (magnetometer, GPS, and accelerometer). These items were not initially considered in the baseline design done in the Conceptual Design Document, however research was done on these items afterwards to determine how the system would actually be controlled in a more detailed level. The controllers used had to be compatible with the amount of sensors used, the type of sensors used, and the communication protocols of the hardware. The software was also another factor that was derived from the type of controllers used. The specific software type that was used would need to be compatible with the controller, so due to this, the specific type of software used was determined after the types of controllers were determined. Lastly, the navigation sensors that were going to be used had been determined, such as using GPS for positioning, or a magnetometer to determine the heading, so trades were not conducted on these items. The analysis done on these components was related to requirement satisfaction instead of options considered. The rest of these details relating to controllers, software, and navigation sensors is discussed in the detailed design section.

4.3.4. Environmental Sensing System

Author: Katelyn Griego
After performing the trade study in the previous section regarding in-plane object detection, it was found that a LiDAR sensor will be the most optimal system. FOV was rated heavily as it is important to be able to detect objects that would potentially be in the MR's path. LiDAR is capable of the necessary range and FOV requirements, and because of the high FOV, only one sensor will be needed. This will make the price range of this LiDAR reasonable. Furthermore, it was found that there is a large quantity of available software which is both easy to access and integrate with the LiDAR system. The RGB D camera ranked second here. This option was ultimately ruled out due to the complexity of the integration needed and the amount of data processing. An RGB D camera is a very sophisticated means of object detection and was ruled to be too complex for the needs of the system. A 360° LiDAR system will therefore be used here A trade study was then performed on sensors to perform discontinuity detection. Here, an accuracy criteria was weighted heavily as a discontinuity is solely 9 in and the sensor must be refined enough to detect this. Results again gave a single beam LiDAR as the best option. A single beam LiDAR has sufficient resolution to detect these relatively small discontinuities, meets the required range, and has documentation to integrate this sensor. The remaining three sensors were ranked in close proximity with one another. These sensors ultimately either did not meet the accuracy needed or were too complex. Therefore, two single beam LiDARs will be utilized to detect discontinuities in front of both front wheels of the CSR.

5. Requirements Development

Author: Chase Pellazar, Alexis Sotomayor

The flowdown requirements were derived from each subsystems shown in the CSR's FBD.This includes Mobility, Communication, C&DH, Sensing, and Power. The requirement ID indicates which subsystem the flowdown requirement belongs to. MOB stands for mobility, COMM for communication, CDH for C&DH, SENS for sensing, and POW for power.

5.1. Functional Requirement 1: CSR.1

CSR.1 : The CSR shall be able to receive commands from the MR or the GS		
Requirement ID	**Description**	**V&V**
COMM.1.1	The CSR Communication system shall receive command packets up to 250 meters in Mission Defined Terrain with no more than a 10 dB link margin *Motivation - Since the CSR will be operating over large distances from the GS, it should be able to receive all commands from the maximum distance a mission will travel*	Test - Communication Demonstration Analysis
CDH.1.1	The CSR C&DH software shall identify the intended receiving subsystem (i.e. Mobility, Sensing, Communication) for received commands *Motivation - Since the CSR system will have multiple subsystems it is necessary that the CD&H subsystem distributes commands to the intended subsystem*	Test - Communication Demonstration
CDH.1.2	The CSR C&DH software shall distribute commands to the intended receiving subsystem (i.e. Mobility, Sensing, Communication) *Motivation - In order for the commands received by the receiver to be issued to the rest of the system, the receiver must interface with the hardware that runs the command handling software*	Test - Communication Demonstration
CDH.1.3	The CSR C&DH system shall interface with the CSR Communication system receiver on a hardware and software level *Motivation - In order for the commands received by the receiver to be issued to the rest of the system, the receiver must interface with the hardware that runs the command handling software*	Test - Communication Demonstration

5.2. Functional Requirement 2: CSR.2

CSR.2 : The CSR shall be able to send image and positioning data to the GS		
Requirement ID	**Description**	**V&V**
COMM.2.1	The CSR Communication system shall send GPS data packets to the GS or the MR through mission defined terrain (See Terrain Definition) upon request from the user *Motivation - Depending on the COTS GPS component, the transmission frequency of the GPS data packets may vary between this range.*[14]	Test - Communication Demonstration

COMM.2.2	The CSR Communication system shall send video frames at a frequency of at least 30 Hz *Motivation - Depending on the capability of the receiver on the MR the CSR transmitter can only send a limited size of imaging data packets*	Test - Communication Demonstration
COMM.2.3	The CSR Communication system shall send video from up to 250 meters (820 ft) to the GS or the MR *Motivation - The CSR will be operating at a maximum distance of 250 meters (820 ft) from the GS, so the CSR should be able to send GPS data packets up to this maximum distance.*	Test - Communication Demonstration Analysis
COMM.2.4	The CSR Communication system shall send GPS data from up to 250 meters (820 ft) to the GS or the MR *Motivation - The CSR will be operating at a maximum distance of 250 meters (820 ft) from the GS, so the CSR should be able to send environmental position data packets up to this maximum distance.*	Test - Communication Demonstration Analysis
COMM.2.5	The CSR Communication system shall send sensor data from up to 250 meters (820 ft) to the GS or the MR *Motivation - The CSR will be operating at a maximum distance of 250 meters (820 ft) from the GS, so the CSR should be able to send imaging data packets up to this maximum distance.*	Test - Communication Demonstration Analysis
CDH.2.1	The CSR C&DH system software shall time stamp collected GPS, obstacle position, and imaging data *Motivation - Since the CSR will be collecting data over the duration of its mission it is necessary to organize the recorded data so that the mission can be understood*	Demonstration
CDH.2.2	The CSR C&DH system shall interface with the CSR Communication system transmitter on a hardware and software level *Motivation - In order for the data collected by the CSR to be transmitted to the GS the transmitter must interface with the hardware that runs the data handling software*	Demonstration

5.3. Functional Requirement 3: CSR.3

CSR.3 : The CSR shall be able to travel to a location of interest		
Requirement ID	**Description**	**V&V**
MOB.3.1	The CSR Mobility system shall be able to perform a 0 meter (0 ft) radius turn up to 360 ^{o} *Motivation - In order for the CSR to maneuver around obstacles it needs to turn, so if it can perform the maximum reorientation it can re-orientate to any degree*	Test - CSR Functional Demonstration Analysis
MOB.3.2	The CSR shall be able to go over discontinuities up to 9 inches *Motivation - While the MR can not go over 1 foot (0.30 m) discontinuities it is advantageous for the CSR to go over a discontinuity in the event that it encounters one while on mission*	Test - Discontinuity Operation Demonstration Analysis

MOB.3.3	The CSR shall drive up or down a slope of 20 ^{o} in type A forest and underbrush terrain (See Terrain Definition) from position hold *Motivation - Since the MR can drive up and down slopes of this degree, the CSR needs to have the capability too*	Test - Inclinations Demonstration Analysis
MOB.3.4	The CSR shall be able to drive in underbrush (See Terrain Definition) *Motivation - The CSR will be operating in forest environment and will encounter varying levels of this type of vegetation*	Test - Environmental Maneuverability
MOB.3.4.1	The CSR Mobility system shall be able to drive the CSR over a 2.4 inch (0.06096 m) step *Motivation - When the CSR must drive over roots of this size when driving through type D underbrush*	Test - Environmental Maneuverability Demonstration Analysis
SENS.3.1	The CSR Sensing system shall detect objects at least 37.5 inches (3.125 ft, 0.9525 m) from the Sensing system *Motivation - In order for the CSR to navigate itself through an unknown environment it needs a way to sense obstacles*	Test - Obstacle Detection Demonstration Analysis
SENS.3.1.1	The CSR Sensing system shall report objects within a field of view of at least 103.5^o of the CSR *Motivation - Available commercial of the shelf devices have a 2D field of view at a minimum of TBD^o*	Test - Obstacle Detection Demonstration Analysis
SENS.3.1.2	The CSR Sensing system shall detect objects at least 1 inch in width *Motivation - Available commercial of the shelf devices have a 2D range up to 4 meters*	Test - Obstacle Detection Demonstration Analysis
SENS.3.2	The CSR Sensing system shall detect discontinuities at least 2.4 inches deep *Motivation - The CSR must map the terrain grades its traversing so that a viable path for the MR can be determined, because the MR has a 20 ^{o} terrain limitation*	Test - Inclinations Demonstration Analysis
CDH.3.1	The CSR C&DH shall interface with the Mobility system's power train on a hardware and software level *Motivation - For the CSR to drive commands must be sent to the power train*	Demonstration
CDH.3.2	The CSR C&DH system software shall store the Location of Interests GPS coordinates in memory. *Motivation - The MR has a width limitation of 5 ft (1.524 meters)*	Test - Obstacle Detection Analysis Demonstration
CDH.3.3	The CSR C&DH system shall determine if the CSR is within +/- 5 meters of the location of interest *Motivation - In order for the CSR to remain on course with the Location of Interest the location must be stored in memory*	Demonstration

CDH.3.4	The CSR C&DH system shall determine the heading of the CSR within 1^o *Motivation - In order for the user to correct the heading of the CSR to be towards the LOI the CSR's current heading must be known*	Demonstration
POW.3.1	The CSR Power system shall provide at least 5400 mAh to the CSR *Motivation - To fulfill its mission the mobility battery must house enough current capacity to do so*	Inspection
POW.3.2	The CSR Power system shall provide at least .25 KW of instantaneous power to the CSR *Motivation - To fulfill its mission the mobility battery must provide enough power to traverse obstacles*	Inspection

5.4. Functional Requirement 4: CSR.4

CSR.4 : The CSR shall travel back to the last recorded waypoint upon loss of communications with the GS		
Requirement ID	**Description**	**V&V**
CDH.4.1	The CSR C&DH software shall store the last recorded pathpoint in memory *Motivation - pathpoints must be stored in memory to be used in the event of off-nominal communication*	Test - Off-Nominal Communication Navigation Demonstration
CDH.4.2	The CSR C&DH software shall detect loss of communications with the MR and the GS *Motivation - In order to react to a loss of comms the CSR must be monitoring communications*	Test - Off-Nominal Communication Navigation Demonstration
CDH.4.3	The CSR C&DH software shall establish a temporary Location of Interest at the last pathpoint *Motivation - To autonomously travel back to the last recorded pathpoint the CSR must know which direction to travel*	Test - Off-Nominal Communication Navigation Demonstration

5.5. Functional Requirement 5: CSR.5

CSR.5 : The CSR shall capture video while driving or in position-hold		
Requirement ID	**Description**	**V&V**
SENS.5.1	The CSR Sensing system shall capture video *Motivation - The sensing system must be capable of capturing video in order for the CSR to capture video*	Test - Camera Operation Demonstration

SENS.5.1.1	The CSR Sensing system shall take video at a rate of 30 fps (TBR) *Motivation - The quality of the video will is being based on INFERNO's frame rate.* [15]	Test - Camera Operation Inspection Demonstration
SENS.5.1.2	The CSR Sensing system shall take video with at least 0.2 Mpa Resolution *Motivation - The video quality is based on the minimum for standard definition.* [15]	Test - Camera Operation Inspection Demonstration
SENS.5.1.3	The CSR Sensing system video device shall have a field of view of at least 100^o *Motivation - Establishes the type of lens incorporated in the camera design*	Test - Camera Operation Inspection Demonstration

6. Detailed Design

6.1. Mobility System Detailed Design

Author: Michely Tenardi, Junzhe He, Alexis Sotomayor, and Colin Chen

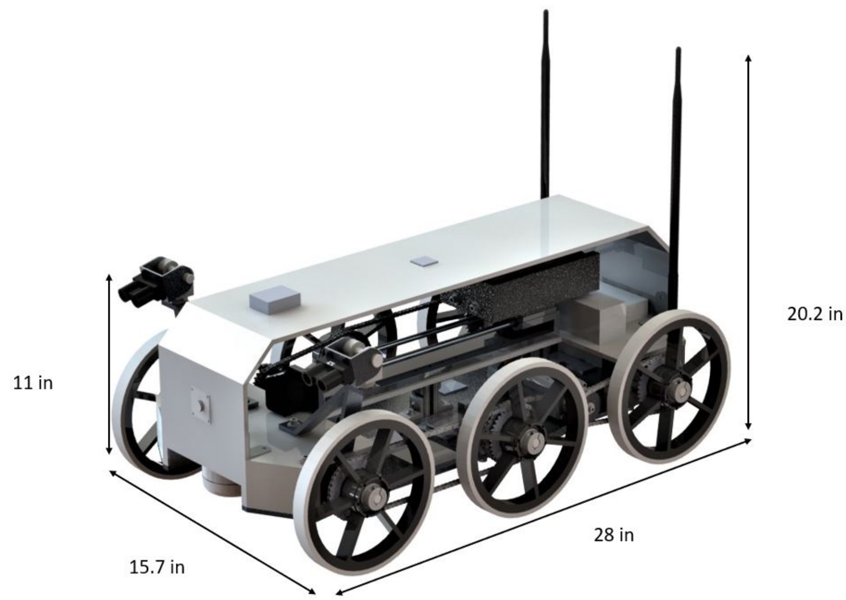

Figure 24: The CSR Final Design

As the CSR must be able to travel through forest fire prone areas to reach the given LOI, mobility system is considered as one of our critical project elements. There are five main specific requirements that drive our mobility system design. Those five requirements are:

- MOB.3.1: The CSR shall be able to perform a 0 meter (0 ft) radius turn up to 360^o.
- MOB.3.2: The CSR shall be able to go over discontinuities up to 9 in. (0.2286 m).
- MOB.3.3: The CSR shall drive up or down a slope of up to 20 in type A terrain (Type A Terrain is described as 0 trees per acre, grain size of 0.00006 - 0.0039 mm, dirt with no vegetation (scattered leaves, etc)).
- MOB.3.4.1: The CSR shall drive over a traversable obstacle up to 2.4 in. (0.06096 m) in height
- POW.3.1: The CSR Mobility power system shall provide at least 5400 mAh to the CSR

To satisfy all these requirements, models of the CSR when traversing all the required obstacles were developed in order to determine feasibility and to derive required specifications for components. Using these derived specifications, components that achieved all the required specifications were selected. This section discusses in detail the mobility subsystem's design, the analytical models developed, and the selected components and their specifications.

6.1.1. Powertrain Analysis and Selection

Overview

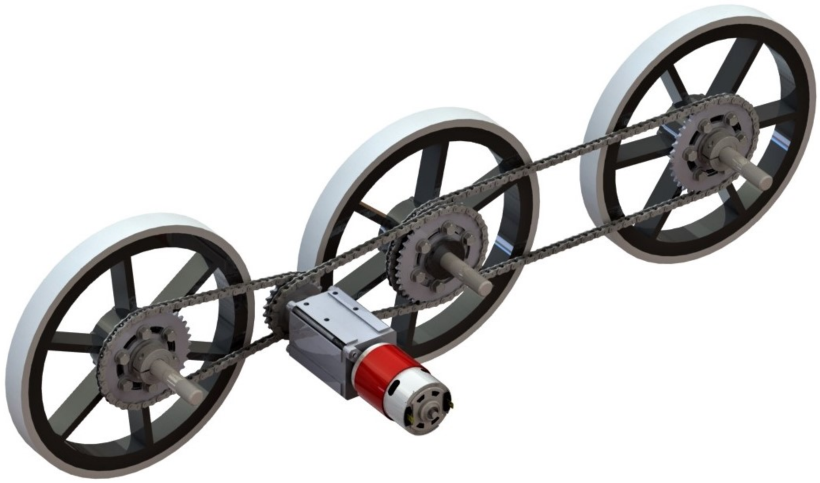

Figure 25: CSR Powertrain CAD Model

As discussed in the Conceptual Design section, the design selected for the mobility system was a six-wheeled, all-wheel drive system, where the wheels on each side of the motor are chained together, and driven by one motor, such that there are two motors in the entire system. A detailed model of the system is shown above in Figure 25. The drivetrain is powered by is an AndyMark 775 Redline Motor Brushed DC Motor. A brushed DC motor was chosen over other types of motors in order to reduce the control complexity and cost of the motors. This motor is mounted to a 64:1 Planetary Gearbox (AndyMark 57 Sport), which is press-fit into two 25-22 tooth, anodized 7075 aluminum sprockets. These gearbox sprockets are chained to the anodized 6061 25-38 tooth sprockets for the front and middle wheels. This combination of 38:22 sprocket reduction and 64:1 gearbox reduction results in a total gear reduction of approximately 110:1. A chain drive was chosen over a belt drive due to the slow rotational speed of the drive, its durability, and lower tension and positioning tolerances required. In order to drive the back wheel, a second sprocket is mounted to the middle wheel which drives the back wheel's sprocket through a chain. The sprockets are bolted to the wheels, which drives their motion. An exploded view of the front or back wheel's mechanical interface can be seen below.

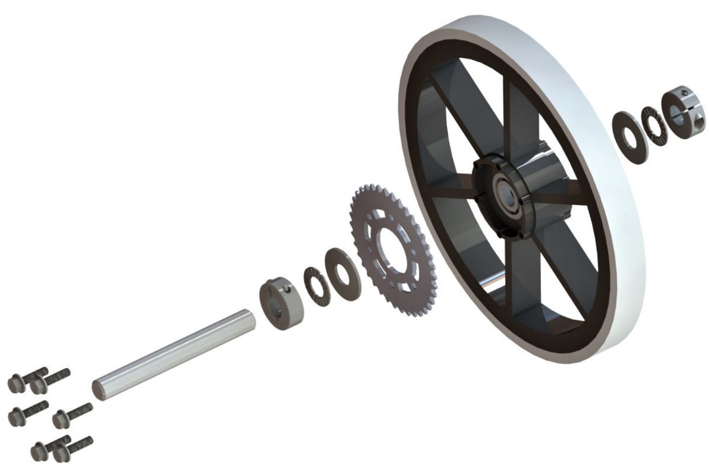

Figure 26: Mechanical Wheel Interface

As seen in the exploded view, the sprocket is directly mounted to the wheel. A 1/2" diameter shaft is placed in the wheel's bearings to support the wheel radially. However, if a radial load were to be applied to the wheel (skid steering, tilted driving, etc), the wheels would potentially fall off, or the non-axially rated bearings could be damaged. In order to mitigate these risks, a combination of washer, needle thrust bearings, and shaft collars fix the wheel to the axle and transfer the axial load to the shaft, rather than the radial ball bearings. Additionally, the thrust bearings allow for smooth wheel rotation with minimal frictional losses.

Torque Model - Slope (MOB.3.3)

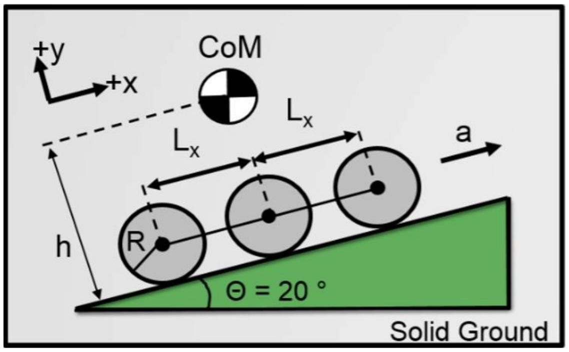

Figure 27: Conceptual Diagram of Slope Model

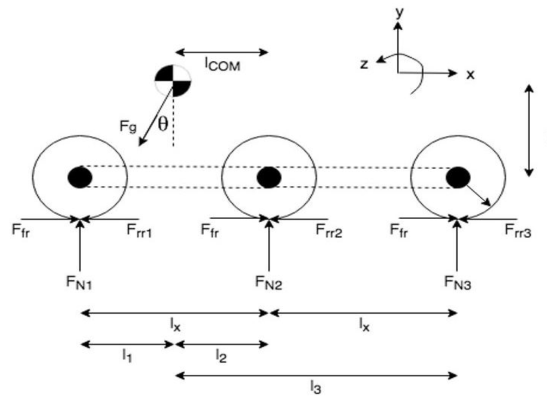

Figure 28: Free Body Diagram of Slope Model

<u>Assumptions</u>

- Coulombic Friction Model with Rolling Resistance - Assumes that the force of friction, which drives the CSR forward, is proportional to the normal force acting on the component experiencing the frictional force. This analysis starts by assuming a roll-no slip condition, and then checks whether the μ_s required is less than or greater than the expected coefficient of friction of rubber on gravel, $\mu_s = 0.7$ approximately. Additionally, assumes that frictional losses can be modelled as rolling resistance, which is proportional to the normal force, $F_{rr} = c_{rr}F_N$, where $c_{rr} = 0.02$ on gravel, approximately.[2]
- Wheels and Moving Mass are Point Masses - In order to approximate the mass distribution of the CSR along the chassis, the mass of the CSR is modeled as four point mass, one on the moving mass, and the other three on the wheels.
- Rigid Chassis - Assumes that there are insignificant energy losses due to deformation of the CSR.
- 2D problem (Side view) - Assumes the CSR travels straight up the slope.
- Negligible aerodynamic drag force.

<u>Baseline Dimensions</u>

- Axle to Axle Distance - $\ell_x = 10in$ $(0.254m)$
- Distance from CSR Center to Moving Mass - $\ell_m = 6in$ $(0.152m)$
- Static Coefficient of Friction - $\mu_s = 0.7$
- Coefficient of Rolling Resistance - $c_{rr} = 0.02$
- Mass of Moving Mass- $m_m = 11lbm$ $(5kg)$
- Mass of CSR Wheel - $m_w = 11lbm$ $(5kg)$
- CSR Center of Mass Height - $h = 6in$ $(0.152m)$
- Wheel Radius - $r = 4in$ $(0.101m)$
- Acceleration - $a = 0in/s^2$ $(0m/s^2)$
- Slope Angle - $\theta = 20^o$
- Gravitational Acceleration - $g = 386.4in/s^2$ $(9.81m/s^2)$

The following variables used in the derivation are defined as follows:

- Distance from Geometric Center to Center of Mass - $\ell_c = \frac{m_m \ell_m}{3m_w + m_m}$
- Distance from Back Wheel Axle to Center of Mass - $\ell_1 = \ell_x - \ell_c$
- Distance from Middle Wheel Axle to Center of Mass - $\ell_2 = \ell_c$
- Distance from Front Wheel Axle to Center of Mass - $\ell_3 = \ell_x + \ell_c$

Derivation

Begin with summation of forces and moments.

$$\sum F_x = ma = F_{f1} + F_{f2} + F_{f3} - F_{g,x} - (F_{r1} + F_{r2} + F_{r3}) \tag{1}$$

$$\sum F_y = 0 = F_{N1} + F_{N2} + F_{N3} - F_{g,y} \tag{2}$$

$$\sum M_z = 0 = h(F_{f1} + F_{f2} + F_{f3}) - h(F_{r1} + F_{r2} + F_{r3}) - F_{N1}\ell_1 + F_{N2}\ell_2 + F_{N3}\ell_3 \tag{3}$$

Note: the effects of the CSR mass distribution on the moment about the center of mass is zero, and therefore the mass terms are not included in the moment balance equation. The effect of the mass distribution on the system is that it determines the location of the center of mass.

Continue with a roll-no slip model. Later, check if the μ_s required is over 0.7. With roll no-slip, the friction/driving forces are all equal, due to the wheels being chained together.

$$F_f = F_{f1} = F_{f2} = F_{f3} \tag{4}$$

Applying this relation, the rolling resistance relationship to F_r, and the incorporating θ, a simplified summation of forces and moments is obtained:

$$\sum F_x = ma = 3F_f - \sin\theta - c_{rr}(F_{N1} + F_{N2} + F_{N3}) \tag{5}$$

$$\sum F_y = 0 = F_{N1} + F_{N2} + F_{N3} - mg\cos\theta \tag{6}$$

$$\sum M_z = 0 = 3hF_f - h(F_{r1} + F_{r2} + F_{r3}) + F_{N1}(-\ell_1 - c_{rr}h) + F_{N2}(\ell_2 - c_{rr}h) + F_{N3}(\ell_3 - c_{rr}h) \tag{7}$$

or

$$\begin{bmatrix} ma + mg\sin\theta \\ mg\cos\theta \\ 0 \end{bmatrix} = \begin{bmatrix} 3 & -c_{rr} & -c_{rr} & -c_{rr} \\ 0 & 1 & 1 & 1 \\ 3h & -\ell_1 - c_{rr}h & \ell_2 - c_{rr}h & \ell_3 - c_{rr}h \end{bmatrix} \begin{bmatrix} F_f \\ F_{N1} \\ F_{N2} \\ F_{N3} \end{bmatrix} \tag{8}$$

As seen, this system of equations is indeterminate. In order to check for feasibility/roll-no slip, set the front wheel's frictional and normal forces to zero, as a worst case check for the behavior in a tipping scenario, where the front wheel is lifted off the ground. Using $\mu_{eff} = F_f/F_N$, if $\mu_{eff1} < (\mu_s = 0.7)$ and $\mu_{eff2} < (\mu_s = 0.7)$ then the CSR can still drive even if the front wheel slips.

After verifying that the CSR can feasibly drive up the slope, the drive torque required per motor can be calculated using the friction force calculated. This is found by summing the torques on each wheel, and dividing it by two, as the model only considers 3 wheels, versus the 6 that actually exist.

$$\tau_{req} = \frac{1}{2}r(F_{f1} + F_{f2} + F_{f3}) = \frac{3}{2}rF_f \tag{9}$$

Results

Using the baseline dimensions above, the lifted front wheel results in $\mu_{eff} = 0.313$. This is significantly below $\mu_s = 0.7$. Therefore, the CSR can travel up the slope without slipping. The output torque required is therefore $\boxed{\tau_{req,slope} = 3.67[Nm] = 32.5[in \cdot lbf]}$. This model can also be used to calculate the nominal, flat driving torque, simply by changing θ to $\theta = 0^o$. This is found to be $\boxed{\tau_{req,flat} = 0.203[Nm] = 1.80[in \cdot lbf]}$.

Before using this value to select powertrain components, the analysis for the obstacle model must also be done. Whichever requires the greatest torques will drive the powertrain design.

Torque Model - Traversable Obstacle (MOB.3.4)
Before beginning the derivation for obstacle traversal, it is worth noting that as the CSR traverses over an obstacle, each wheel will drive over the bump. These stages are referred to in the derivation as Case A, B, and C, corresponding with the front, middle, and back wheels driving over the obstacle, respectively. The free-body diagrams for each case are shown below in Figures 29, 30, and 31. The model takes advantage of the fact that the maximum torque occurs when the wheel begins to drive over the obstacle. Additionally, for each case, one wheel will not make contact with the ground, visualized in the FBD's.

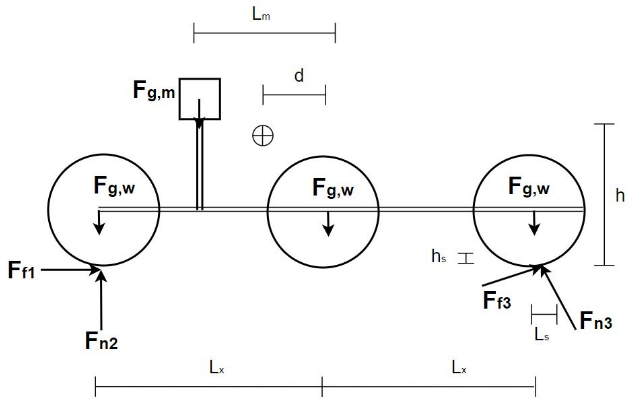

Figure 29: Obstacle Free Body Diagram - Case A

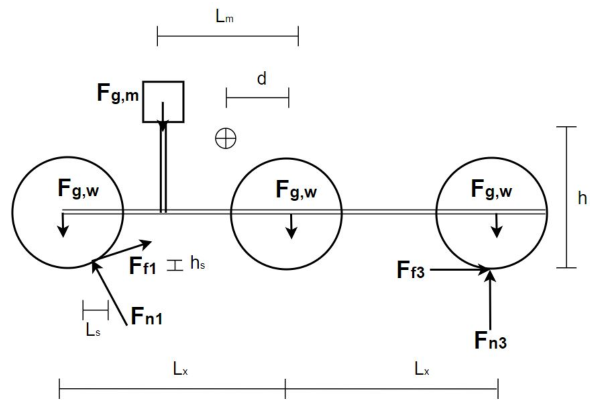

Figure 30: Obstacle Free Body Diagram - Case C

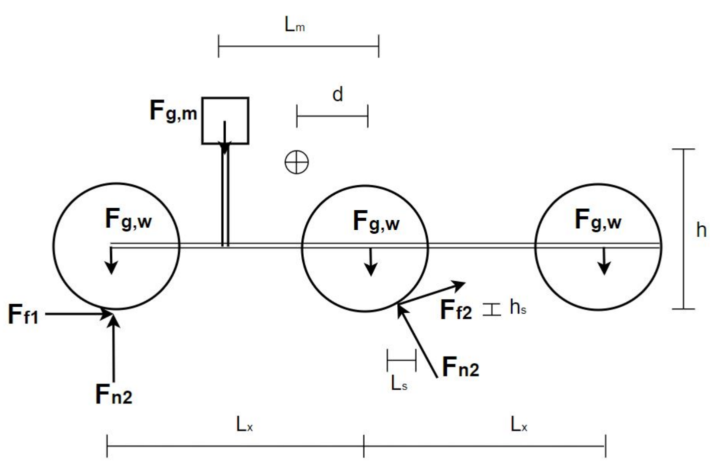

Figure 31: Obstacle Free Body Diagram - Case B

Assumptions

- Coulombic Friction Model - Assumes that the force of friction, which drives the CSR forward, is proportional to the normal force acting on the component experiencing the frictional force. This analysis starts by assuming a roll-no slip condition, and then checks whether the μ_s required is less than or greater than the expected coefficient of friction of rubber on wood[3], $\mu_s = 0.7$
- Steady State - Assumes there is no significant net acceleration.
- Negligible rolling resistance - Assumes that the rolling resistance between wood and a tire is negligible.
- Rigid Chassis - Assumes that there are insignificant energy losses due to deformation of the CSR.

- 2D Problem (Side view) - Assumes the left and right side of the CSR are the same.
- Negligible kinetic energy - Assumes that all of the work required to lift the CSR over the obstacle is from the wheels and motor, rather than due to existing momentum.
- Negligible aerodynamic drag force.

Baseline Dimensions

- Axle to Axle Distance - $\ell_x = 10in$ $(0.254m)$
- Distance from CSR Center to Moving Mass - $\ell_m = 6in$ $(0.152m)$
- Height of the Obstacle - ℓ_s
- Static Coefficient of Friction - $\mu_s = 0.7$
- Mass of Moving Mass- $m_m = 11lbm$ $(5kg)$
- Mass of CSR Wheel - $m_w = 11lbm$ $(5kg)$
- CSR Center of Mass Height - $h = 6in$ $(0.152m)$
- Wheel Radius - $r = 4in$ $(0.101m)$
- Gravitational Acceleration - $g = 386.4in/s^2$ $(9.81m/s^2)$

Note: The coefficient of friction and height of obstacle used in the analysis are driven by the derived requirement Mob.3.4.1, which required that CSR shall be able to traverse an obstacle up to 2.4 in height. The customer levied requirement for traversing obstacles such as roots and rocks, and allowed the project team to define maximum height that that CSR would be able to drive over. After looking at average root size and rock dimensions in a forest environment, 2.4 in came to be the benchmark for obstacles we wanted the ability to traverse. Using this terrain, the coefficient of friction was found to be approximately 0.7.

The following variables used in the derivation are defined as follows:

- Impact Incidence Angle - $\theta = \arccos \frac{r-h_s}{r}$
- Distance from Geometric Center to Center of Mass - $\ell_c = \frac{m_m \ell_m}{3m_w + m_m}$
- Distance from Back Wheel Axle to Center of Mass - $\ell_1 = \ell_x - \ell_c$
- Distance from Middle Wheel Axle to Center of Mass - $\ell_2 = \ell_c$
- Distance from Front Wheel Axle to Center of Mass - $\ell_3 = \ell_x + \ell_c$
- Distance between Obstacle Impact Point and Impact Wheel Axle - $\ell_s = r \sin\theta$

Derivation - Case A:

This case has the back wheel (wheel 1) on the ground, the middle wheel (wheel 2) elevated and not contacting the ground, and the front wheel (wheel 3) impacting the obstacle

$$\sum F_x = 0 = F_{f1} + F_{f3}\cos\theta - F_{N3}\sin\theta \tag{10}$$

$$\sum F_y = 0 = F_{f3}\sin\theta + F_{N1} + F_{N3}\cos\theta - mg \tag{11}$$

$$\sum M_z = 0 = F_{f1}r + F_{f3}\sin\theta\ell_s + F_{f3}\cos\theta(r - h_s) - F_{N1}\ell_1 - F_{N3}\sin\theta(h - R) + F_{N3}\cos\theta\ell_3 \tag{12}$$

Again, applying the roll-no slip assumption (to be back checked) to the chained system results in the following system of equations.

$$\sum F_x = 0 = F_f(1 + \cos\theta) - F_{N3}\sin\theta \tag{13}$$

$$\sum F_y = 0 = F_f\sin\theta + F_{N1} + F_{N3}\cos\theta - mg \tag{14}$$

$$\sum M_z = 0 = F_f[r + \sin\theta\ell_s + \cos\theta(r - h_s)] - F_{N1}\ell_1 + F_{N3}(-\sin\theta(h - R) + \cos\theta\ell_3) \tag{15}$$

This can be represented as the solvable 3x3 matrix:

$$\begin{bmatrix} 0\sin\theta \\ mg\cos\theta \\ 0 \end{bmatrix} = \begin{bmatrix} 1+\cos\theta & 0 & -\sin\theta \\ \sin\theta & 1 & \cos\theta \\ r + \ell_s\sin\theta + (r - h_s)\cos\theta & -\ell_1 & -(h-R)\sin\theta + \ell_3\cos\theta \end{bmatrix} \begin{bmatrix} F_f \\ F_{N1} \\ F_{N3} \end{bmatrix} \tag{16}$$

After solving for F_f and verifying the coefficient of friction is valid, the output torque required for one motor/reducer combination can be solved using Equation 9 from the slope analysis above.

Derivation - Case B:

This case has the back wheel (wheel 1) on the ground, the middle wheel (wheel 2) impacting the obstacle, and the front wheel (wheel 3) elevated and not contacting the ground. The derivation is nearly the same as that for Case A, except in the moment balance equation, ℓ_2 and F_{N2} are used and solved for instead of ℓ_3 and $_{N3}$. Thus, the system of equations in matrix form is shown below:

$$\begin{bmatrix} 0\sin\theta \\ mg\cos\theta \\ 0 \end{bmatrix} = \begin{bmatrix} 1+\cos\theta & 0 & -\sin\theta \\ \sin\theta & 1 & \cos\theta \\ r + \ell_s\sin\theta + (r - h_s)\cos\theta & -\ell_1 & -(h-R)\sin\theta + \ell_2\cos\theta \end{bmatrix} \begin{bmatrix} F_f \\ F_{N1} \\ F_{N2} \end{bmatrix} \tag{17}$$

Derivation - Case C:

This case has the back wheel (wheel 1) impacting the obstacle, the middle wheel (wheel 2) elevated and not contacting the ground, and the front wheel (wheel 3) on the ground. This derivation is quite similar to those of Case's A and B. However, the moment balance equation is slightly altered, due to the impact occurring behind the center of mass, rather than in front of it.

The altered moment balance equation is shown below:

$$\begin{aligned} \sum M_z = 0 &= F_{f1}\sin\theta\ell_s + F_{f1}\cos\theta(r - h_s) + F_{f3}r - F_{N1}\sin\theta(h - R) - F_{N1}\cos\theta\ell_1 + F_{N3}\ell_3 \\ &= F_f[r + \sin\theta\ell_s + \cos\theta(r - h_s)] - F_{N1}[\sin\theta(h - R) + \cos\theta\ell_1] + F_{N3}\ell_3 \end{aligned} \tag{18}$$

Using this new moment balance equation, Equation 18, the system matrix can be solved:

$$\begin{bmatrix} 0\sin\theta \\ mg\cos\theta \\ 0 \end{bmatrix} = \begin{bmatrix} 1+\cos\theta & 0 & -\sin\theta \\ \sin\theta & 1 & \cos\theta \\ r + \ell_s\sin\theta + (r - h_s)\cos\theta & -(h-R)\sin\theta - \ell_1\cos\theta & \ell_3 \end{bmatrix} \begin{bmatrix} F_f \\ F_{N1} \\ F_{N2} \end{bmatrix} \tag{19}$$

Results

Using the system of equations for Case's A, B, and C, and the baseline dimensions given above, the torques and required coefficients of frictions are shown in Table 38 below.

	Case A	Case B	Case C	Slope
Torque Required [Nm]	9.28	13.2	4.01	3.67
μ_{eff}	0.654	0.654	0.645	0.313

Table 38: Torque and Coefficient of Friction Requirements

It is can also be found that the minimum wheel radius that can be reached before slipping using the estimated $\mu_s = 0.7$ value is 3.7 in.

Component Specifications and Analytical Results

As seen in Table 39, Case B of the Traversable Obstacle Model drives the powertrain design and wheel selection. The powertrain design began with the motor.

The motor chosen must able to provide the required torque and speed to power the CSR over an obstacle at a peak speed of 1 m/s (3.28 ft/s). Note, the CSR is planned to nominally operate at 0.5 m/s; however a margin was implemented to allow for flexibility with operations. This linear velocity of 1 m/s translates to a wheel rotational velocity of 94 rpm. Due to the slow rotational velocity of wheel compared to the fast operating speeds of a DC motor, a motor that is smaller, less powerful, and cheaper than one that can directly provide 13.2 Nm of torque can be selected by gearing it down. Additionally, in order to avoid overheating the motor, a factor of safety of 4 is selected for the stall torque vs expected output torque. This large factor of safety is selected not only to account of the assumptions made in the calculations, but to ensure the motor does not regularly operate near the stall torque of the motor. Using these design requirements, the AndyMark 775 Redline Brushed DC Motor was selected. Implementing a gear ratio ($n = 84 : 1$) to achieve a factor of safety of 4, the wheel can rotate at a rate of 178 rpm, which provides a linear velocity of 1.89 m/s, comfortably achieving our required specifications and desired factor of safety.

Figure 32: AndyMark Redline 775 Motor - Photo Source: AndyMark Website

With the motor selected a gearbox and reduction system must be selected. As the gear ratio of $n = 84 : 1$ overshoots the desired wheel angular velocity, the reduction system can further gear down the motor. Using a 64:1 Planetary Gearbox (AndyMark 57 Sport) in tandem with the wheel:gearbox hub sprocket system pictured in Figure 25, a gear ratio of $n = 110 : 1$ is reached. This results in an output angular velocity of up to 145 rpm, or 1.54 m/s, at 13.2 Nm, comfortably reaching our required specifications.

Finally the obstacle analysis drives the wheel selection. As seen in the analysis above, the wheel must have a radius of 3.7 in to traverse over the obstacle without slipping. Therefore, a wheel with a radius of 4 in was selected. However, as this is fairly close to the 3.7 in required value, the wheel will be ordered once funding is received, and its coefficient of friction over wood will be tested. If the coefficient of friction measured is unsatisfactory, a few off-ramps can be taken. First, the tire can be modified to provide a greater coefficient of friction. If that does not work, a large wheel can be selected. With the current design, a wheel with a radius of up to 5 in can be used without major modifications.

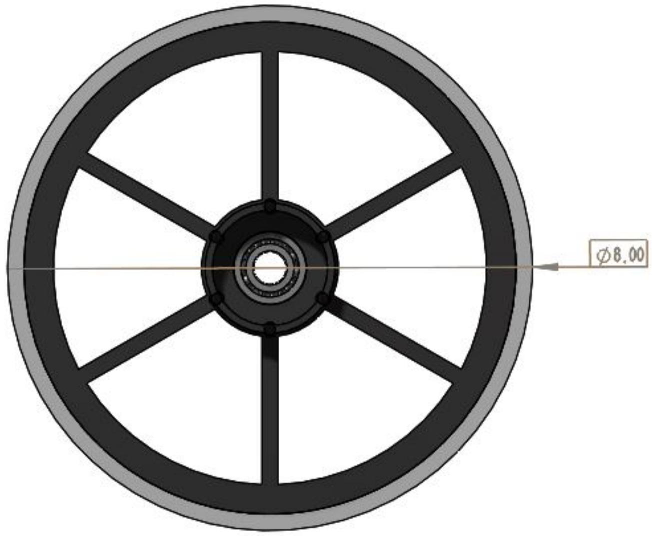

Figure 33: 4” Radius (8” OD) Rubber Treaded Wheel

Structural Analysis - Gearbox Sprocket (MOB.3.3, MOB.3.4)

A concern with the drive system is the shearing between the gearbox shaft and the sprockets which are coupled to it. Although the output torque of the system is 13.2 Nm, the drive shaft only feels a torque of 7.64 Nm, due to the gearing between the drive sprocket and the wheel sprockets. First, looking at the gearbox shaft, the manufacturer states that the entire gearbox assembly, of which the shaft is a part of, is rated for torques up to 217 Nm. This is over 28x our expected output on this shaft, thus the shaft is unlikely to shear. The other component that is in danger of shearing is the 7075 aluminum drive sprocket. A SolidWorks FEM analysis was performed. As there are two sprockets that share the torque load (one sprocket sends half of the torque to the back wheel, and the other sends the other half to the middle wheel), each sprocket only experiences 3.82 Nm of torque. This analysis fixed the teeth of the sprocket, and placed the torque of 3.82 Nm inside the hexagon face. The results of the FEM analysis are shown below.

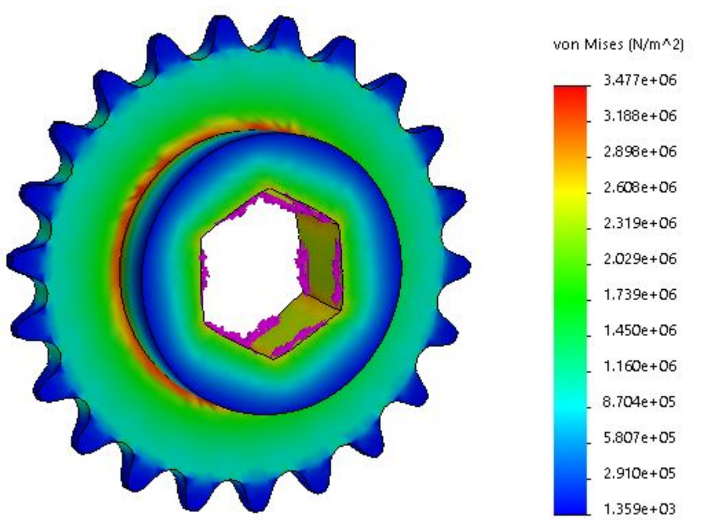

Figure 34: Gearbox Drive Sprocket FEM Analysis

It can be seen that according to the FEM model, the greatest load occurs inside the hexagonal face, and where the protrusion contacts the sprocket face. The latter stress concentration is likely due to the limitations of FEM with sharp corners. Looking at the hexagonal face, it appears the stress never exceeds $3.48 * 10^6 N/m^2$, while the yield strength of 7075 aluminum is $4.35 * 10^8 N/m^2$. This provides a factor of safety of 125. Although FEM has limitations, and the model assumes a perfect press-fit contact is being made between the shaft and the sprocket, the factor of safety is large enough to be confident with the design moving forward. If, however, these COTS components are found to be manufactured with poor tolerances, there are possibilities for mitigating this failure mode, such as utilizing set screws, pins, and shaft keys.

Structural Analysis - Drive Chain

In addition to calculating if the sprocket can handle the expected loads, the drive chain's must be capable of handling the forces travelling through them. The scenario that results in the greatest working load on the chain is when the CSR is overcoming an obstacle on its middle wheel. Here, the torque expected is 13.2 Nm, and it is divided two, as only the back and middle wheels are resisting the motor. The wheel sprockets have a pitch diameter of 3.03", or 0.077 m. This results in a working load of 85.7 N, or 19.3 lbf. The chains used are capable of providing 378, or 85 lbf. Therefore, the chain meets the required specification, which a factor of safety of 4.4.

Structural Analysis - Axial Load (MOB.3.1)

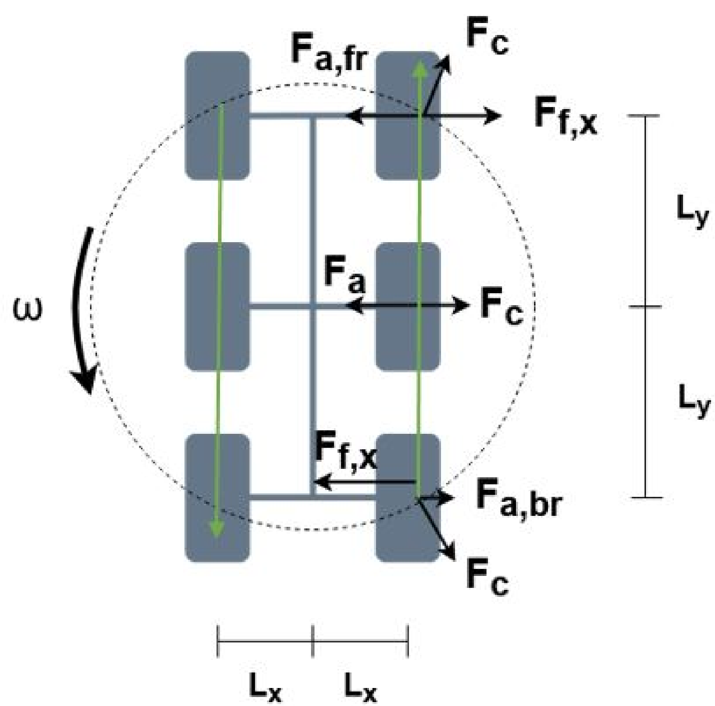

Figure 35: Axial Load from Skid Steer Free Body Diagram

Assumptions

- Coulombic Friction Model - Assumes that the force of friction, a significant component of the axial load, is proportional to the normal force acting on the wheels, as per the relationship $F_{fr} = \mu_k F_N$
- Skidding on gravel terrain, $\mu_k = 0.7$, approximately.[4]
- Geometrically Centered Center of Mass - Assumes the effect of the offset center of mass is insignificant on the axial load acting on the CSR wheels.
- Rigid Chassis - Assumes that there are insignificant energy losses due to deformation of the CSR.
- 2D Problem (Top view) - Assumes there is no rolling moment acting on the CSR, and that the normal forces acting on each wheel are the same.

Baseline Dimensions

- CSR Width (Center of Left Wheel to Center of Right Wheel) - $\ell_x = 5in$ $(0.127m)$
- Axle to Axle Distance - $\ell_y = 10in$ $(0.254m)$
- Kinetic Coefficient of Friction - $\mu_s = 0.7$
- Mass of CSR - $m_w = 11lbm$ $(5kg)$
- Angular Velocity of Skid Steer - $\omega = 1rad$

Note: The angular velocity used in this calculation is not a requirement. It is based on the linear velocity of the CSR; if the wheels spin at a rate to move each side at 0.5 m/s, the angular velocity is 0.89 rad/s. Thus, a value of 1 rad/s is used to overestimate the axial force experienced.
Derivation This analysis is performed by looking at the loads acting on each wheel. Due to the 2D assumption, only the summation of forces on each individual wheel, not moments, are required. Additionally, looking at the FBD, it can be seen that the front right (and back left) wheels will be feeling the greatest axial force, due to the summation of the centripetal and sliding friction force. Therefore, only the derivation for this wheel is shown:

$$\sum F_x = -F_{centripetal}\frac{\ell_y}{\sqrt{\ell_x^2+\ell_y^2}} = -F_a + F_f\frac{\ell_y}{\sqrt{\ell_x^2+\ell_y^2}} \tag{20}$$

$$\sum F_y = -F_{centripetal}\frac{\ell_x}{\sqrt{\ell_x^2+\ell_y^2}} = F_{wheel} + F_f\frac{\ell_y}{\sqrt{\ell_x^2+\ell_y^2}} \tag{21}$$

This simplifies down to:

$$F_a = \frac{m}{6\sqrt{\ell_x^2+\ell_y^2}}(\mu_k g\ell_y + \omega^2\ell_x\sqrt{l_x^2+\ell_y^2}) \tag{22}$$

Results
Using the baseline dimensions, the expected axial force is 20.9 N, or 4.7 lbm. While this load is not extremely large, it could potentially damage the wheel's radial ball bearings, especially with repeated loads. Additionally, without reinforcement, the bearings or shaft could be pulled out of their fittings In order to prevent this failure, aluminum 2024 shaft collars and needle thrust bearings are installed to the shafts, as seen above in Figure 35. The thrust bearings are rated to 8450 N, or 1900 lbf. The shaft collars' holding force is dependent on the shaft/hub tolerance, but can be expected to be around 500 N, or 112 lbf.[5]. This interface therefore has a factor of safety of over 23.

Structural Analysis - Wheel Shaft (MOB.3.2, MOB.3.4.1)
In order to ensure that the wheel shaft can handle the loads during the entire mission, forces analysis on the shaft were conducted. The shafts are supporting the chassis right in the middle while supporting brackets are fixed on one side and the wheels are attached on the other side. Since there are six wheel shafts in total, each shaft supports $\frac{1}{6}$ weight of the chassis in regular position. With 45,000 psi in yield strength, the chosen wheel shaft was proved to be able to handle the maximum shear stress during regular position which is 2,469 psi. As the bending moment has the capability of 26,595 lbf in, the shaft will also be able to handle the maximum bending moment in regular condition which is proved to be 397.2 lbf in. These calculations have already taken safety factor of 3 into account. This is due to neglecting the force in the X direction of the wheel and other forces, since it is a lot smaller compared to gravity force. Thus, bigger safety factor value was chosen.

The primary concerns are when the CSR goes over the 9 in. discontinuities (MOB.3.2) and drives over an obstacle up to 2.4 in. in height (MOB.3.4.1). There are possibilities of only four or even two wheels that are intact to the ground. Further calculations found that the maximum shear stress when each shaft supports $\frac{1}{4}$ weight of the chassis ($W_{chassis}$) is 3,704 psi and 7,407 psi when each shaft supports $\frac{1}{2}$ weight of the chassis. This is still significant less than 45,000 psi of shaft capability. For the maximum bending moment, the $\frac{1}{4}$ $W_{chassis}$ case has a maximum of 595.8 lbf in and the $\frac{1}{2}$ $W_{chassis}$ case has a maximum of 1,192 lbf in. These calculations also accounted for safety factor of 3. Thus, the chosen wheel shaft was proved capable to experience the maximum shear stress and maximum bending moment in any cases.

Wheel shafts are not experiencing torsion because the wheels are coupled to the shaft through bearings. The sprockets are fixed to the wheels, which are driving the wheels. Thus, no calculation was conducted for wheel shaft torsion. Only the gearbox shaft that is experiencing torsion. As the full gearbox assembly is rated three times of our expected load (40 Nm versus 12 Nm), the requirement is still satisfied.

6.1.2. *Linear Mass Stage Analysis and Selection*

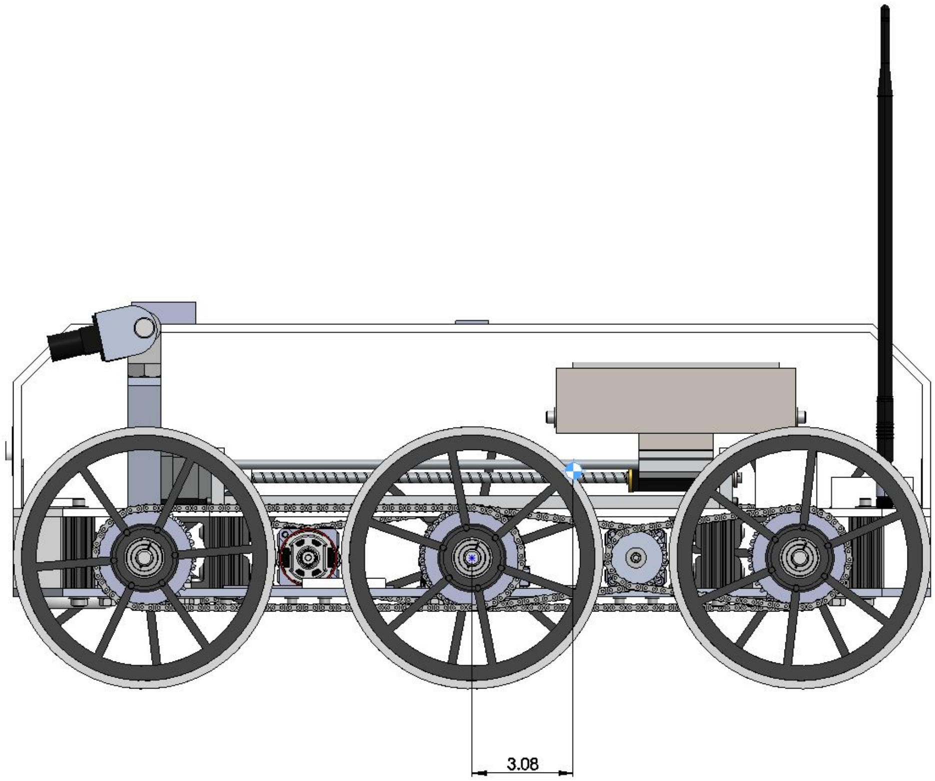

Figure 36: Effect of Linear Mass Stage on CSR Center of Mass

The linear mass stage is required to cross the 9” discontinuity, as defined by the requirement MOB.3.2. This linear mass stage design was driven by the desire to maintain a small rover design, rather that using wheels that are as big as those of the mother rover. The linear mass stage works in three main steps. First, the stage lies in the back of the CSR, putting the center of mass behind the center wheel, allowing the front wheel to be unsupported over the discontinuity without tipping. Next, the CSR drives until both the front and back wheels are supported, and the middle wheel is over the discontinuity. Here, the moving mass stage is moved the the front of the CSR, such that the CSR doesn’t tip when the back wheel is over the gap. Once the back wheel crosses the gap and the CSR is fully supported, the mass stage returns to the back of the CSR. This is visualized in Figure 37 below. A more in-depth description of the discontinuity traversal procedure is detailed in the Guidance, Navigation, and Control Detail Design section, on Figure 66.

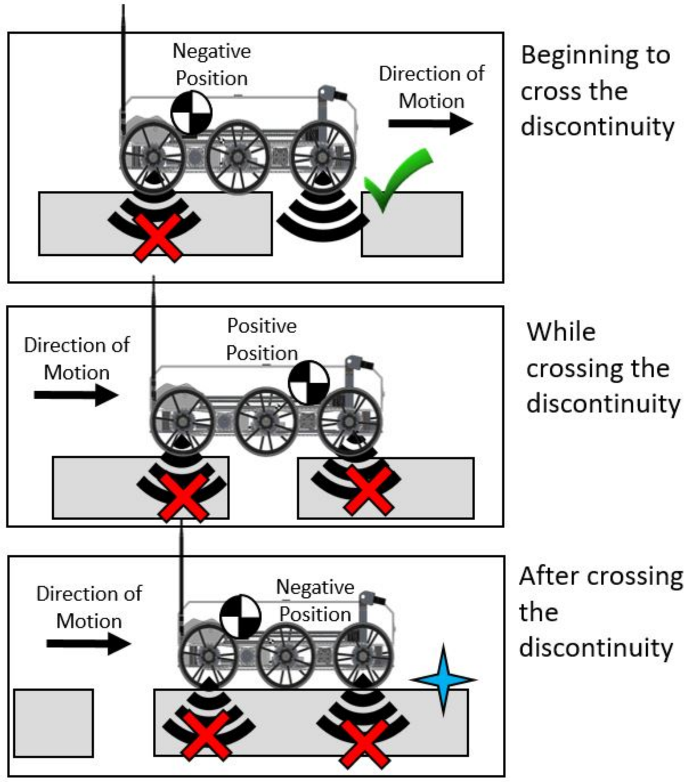

Figure 37: Conceptual Diagram of the Discontinuity Traversal

The motor torque required to cross the discontinuity is the same as that of flat ground. This is due to the chained design of the drive train; when one wheel is not experiencing a reaction friction force from the ground, it does not react to the drive shaft, outside of the inertia of the wheel and internal friction. Therefore, the torque output from the drive shaft is distributed to the remaining wheels, and the net output force and torque remain the same.

6.1.3. Power Analysis and Selection

A key driver in the selection of the battery for the mobility system is the battery's ability to provide instantaneous power, and the battery's ability to provide that power multiple times (for short periods) throughout the duration of a mission. Although JPL did not provide specific power requirements in the Statement of Work, the team was able to derive a power capacity needed for a mission from the 250 m distance requirement. A difficult mission terrain with ample obstacles and slopes was then developed to provide us with a baseline for the expected power consumption of the mobility system. The power spike analysis primarily stemmed from requirements MOB 3.3 and MOB 3.4.1. The expected power consumption is derived from the expected torques on gravel, as well as the wheel design and mission speed. The equation for this power consumption is shown below[33]. Total current can then be extrapolated from calculated power consumption using the relation between voltage, current, and power; these currents are later coupled with a a mission scenario to determine the energy capacity required for a mission.

$$Power[W] = \left(\frac{TotalTorque[Nm] \cdot Speed[Rpm]}{9.549}\right) \tag{23}$$

MOB 3.3 is the requirement stating the CSR shall be able to drive up or down an inclined slope of 20^o (without obstacles or trees, per JPL). To determine required power for this maneuver, the total torque at a speed of 1 m/s travelling up an inclined slope of 20 ° on light gravel was used. Although the CSR is expected to only travel at 0.5 m/s, the calculations were done at 1 m/s to add a level of safety margin in the calculations. As the combined gear ratio of the sprocket/gearbox reducing system, is approximately $n = 110 : 1$, the output torque and RPM of the wheel must be scaled as such. This brings the required motor torque output down to $\tau_{motor} = 33.4$ mNm and the desired RPM to $\omega = 10300$ RPM. Using the motor data sheet below, the current draw of the motor at max speed of for τ_{motor} is found to be approximately 11 A/motor. However, as this max speed corresponds to a linear velocity of 1.96 m/s, this value can be scaled down to 5.6 A/motor for the 1 m/s velocity of the CSR. This results in an effective power draw of 67 W for a slope maneuver.

MOB 3.4.1 is the requirement the CSR must drive over obstacles up to 2.4 in. This requirement lends to the largest power spikes. Using the model discussed in the powertrain section above, an output torque of for each drive shaft is 13.2 Nm. Using the motor torque curve provided by the manufacturer and the analysis above, the expected and scaled motor current draw at 13.2 Nm and 1 m/s is 11.43 A/motor, or a power draw of 137 W/motor. It is again worth noting that the actual power draw of the motor is expected to be approximately half of the calculated values used for component specifications.

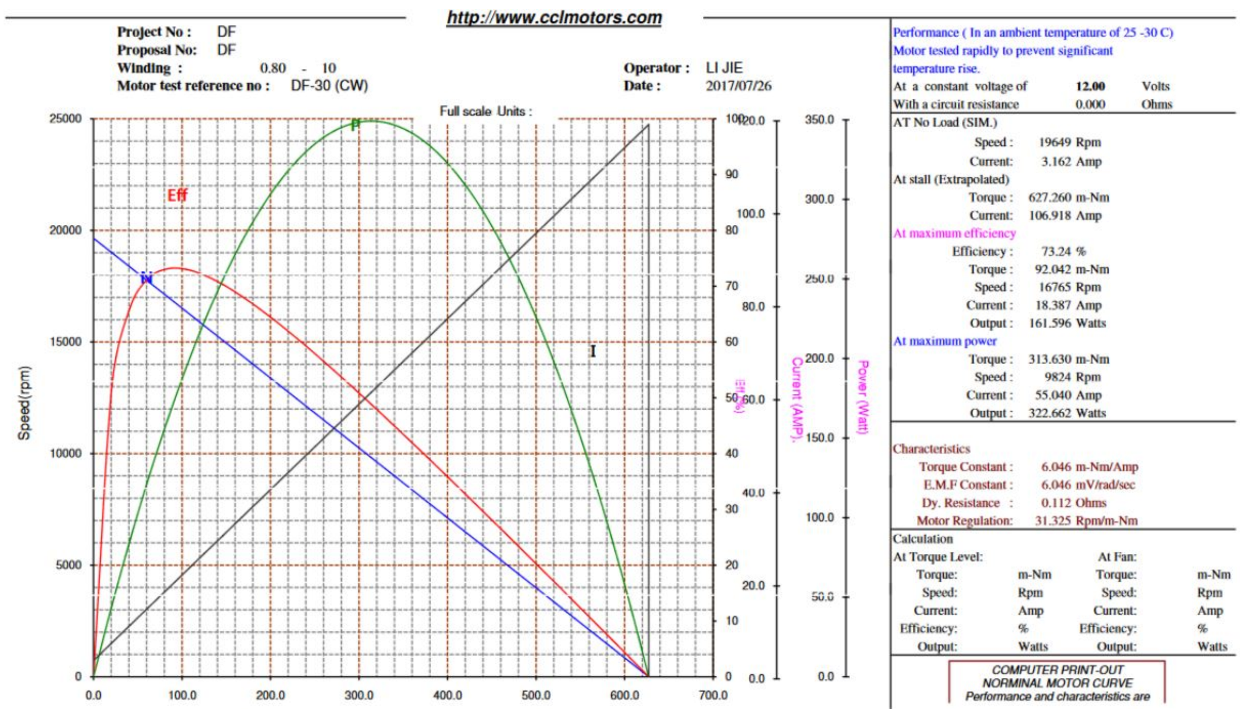

Figure 38: AndyMark 775 Redline Motor Torque Datasheet - Torque in mNm

The next step in formulating the derived power requirements was to create the simulated mission. For a mission distance of 250 meters from the MR, at an average speed of 0.5 m/s and top speed of 1 m/s,we accounted for losses in mission time for crossing discontinuities and turning around trees. Moreover, dynamical analysis indicated that the CSR would take around 4.66 secs for the CSR to traverse a 2.4 in obstacle, of which we assumed 30 of these large obstacles for the mission. We do not expect to see heavy slopes on our terrain, but we accounted for 6 total minutes of inclined slope travel at 20 °. The total mission time came out to approximately 40 minutes, with another 20 minutes added on as a safety factor to place the mission estimate at 1 hour.

The graph below displays the projected current consumption for the hour long mission, with different levels of power spikes for incline slope traversal and obstacle traversal. A key assumption in this analysis is that this is a piecewise function, with immediate spikes in current consumption. This assumption can be made because the current will change over such a short time that we can assume the spike in power occurs almost instantly. Integrating this piecewise function delivers the total current capacity required for the mission.

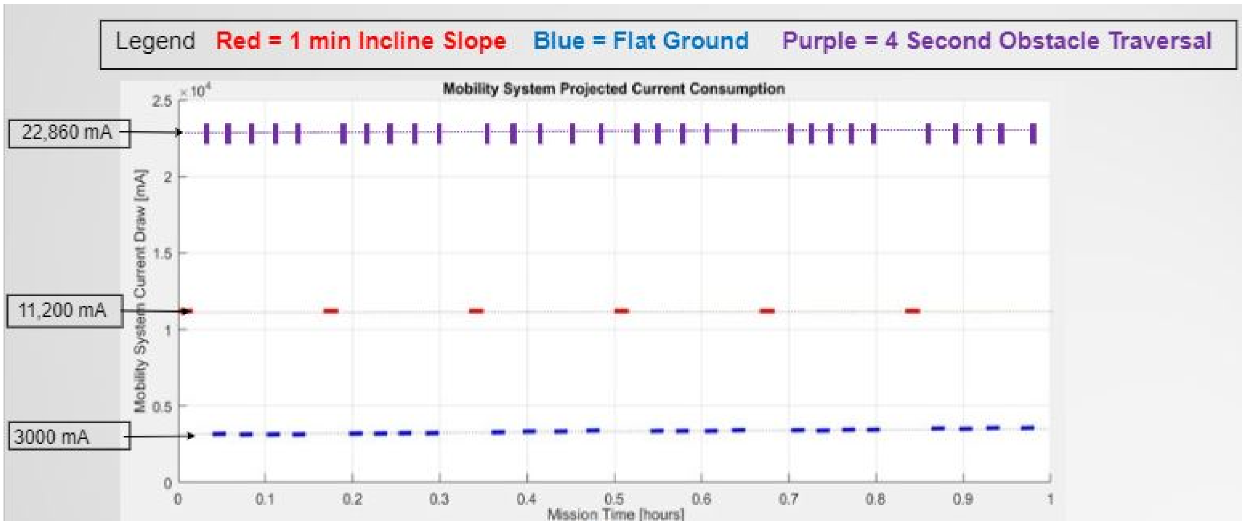

Figure 39: CSR Simulated Mission - Projected Current Consumption

Integrating the graph is simply a multiplication of the current consumption by the total time of that consumption, and provides a required capacity for each maneuver; this is noted in the third row of the table above. Accounting for a 20 percent inefficiency in the conversion from electrical to mechanical power, the total required battery capacity for one mission is 5400 mAh.

Obstacle	Flat Ground	Inclined Slopes	Obstacles (2.4 [in])
Current Draw	3000 mA	11200 mA	22,860 mA
Total Time	52 min (.87 h)	6 min (.1 h)	2 min (.03 h)
Required Capacity	2600 mAh	1120 mAh	762 mAh

Figure 40: Projected Current Consumption Calculations

The battery selected has a capacity of 7500 mAh, as well as the ability to provide 11.4 kW of instant power if needed. The highest power that the CSR would need is for obstacles, in which case the CSR would need about 0.275 KW; this provides a very large margin for instantaneous power.

The battery selection provides us with a 28 percent margin on a very difficult mission, therefore our derived power requirement POW 3.1 can be satisfied. This battery selection for the mobility system is the Gens Ace 4S LiHV 100C LiPo Battery Pack, operating at 15.2 Volts with a minimum capacity of 7500 mAh.

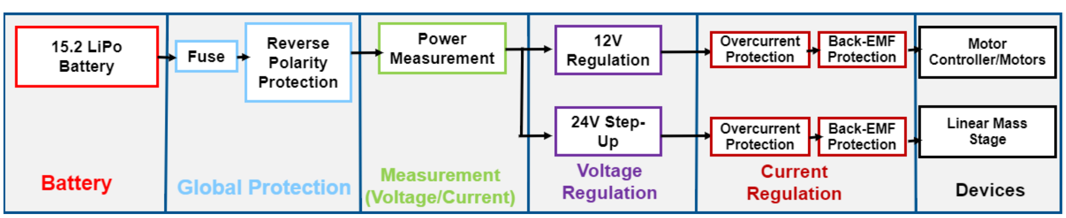

Figure 41: Power Distribution Block Diagram (Mobility)

6.1.4. *Chassis Material Analysis and Selection*

The goal for the chassis design is to make the CSR to be lightweight and low-cost, while still being capable of supporting itself and the CSR's components. The base plate will be manufactured from 1/4 in. 6061 aluminum, and the upper two levels will be acrylic plates. The middle acrylic plate is supported and mounted to the aluminum base plate using 80/20 struts. The base plate is made from 6061 aluminum as it provides the strength required to support the entirety of the CSR. Additionally, it is relatively lightweight, easy to use for manufacturing (in terms of formability, weldability, machining, etc). It has high corrosion and heat resistant, which is compatible for the CSR as it will travel in the forest fire prone areas and has a lot of electronic components on it. To ensure the base plate provides the structural support necessary, an FEM analysis on the base plate was performed.

The FEM analysis was set up by setting the wheel shaft mount's mounting holes as fixed. The weight of the base plate itself was incorporated using the gravity function. Next, the weight of the 80/20 struts and all of the upper two housings and its components were placed on the 80/20's mounting holes, which is 112 N. This was rounded up for the FEM to 120 N. Next, the weight of the gearbox/motor assembly was applied to their respective mounting holes, which is approximately 10 N per assembly. Finally, the remaining components that lie on the bottom housing, such as small batteries and electronics are rounded up to 10 N, distributed evenly across the board. The results of this SolidWorks simulation are shown below in Figure 42. It can be seen that the peak stresses occur in this model at one set of the fixed mounting holes, at $5.5 * 10^6 N^2$. Taking this for face value, the baseplate therefore has a factor of safety of 10, as its yield stress is $5.5 * 10^7 N/m^2$. However, the SolidWorks simulation is liking overestimating the true stress at this point, as the load will not be truly concentrated on the mounting holes, but spread out across the mounting plate surfaces (brackets, 80/20, shaft mount). Therefore, the actual load is expected to be much less than this. Accounting for the overestimation due to the stress concentration about the mounting holes, the factor of safety of 10 provides confidence than the aluminum base plate can handle the expected loads.

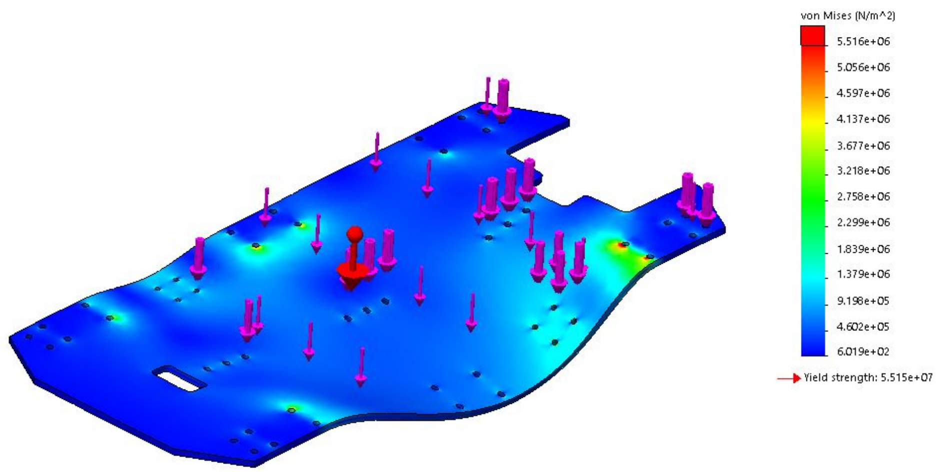

Figure 42: Aluminum Base Plate FEM Model

Acrylic is used to manufacture the top two levels as it is straightforward to machine using a laser cutter and is able to provide a solid frame for the CSR. Additionally, acrylic is 2.3 times lighter than aluminum. While ac is not as strong as aluminum, it is still capable of supporting the loads it will experience, as seen by the FEM analysis below. The middle, acrylic, chassis plate SolidWorks Stress Simulation is shown in Figure 43. The model uses its 80/20 mounting holes as its fixed geometry. Like the base plate model, the component loads were applied to the model. First, the weight of the plate itself was applied, which is approximately 9 N. Then, the loads from the moving mass stage, the batteries, the single-beam LiDARs, and the top acrylic housing were applied, which have a collective weight of 90 N. This load was applied uniformly across the surface. As seen in the result, the peak stresses occur near the fixed holes. Like with the base plate model, these stress concentrations will not occur on the actual model, as they will be spread out with the mounting hardware. Even with these concentrated stresses, the peak stress experienced is $1.6 * 10^6 N/m^2$, whereas the yield stress is $4.5 * 10^7 N/m^2$. This results in a factor of safety of 28, even with the concentrated stresses. Therefore, this platform will be able to support the loads it will experience.

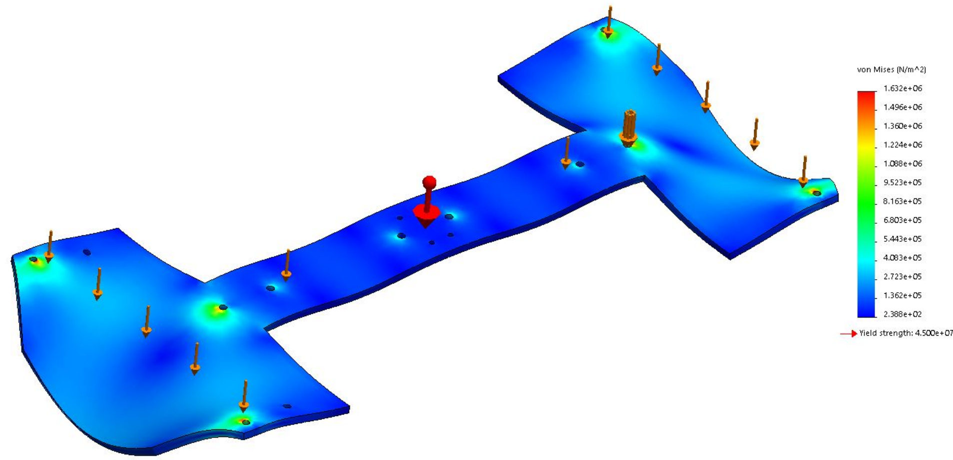

Figure 43: Middle Acrylic Plate FEM Model

Finally, the top housing was modelled; the main concern with the top acrylic housing is its bending in the middle, as only the ends of the 2 ft long plate are supported. Additionally, this housing has a magnetometer/accelerometer on top of it, therefore significant deformation of the housing is undesirable. Therefore, the strain model is included in addition to the stress model. This model has the side walls fixed, and the loads applied are its own weight, and the weights of the GPS antenna and the magnetometer chip. This results in the stress result in Figure 44 and the strain result in Figure 45. As seen, the peak stress is $3.5 * 10^5 N/m^2$. This results in a factor of safety of 128. Additionally, the deformation across the middle is only 0.5 mm. Despite these reassuring values, the true behavior of the system when manufactured will be tested, and if the deformation is too large, a supporting strut will be incorporated across the top housing.

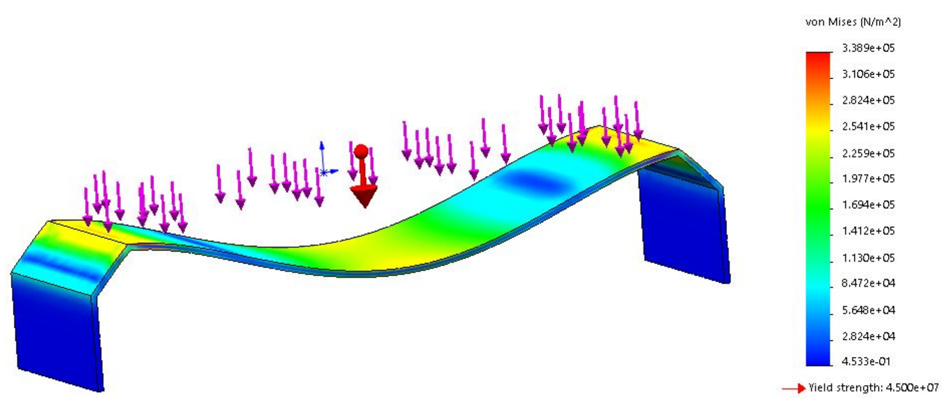

Figure 44: Top Acrylic Plate FEM Model - Stress

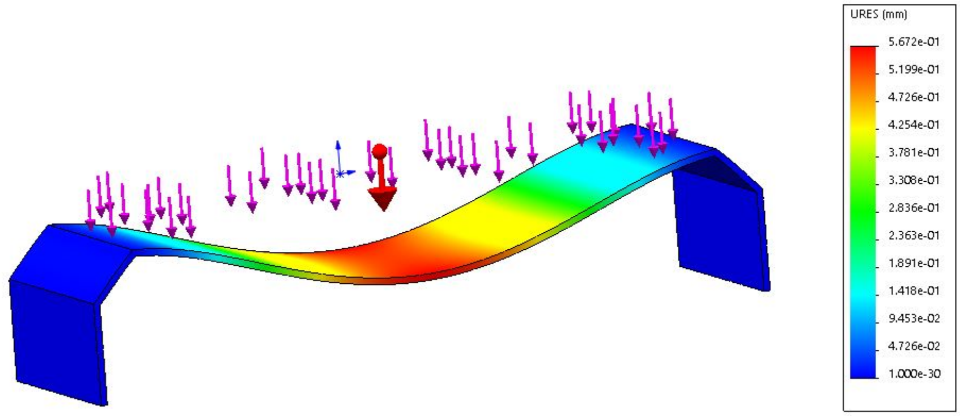

Figure 45: Top Acrylic Plate FEM Model - Strain

6.1.5. Mobility Control

Author: Alexander Sandoval

The main pieces of hardware that are needed to be able to control the motors and the linear mass stage is the motor controller and the stepper motor driver. This allows simplicity for issuing commands for both the motors and the linear mass stage. The benefit in using this motor controller is because of the driver software available which can allow simple commands to be issued such as speed, direction, start, and stop. The benefit in using the stepper motor driver is again for simplicity of issuing commands due to the available driver software. Commands can be issued to initiate a certain number of steps which allows the distance to be controlled of the mass stage. We also will be attaching encoders to the motors to make sure the speed will stay constant for both wheels to ensure a straight traversal path. This hardware is shown in Figure 46.

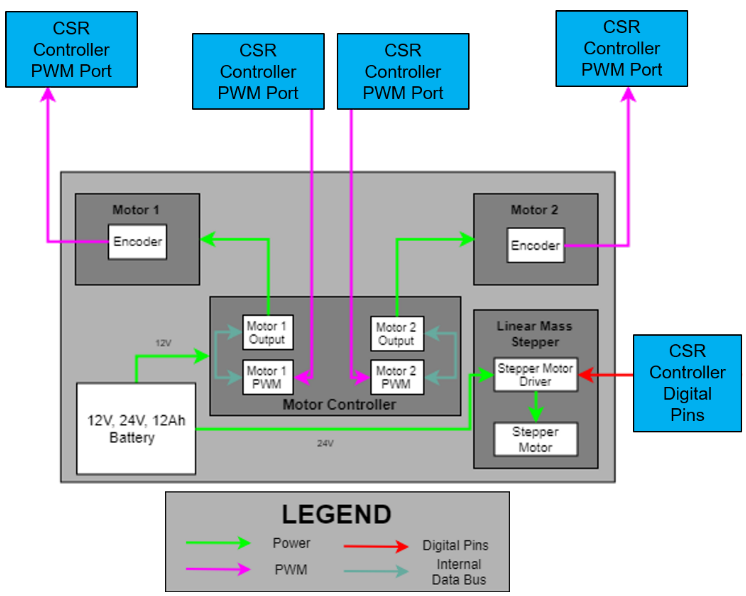

Figure 46: The hardware interface diagram for mobility control.

6.2. Communications Detailed Design

Author: Alexander Sandoval and Brindan Adhikari

For the CSR to carry out the main purpose of the mission of sending back a viable path for the MR, a working communication system needs to be established. Given the terrain of the mission, this task becomes more difficult as this requires HERMES to not only establish communication up to 250m (820 ft) but do so through potential obstructions such as trees, brushes, and hills. To be able to fulfill this level of communication there are three specific requirements that shall be met which are:

- CSR.1: The CSR shall be able to receive commands from the MR or the GS.
- CSR.2: The CSR shall send video and GPS coordinates to the GS or the MR through mission defined terrain.
- CSR.4 : The CSR shall travel back to the last recorded waypoint upon loss of communications with the GS.

To meet these requirements, three driving sections are presented which lead to the conclusion of requirement satisfaction. The sections that will be included will describe the hardware integration and setup, the link budget analysis, and the data budget analysis. The hardware integration and setup will explain how the communications hardware will be integrated across all systems and how the system will communicate. The link budget analysis will explain the calculations needed to meet a 10-dB link margin. The data budget analysis will explain how the data being sent and received meets the data bandwidth available from the radios.

6.2.1. Hardware Integration and Setup

6.2.1.1 Hardware Integration

Creating the PtMP Wi-Fi approach must include the same long-range link radios for the GS, CSR, and MR systems. This is because the radios can only talk to one another and no other hardware. Thus, this creates a universal setup among the GS, CSR, and MR with only small individual additions to carry specific purposes for the individual needs of these systems. This universal setup includes a battery, a POE injector, a long-range radio, and antenna. This long-range radio is a high data bandwidth radio which communicates over a 900 MHz frequency. This radio allows for an easy setup and creation of a communication link to other radios. The POE injector essentially is a DC-DC step up converter that takes in a 12 V battery and data input from the controller and steps up the voltage to 24 V to supply both power and data to the radio. Since this radio supports multiple-input multiple-output (MIMO) functionality which improves link quality and reliability, the need for two antennas is necessary[26]. A summary of characteristics for this universal setup is shown in Table 39.

	Frequency (MHz)	Gain (dBi)	Horizontal Beamwidth (Degrees)	Vertical Beamwidth (Degrees)	Interface
Omni-Directional Antenna	900	5	360	25	RP-SMA Female
	Data Bandwidth (Mbps)	Transmission Power (dBm)	Receiver Sensitivity (dBm)	Interface	
Ubiquiti Radio Rocket M900 (Radio)	10 Mbps	28	-96	Ethernet	
	Voltage Input (V)	Voltage Output (V)	Interface		
TP-DCDC-1224 (POE Injector)	12	24	Ethernet/DC Barrel Jack		
	Voltage (V)	Amp-Hour (Ah)	Interface		
Battery	12	3	DC Barrel Jack		

Table 39: Universal communication setup hardware characteristics.

For the CSR's communication system, there is only the need for the universal setup. This is shown in Figure 47. For the GS communication system, there is the need to integrate a GPS base station along with the universal setup. This is because the GPS implementation, which will be discussed further, demands the GS to continuously send correction bytes to the CSR. This setup is shown in Figure 48. For the MR communication system, there is the need to integrate the universal setup into last years controller. This is as simple as connecting an ethernet shield to the existing Arduino to be able to send commands through the radios. This setup is shown in Figure 49. Also shown is the power distribution that will be needed to ensure the radio receives the optimal amount. This is shown in Figure 50.

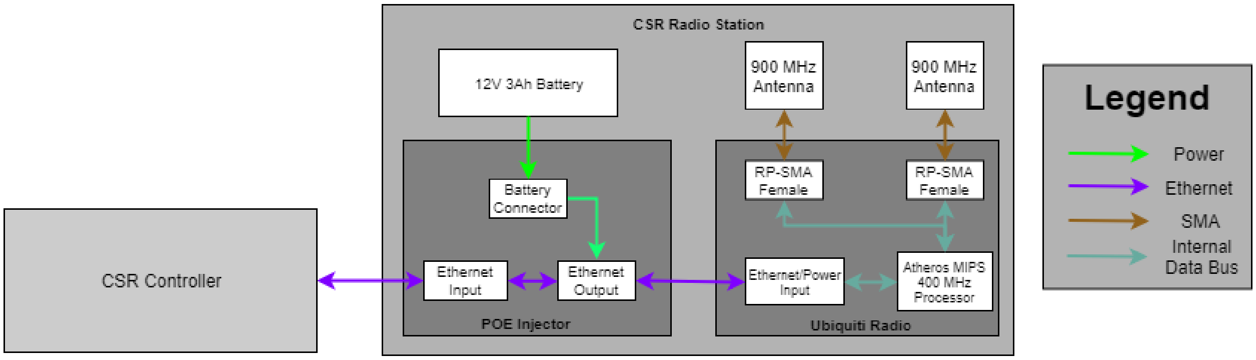

Figure 47: CSR communication hardware interface diagram.

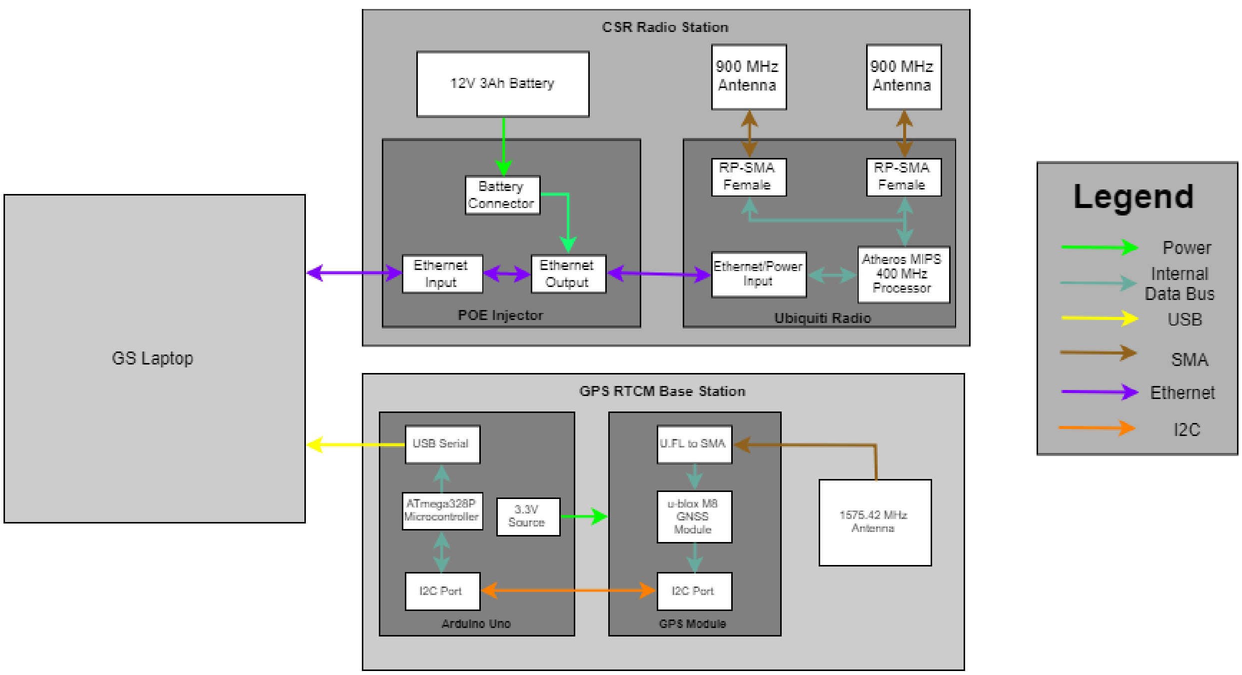

Figure 48: GS communication hardware interface diagram.

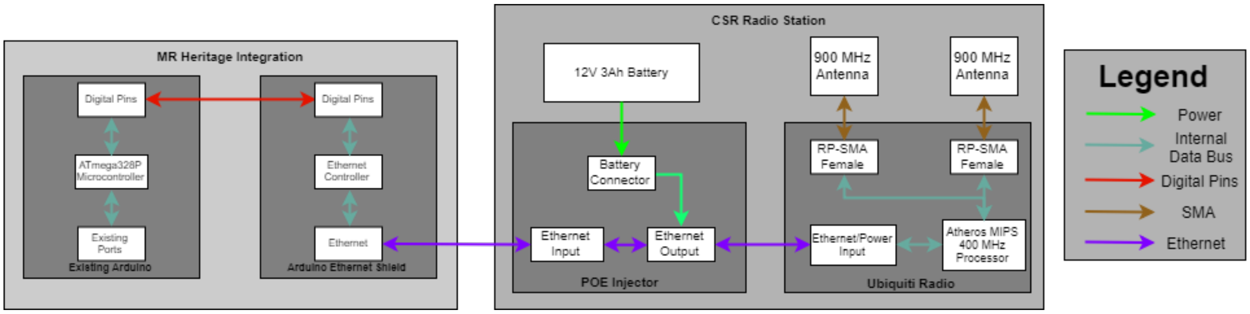

Figure 49: MR communication hardware interface diagram.

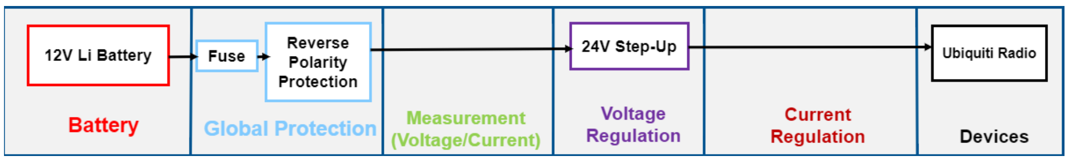

Figure 50: Power distribution block diagram (communications).

The power budget and battery selection for the communications was done the same way as the CD&H and Sensing subsystem, assuming continuous operation for a one hour mission. The energy capacity required for the communications subsystem for a one hour mission is 1.65 Ah. The selected battery is the TalentCell Rechargeable 12V 3000mAh Lithium Ion Battery Pack, which provides 3 Ah of battery capacity. This makes for a 45 percent margin on the endurance mission.

6.2.1.2 Setup

The way these long-range radios communicate is over Transmission Control Protocol (TCP) which is more commonly abbreviated as TCP/IP. This protocol essentially has the transmitter wrap a data package and address it to a receiver in which the receiver then unwraps the data package. To be able to properly address each transmitter and receiver, the need for assigning static IP addresses among our devices is critical for assuring the right data packages are sent to the correct places. While TCP/IP handles how to wirelessly transfer data packages, Wi-Fi handles how the data packages are being created, sent, and received. This capability is already built into the controller, the laptop, and shield being used which handles this complexity for this mission. Thus, the group of devices and radios create a LAN which is shown in Figure 51.

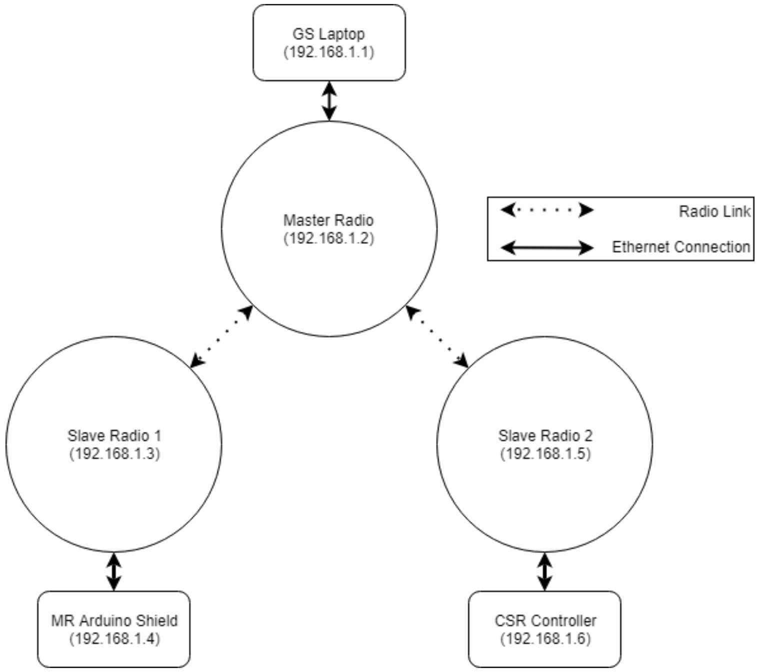

Figure 51: The communications setup between all our systems that creates a Local Area Network.

6.2.2. *Link Budget Analysis*

After choosing the best communication system available, it was vital to establish a link budget to ensure that communication can take place at a distance of 250 m between the GS/MR and the CSR. While establishing a link budget, eight factors were considered: power transmission of the radio, antenna gain of the GS radio, antenna gain of the CSR radio, cable loss within the CSR, cable loss within the GS, free-space path loss, receiver sensitivity, and loss due to trees. The first six factors were extracted from the manufacturer's specification sheet of the selected products. In order to calculate the free-space path loss, Equation 24 was used.

$$FSPL = 10log_{10}d + 20log_{10}f - 147.55 \tag{24}$$

- d = distance of communication [m]
- f = frequency [Hz]

First, the link margin was calculated at a distance of 250 meters without accounting for obstacles. This is shown in Figure 55a. Then, the next step was to account for the trees. Instead of getting involved into the option of calculating the loss due to trees using numerous unfamiliar equations and factors, it was a safer option to select an experimental model to avoid miscalculation. We chose to conduct our calculations using a experimental research paper written by Radio Science, a scientific journal[27]. In this study, the characteristics of the vegetation were accounted for as an experimental average in a forest terrain. This is one of the flaws in this model as it does not give a definitive size of the trees over which communication is taking place. However, due to the fact that this model is based off average tree characteristics (height, trunk size, leaf size, leaf density, tree density etc) in a forest terrain, it was the most accurate and reliable option available. The equation used to calculate attenuation due to trees is shown in Equation 25. The value received from this equation is subtracted from the FSPL link margin to get the final link margin.

$$Attenuation_{trees} = R_{\infty}d + k[1 - exp(-\frac{R - R_{\infty}}{k})d] \tag{25}$$

The variable "d" is the vegetation depth in meters. Tree depth is the depth of vegetation in the total communication range. This is shown in Figure 52. The variables R_{∞}, k, and R are a function of the communication frequency and the vegetation scenario. Radio Science took into account ten scenarios. Out of these scenarios, three were selected on its likelihood of occurrence during the HERMES mission. These scenarios were: into vegetation, edge of vegetation, and line of vegetation. This is illustrated in Figure 53.

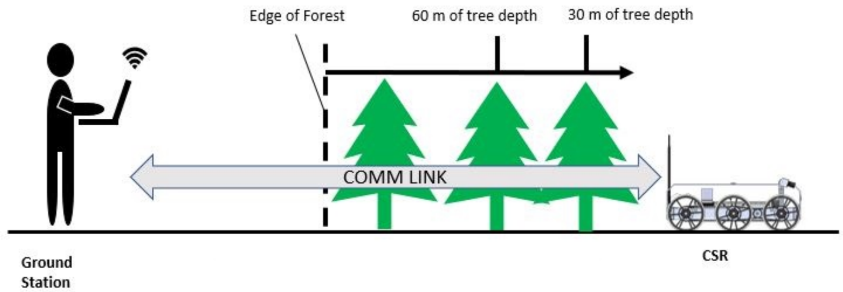

Figure 52: Tree depth visualization.

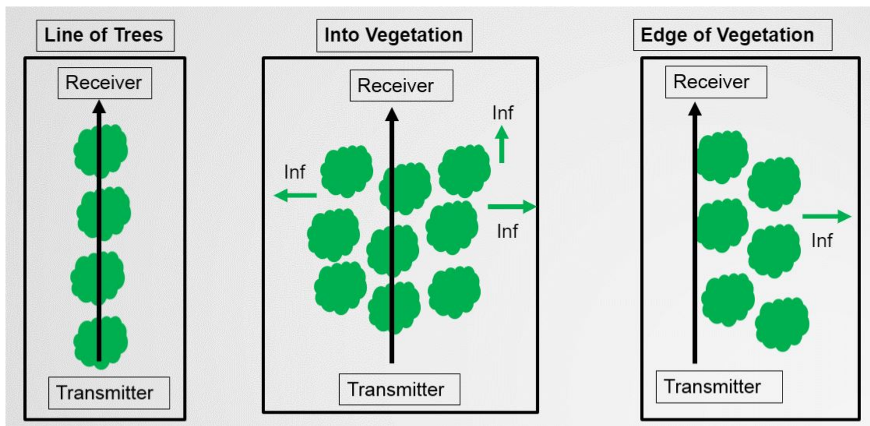

Figure 53: Vegetation scenarios.

After consulting with a few professors with expertise in communications along with research, it was decided that the goal of the HERMES communication system would be to have a link margin of at least 10 dB at a distance of 250 meters. Using Table 5. in the Radio Science's research paper, attenuation due to trees was plotted against the communication distance with various tree depths tested in these three scenarios. These plots are shown in Figures 54a-54c. From these plots, it can be seen that the worst case scenario in terms of attenuation at a distance of 250 m would is the "into vegetation" scenario as it allows the least depth of trees (70m) to stay under the 10 dB Link margin.

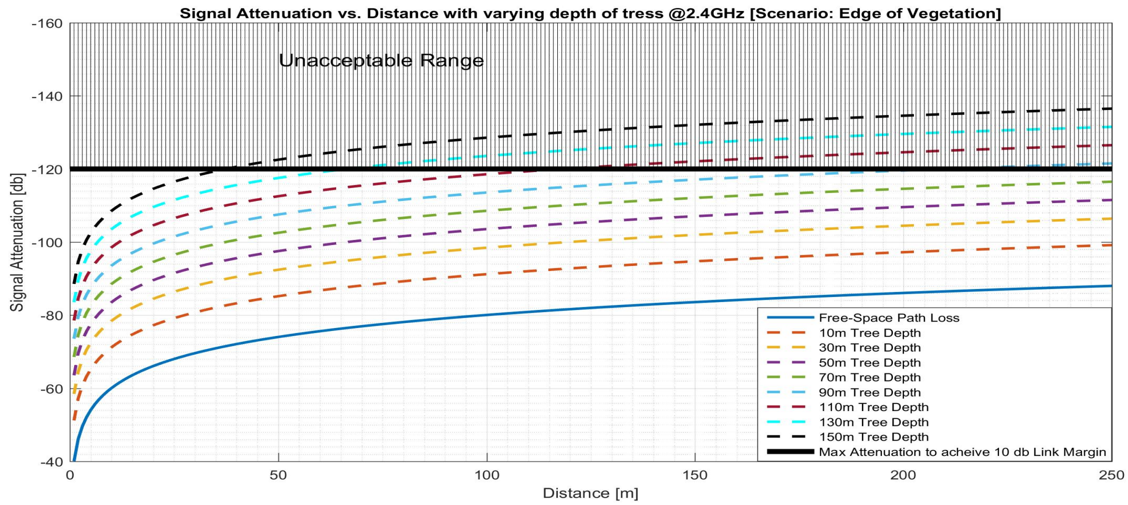

a) Edge of vegetation.

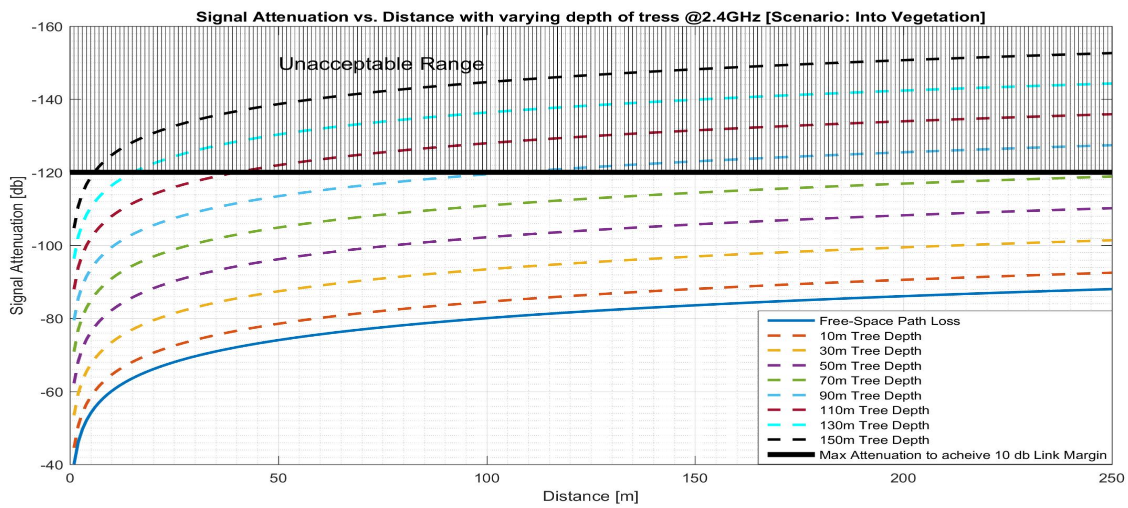

b) Into vegetation.

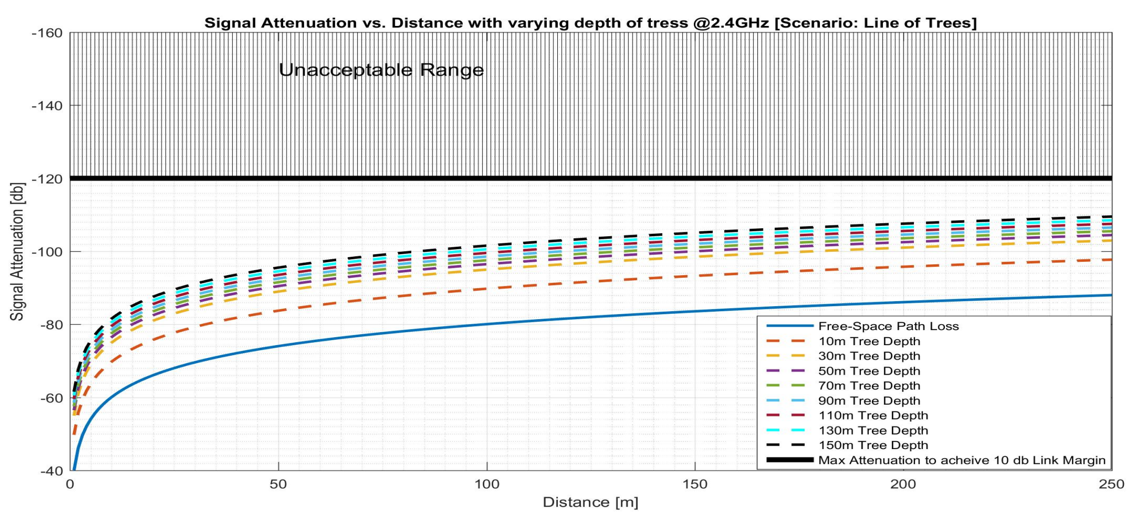

c) Line of vegetation.

Figure 54: Attenuation due to trees in different scenarios at various tree depths.

For a safety factor, the worst case scenario was chosen in order to finalize the link budget. It was concluded that the worst case scenario was "Into Vegetation" and a 10 dB link margin could be achieved as long as the tree depth is less than or equal to 70 meters. This is also shown in Figure 55b.

Power transmission (dBm)	28
Antenna Gain transmitter (dBi)	5
Antenna Gain receiver (dBi)	5
Cable Loss of transmitter (dB)	-2
Cable Loss of receiver (dB)	-2
Free-Space Path Loss (dB)	-88.01302501
Receiver Sensitivity (dBm)	-96
Link margin w/o obstacles (dB):	**41.98697499**

a) Link margin (No obstacles)

Tree Depth	Attenuation (dB)	Link Margin (dB):
10m	-4.4854	37.50157499
20m	-8.9423	33.04467499
30m	-13.3715	28.61547499
40m	-17.7737	24.21327499
50m	-22.1497	19.83727499
60m	-26.5004	15.48657499
70m	-30.8264	11.16057499
80m	-35.1285	6.858474992

b) Link margin with varying tree depth (Into vegetation)

Figure 55: Link budget calculation.

6.2.3. Data Budget Analysis

In addition to the link budget, it is essential to establish a data budget to ensure communication between the CSR, GS, and the MR. The link budget shows that our communication device has enough transmission power to send data at a distance of 250 m with 70 m tree depth. However, another aspect to take into account is how much data can be sent through that distance. During the mission, there will be various data transmitted through the communication system. These data include:

- 1) Commands from the GS/MR to the CSR.
- 2) Live video feed from the CSR to the GS.
- 3) Magnetometer/Accelerometer data from the CSR to the GS.

The commands that will be sent to the CSR will be 10 bit packets. In order to calculate the bandwidth requirement for the live video feed, Equation 26 was used. The camera selected for the HERMES mission is the "180^o Fisheye Lens 1080p Wide Angle Pc Web USB Camera." Since the camera captures color videos and images, there are 24 bits per pixel (3 bytes per color in RGB). The camera uses a MJPEG video compression format which allows a compression ratio of 10 and allows various combinations of frame speed and pixels per frame. These combinations are shown in Table 40 with the required bandwidth for that combination. Finally, the GPS data and the magnetometer data will be sent to the CSR at a frequency of 1Hz as string characters of approximately 30 characters. Since 1 character is 1 byte, the total bandwidth required would be 240 Bits/s.

$$Bandwidth = \frac{(\frac{Frames}{s}) * (\frac{Pixels}{Frame}) * (\frac{Bits}{Pixel})}{CompressionRatio} = \frac{Bits}{s} \tag{26}$$

Frames/s	Resolution (Bits)	Required Bandwidth (Mbps/s)
6	1920x1080	2.986
6	1280x1024	1.887
9	1280x720	1.991
9	1024x768	1.699
21	800x600	2.419
30	640x480	2.212
30	352x288	0.729
30	320x240	0.553

Table 40: Required bandwidth for camera.

The radios used by the HERMES mission allows a total bandwidth of 15 Mbps. Table 41 shows the data rate margin assuming transmission of all data at a given time of a second and the highest bandwidth requirement for the camera. As shown in the table, this allows for a total data rate margin of 12.014 Mbps. Therefore, in addition to having a link margin of atleast 10 dB at a distance of 250 meters, HERMES will have the capability to transmit and receive all the required data for the entirety of the mission.

Data Type	Bandwidth Required
Commands to the CSR	10 Bits
Video Feed	2.986 Mbits
GPS/Magnetometer	240 Bits
Total BandWidth	**2.986 Mbits**
Data Rate Margin	**12.014 Mbps**

Table 41: Data rate margin.

6.3. Guidance, Navigation, and Control Detailed Design

Author: Brandon Santori, Alexander Sandoval, Marcos Mejia

In order for the CSR to traverse forested terrain and arrive at an LOI, the guidance, navigation, and control system (GNC) is required to allow actual controlled maneuvering. As such, it has been considered a critical project element. For this system, there are 5 primary requirements:

- CSR.3: The CSR shall drive to a location of interest through mission defined terrain
- CDH.3.3: The CSR CDH system shall determine if the CSR is within 5 meters of the location of interest
- CDH.3.4: The CSR CDH system shall determine the heading of the CSR
- MOB.3.2: The CSR shall be able to go over discontinuities up to 9 inches
- SENS.5.1.3: The CSR Sensing system shall capture video with a field of view of at least 100 ^{o}

6.3.1. Hardware Selection

For these requirements to be satisfied, basic guidelines for hardware selection were developed. In order to satisfy CHD.3.3, a GPS with an accuracy of ±5 m is required. For CDH.3.4, it was determined that the selected magnetometer will require an accuracy of at least 1 μT. Finally, SENS.5.1.3 requires a lens with greater than 100 ° FOV as stated. The remaining requirements will be fulfilled with software created for the CSR. The hardware solutions selected to satisfy these baseline requirements as well as the corresponding specifications are shown below in Table 42. On top of these required components, there will be further discussion for the controller being used to integrate everything.

Component Type	Specific Component	Required Specs	Achieved Specs
GPS	GPS-RTK Board NEO M8P-2	5 m accuracy	0.025 m accuracy
Magnetometer and Accelerometer	LSM303	1 μT accuracy	0.058 μT accuracy
Lens	Fisheye Lens	100° FoV	180° FoV

Table 42: GNC Hardware Selection

6.3.1.1 Guidance and Navigation

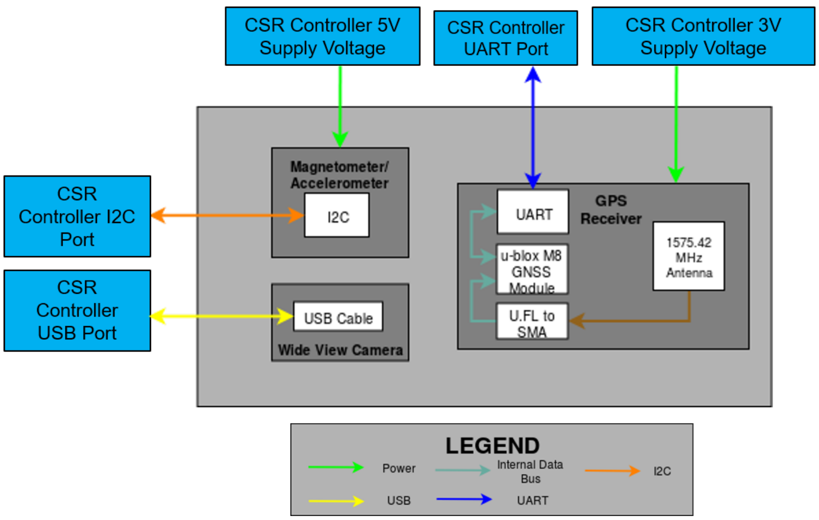

Figure 56: The hardware interface diagram for guidance and navigation which comprises of a GPS, Magnetometer/Accelerometer, and Camera.

The interface diagram shows that the magnetometer will be powered using a 5V supply voltage, and be communicating to the CSR controller through I2C protocol. The GPS reciever will be powered by a 3V supply voltage, and communicate to the CSR controller through UART, and lastly the wide view camera will be communicating and powered over USB to the controller.

6.3.1.1.1. Global Positioning System

In order for the CSR to determine it's own location GPS is going to be used. This would be to satisfy requirement CDH.3.3 which requires the CSR to be within 5 meters of the location of interest. To do this, a GPS with an accuracy of 2.5 cm was chosen. This GPS, the GPS-RTK Board NEO M8P - 2, uses a method called Real Time Kinetics (RTK) which uses two GPS modules, one as a base station and another as a rover station. The rover will be placed on the CSR and be sent GPS correction bytes from the ground station which produces the correction bytes. Both GPS modules receive NMEA messages from the Global Navigation Satellite System. The rover module receives RTCM corrections data at a rate of 350 bytes/second, while the rover will send the GPS data packets to the ground station on command. The diagram below shows how the satellites, the GPS modules, the controllers, and radios interface. The diagram also shows what software would be needed to receive messages, parse them, and send the correction data to the CSR.

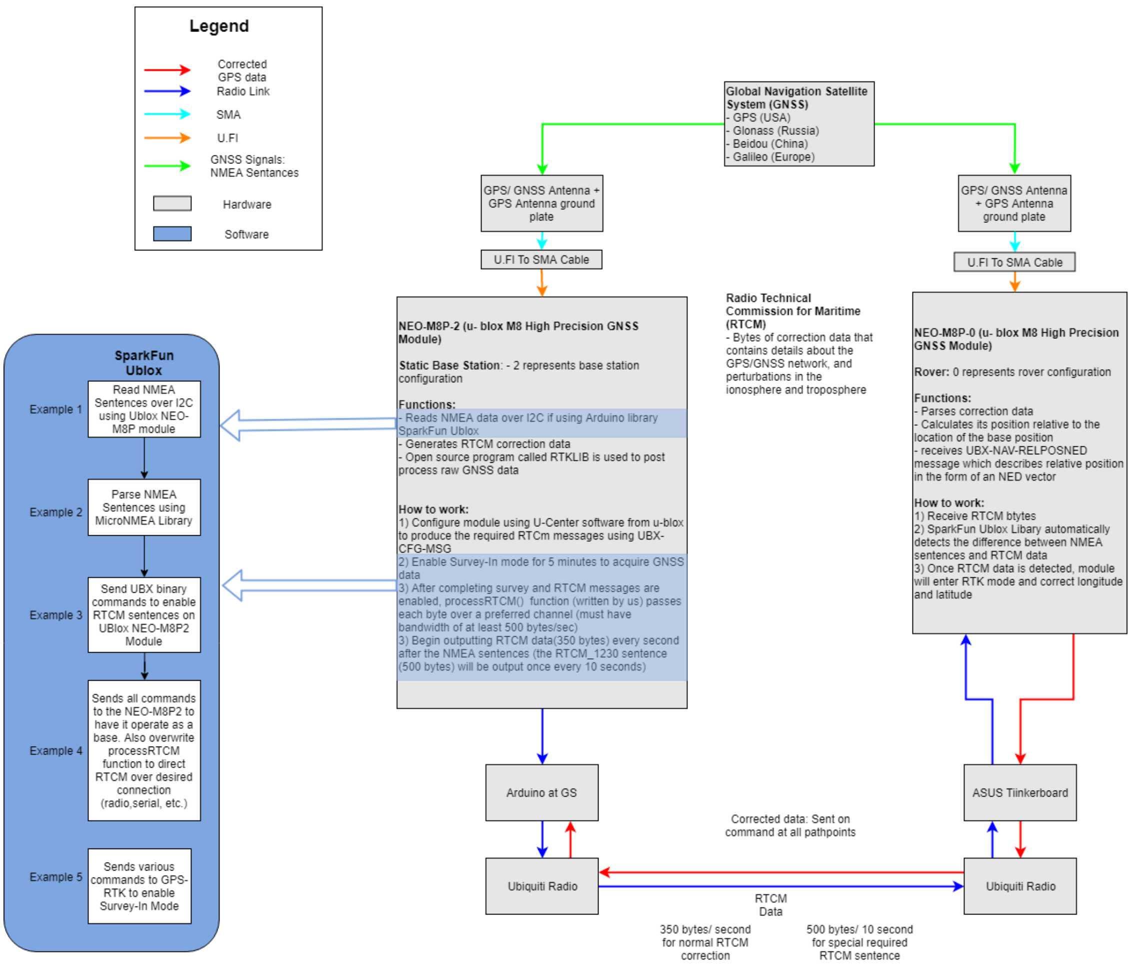

Figure 57: GPS Interface

6.3.1.1.2. Magnetometer

In order for the CSR to determine it's heading a magnetometer will be used. Specifically the Magnetometer and Accelerometer LSM303, which has a 0.058 μT accuracy. This meets the required 1 μT accuracy requirement which was derived from the CSR being 250 meters away from the ground station, and needed to know the LOI's heading within 5 m of accuracy. At 250 meters this would translate to a required heading accuracy to be 1.1 ^{o}, while the LSM303 has a heading accuracy of .133^o. The heading accuracy,f, was determined using the equation below:

$$f = tan^{-1}(r/m) \tag{27}$$

Where r is the sensor resolution, and m is the magnitude of Earth's magnetic field.

This is shown in the figure below:

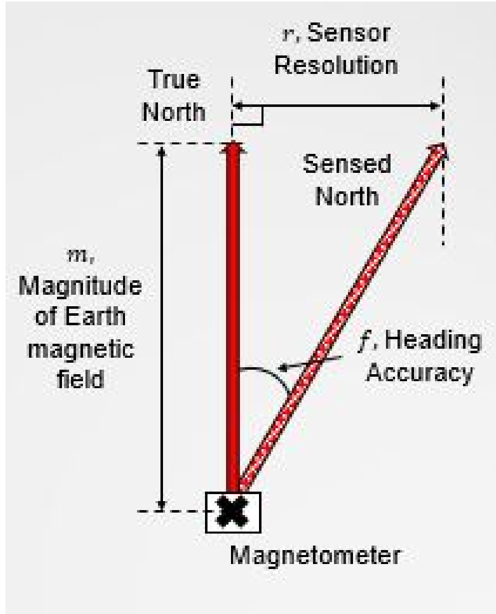

Figure 58: Magnetometer Diagrams

Another concern with the magnetometer would be noise from other components. Specifically the most concerning component would be the motor due to the noise generated while powered. Due to this, preliminary tests were conducted to determine how the magnetometer would be affected by the motor. A motor was placed on a stand and powered to generate noise. Then using a phone with three different magnetometer applications, measurements were taken at 15 - 60 cm in 15 cm increments. For each position, the x, y, and z magnetometer measurements were recorded for the motor being powered on, powered off, and powered on for 5 seconds before taking the measurement. The test results showed that at the closest location of 15 cm the difference in the magnetic field for no motor, a non- powered motor, and a powered motor was insignificant (+/- $/mu$T). Due to this preliminary test, there is confidence that interference will not be an issue. However later on in the semester whenever integration begins, if interference poses to be a significant issue, then design alternatives exist. One of these design alternatives would be mu-metal foil shielding around the motor which would reduce generated noise, or the magnetometer could be placed on a boom to extend the distance from the motor.

6.3.1.1.3. Imaging System

The imaging system that will satisfy the video and imaging requirements will be a 180^o Fisheye Lens 1080p Wide Angle Camera. It was a 2 MegaPixel 1920x1080 pixel, with a USB 2.0 interface. This camera will be used to send continuous video feed back to the ground station, and it will be critical to use whenever the operator is travelling around an obstacle, or when it encounters a discontinuity, or a slope. The user at the ground station will have the ability to take time stamped screen shots of the video feed, which would satisfy requirement CDH.2.1, where the CSR is required to send time stamped imaging data.

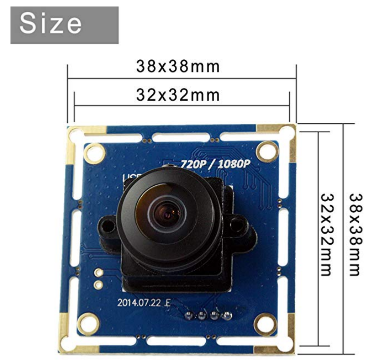

Figure 59: Imaging System

6.3.1.2 Control

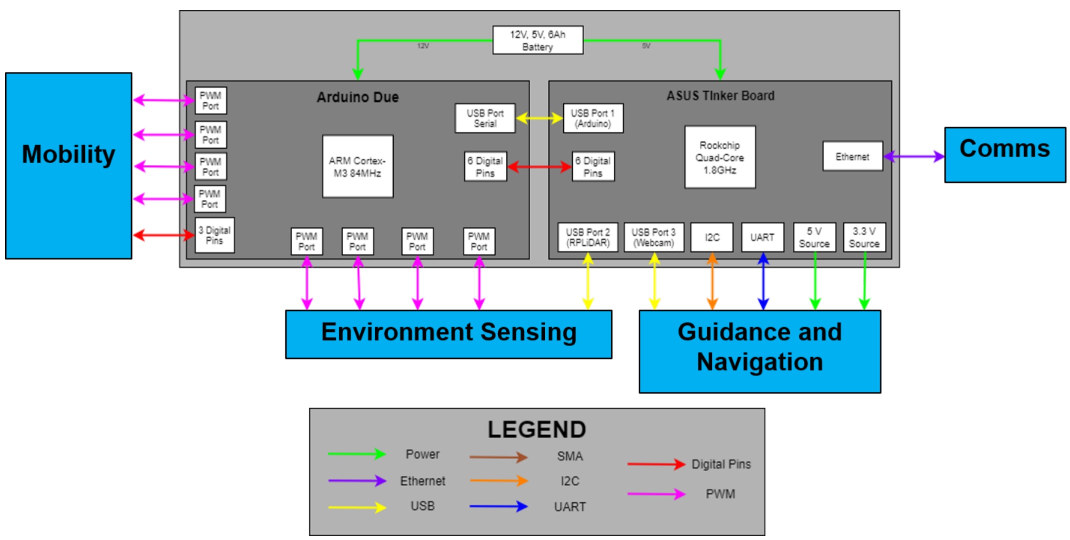

Figure 60: The hardware interface diagram for the main controller comprising of a ASUS Tinker Board and Arduino Due.

	CPU (MHz)	USB	I2C	UART	PWM	Digital Pins	Analog Pins
ASUS Tinker Board (SBC)	1800	4	2	4	2	28	0
Arduino Due (MCU)	84	1 Micro	2	4	12	54	12

Table 43: The CSR controller characteristics for both the ASUS Tinker Board and Arduino Due.

6.3.1.3 Power

In order for the controls hardware to be active for operation there is a dedicated power supply for the Arduino Due and ASUS Tinker Board. The diagram below primarily focuses on the voltages seen within the system however the battery being used contains enough capacity to provide sufficient power to the two devices for the estimated mission time. In addition, one battery can be used for both devices by linking the devices in parallel to the battery.

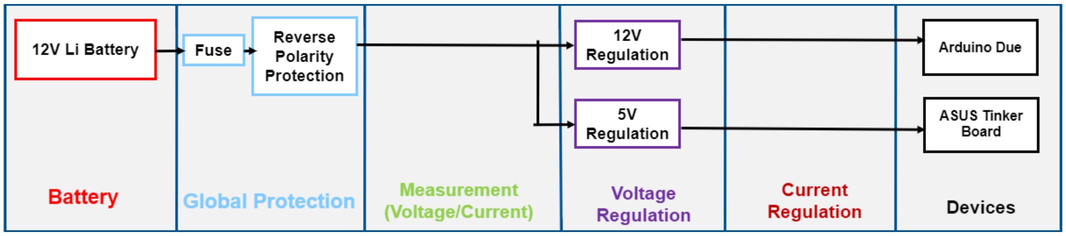

Figure 61: Power Distribution Block Diagram (C&DH)

The battery selected for the C&DH subsystem is the TalentCell Rechargeable Portable Lithiom Ion battery,operating at 12 Volts, with a capacity of 6000 mAh. For a one hour mission, the expected current consumption of this subsystem is 2.31 A continuously for one hour. As the total capacity of the battery is 6Ah, the battery provides a 62 percent margin, even for an extended mission.

6.3.2. CSR Robot Operating System Utilization

In order to create software that will be capable of meeting all requirements, it was determined that the Robot Operating System (ROS) will utilized. ROS allows for multiple processes to occur at the same time without the need for extensive programming to handle the challenges normally associated with multi-threading. Additionally, it allows for easy communication between multiple devices which will be largely beneficial as the CSR must constantly communicate with the GS. It is important to note that the CSR will utilize two onboard processors; these being the ASUS Tinkerboard and the Arduino Due. The Asus will be the primary controller and thus it will run Python with the ROS Python libraries. The Arduino will communicate with the Asus through a series of digital pins as well as a USB connection. However, the Arduino will be running the base Arduino language and thus will not be running ROS. As a result of the differences in these processors, the bulk of the CSR code will be within the Asus.

In order to allow multiple processes to run in parallel, ROS creates independent executables known as nodes. These are then able to communicate with each by creating topics which may be published to or subscribed to by any other number of nodes. This allows for rapid sharing of information between different programs which will be very valuable as will be discussed within the next sections.

6.3.3. CSR Control Software Design

To meet all the GNC specific requirements, the CSR will operate within 6 different modes. The CSR will switch between modes manually after receiving commands from the GS or autonomously if a separate mode determines it is necessary. This architecture is divided into two main categories: initialization/ending modes and traversal modes. The Initialization and ending modes include modes 0 and 5 while the traversal modes are 1-4. These modes are described below in Table 44.

Mode Name	Mode Number	Mode Description
Initialization	0	Performs initialization actions needed within the CSR as well as receiving the LOI GPS coordinates
Manual	1	Allows manual navigation of the CSR. Processes directional mobility commands from the user
Semi-Autonomous	2	Drives the CSR forward until an obstacle, heading error, or loss of communications is detected
Discontinuity Traversal	3	Allows for autonomous crossing of discontinuities up to 9 inches in length
Loss of Communications	4	Autonomously returns the CSR to the last confirmed pathpoint
LOI Reached	5	Informs the GS that a viable path has been determined for the MR to reach the LOI

Table 44: CSR Software Modes

These different modes will be primarily contained within a single main loop. This will allow for the CSR to quickly switch between modes if the mode number is changed. The general structure is shown below in Figure 62 as well as the corresponding pseudocode.

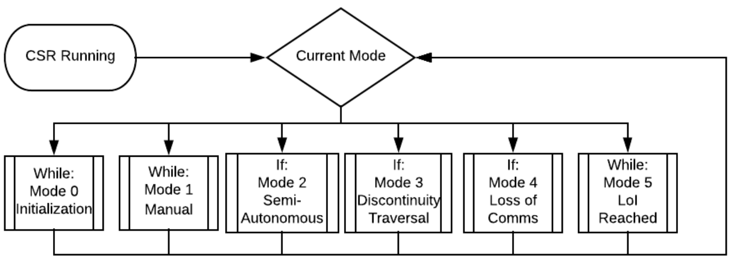

a) Main Loop Flow Diagram

```
While (roscore)
        getMode()
        While (mode == 0):
                Initialization mode
        End
        While (mode == 1):
                Manual mode
        End
        If (mode == 2):
                Semi-Autonomous mode
        End
        If (mode == 3):
                Discontinuity traversal mode
        End
        If (mode == 4):
                Loss of comms mode
        End
        While (mode == 5):
                LOI arrival mode
        End
End
```

b) Main Loop Pseudocode

Figure 62: CSR Main Loop

The initialization mode is comprised of overall system initialization and the reception of the LOI coordinates. The structure of mode 0 is shown below in Figure 63

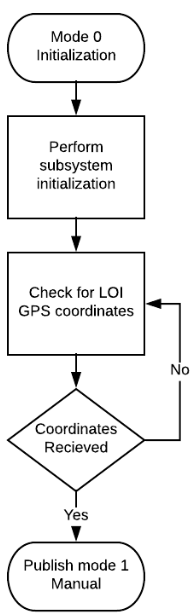

a) Mode 0 Flow Diagram

```
While (mode == 0):
        If (received_GPS):
                mode == 1
                Publish.mode
        End
End
```

b) Mode 0 Pseudocode

Figure 63: CSR Initialization Mode

The CSR manual mode will handle manual maneuvering as well as the primary placement of GPS pathpoints to form the viable path for the MR. Upon detecting a change in user input, the CSR will send the mobility command to the Arduino which connects to the motor controllers. If this command is a turn, it will then drop a pathpoint. This is shown below in Figure 64

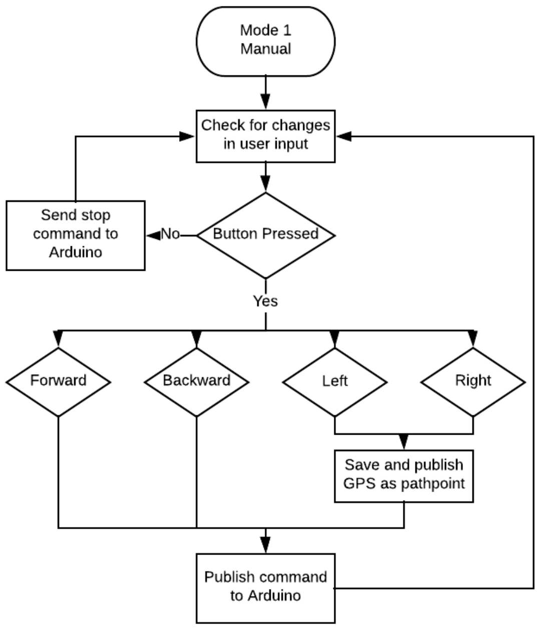

a) Mode 1 Flow Diagram

```
While (mode == 1):
        If(button_pressed):
                If (button_type == forward):
                        controlMotors(forward)
                End

                If (button_type == backward):
                        controlMotors(backward)
                End

                If (button_type == left):
                        saveAndSendGPS()
                        controlMotors(left)
                End

                If (button_type == right):
                        saveAndSendGPS()
                        controlMotors(right)
                End

                While (button_pressed And (not loss_comms)
                        And (not reached_loi) And (not discontinuity)
                        And (not mode_switch)):

                        checkCommands()
                End

                stopMotors()
        End
End
```

b) Mode 1 Pseudocode

Figure 64: CSR Manual Mode

The semi-autonomous mode drives the CSR in a straight line until an obstacle is met, the heading drifts too far, or a mode change occurs. The structure of this mode is shown in Figure 65.

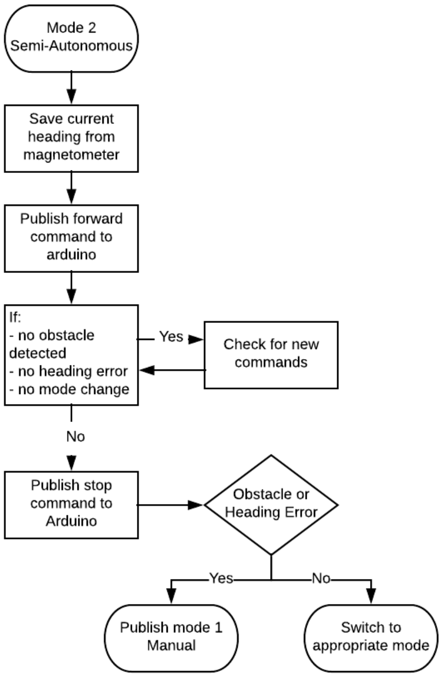

a) **Mode 2 Flow Diagram**

```
If (mode == 2):

        fixOrientation()

        goForward()

        While ((not object_detected) And (not loss_comms)
                And (not reached_loi) And (not discontinuity)
                And (not mode_switch)):

                checkCommands()
        End

        stopMotors()
End
```

b) **Mode 2 Pseudocode**

Figure 65: CSR Semi-Autonomous Mode

Mode 3 is the discontinuity traversal mode. This mode will handle crossing a 9 in horizontal discontinuity which will require the utilization of the ultrasonic sensors as well as the movement of the linear mass stage to maintain stability. The structure of this mode is presented in Figure 66 below.

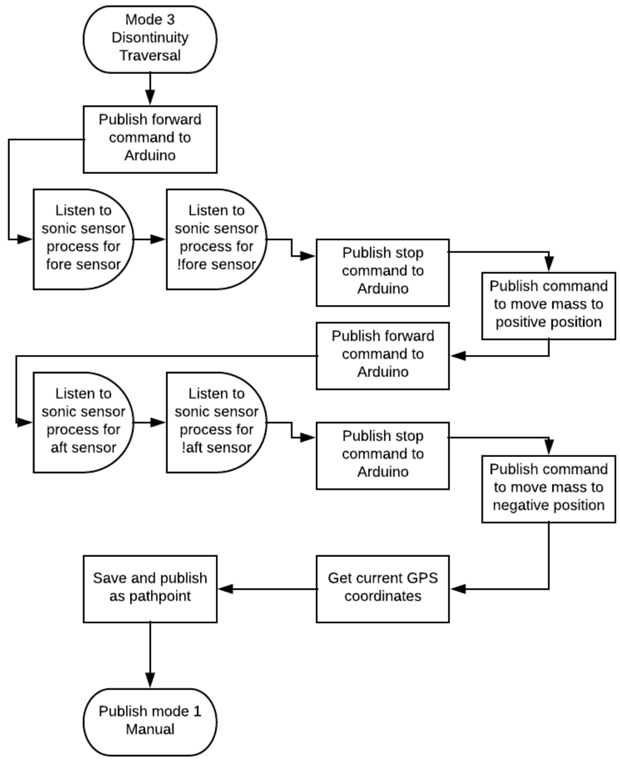

a) Mode 3 Flow Diagram

```
If (mode == 3)
        reduceSpeed()
        goForward()

        # drive forward until front wheel over gap
        while(checkFrontGap()):end

        # drive forward until front wheel is across gap
        while(!checkFrontGap()):end
        stopMotors()
        moveMass(front)
        goForward()

        # drive forward until back wheel over gap
        while(checkBackGap()):end

        # drive forward until back wheel is across gap
        while(!checkBackGap()):end
        stopMotors()
        moveMass(back)
        increaseSpeed()
        saveAndSendGPS()
        setMode(1)
end
```

b) Mode 3 Pseudocode

Figure 66: CSR Discontinuity Traversal Mode

The 5th CSR mode is the loss of communications mode. This mode is entered when either the latency between the CSR and the GS so large that manual control becomes unfeasible or when communication is entirely lost. Upon entering this mode, the CSR will turn to face towards the last confirmed pathpoint and will then drive forward until it is within 5 m of this location. The overall structure of this mode is shown below in Figure 67.

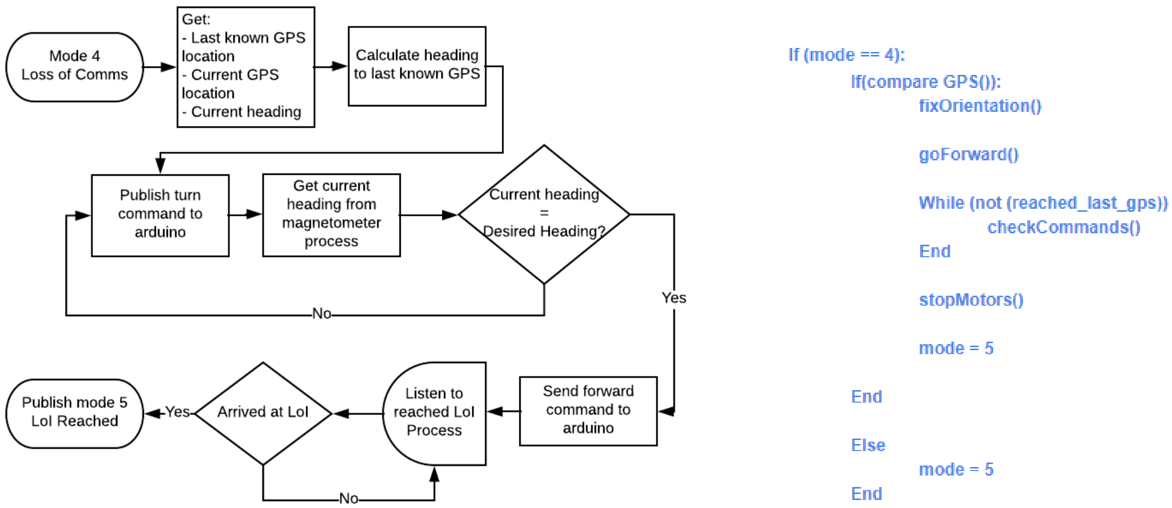

a) Mode 4 Flow Diagram **b) Mode 4 Pseudocode**

Figure 67: CSR Loss of Communications Mode

The final CSR mode is the LOI arrival mode. This mode is entered in two scenarios. Either the CSR is within 5 m of the LOI and thus mission success occurs or the CSR loses communications and has returned to within 5 m of the last pathpoint. Upon entering this mode, the CSR will send stop commands to all motors and try to send a mission complete signal to the GS. The overal function of this mode is shown in Figure 68.

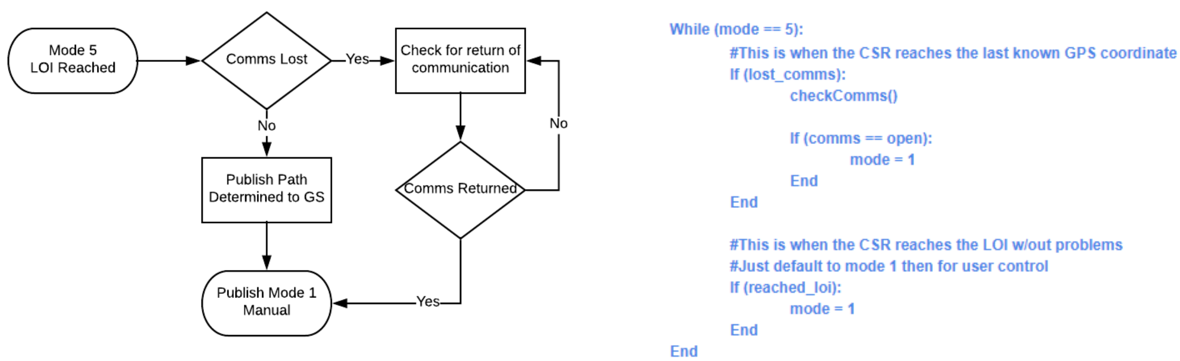

a) Mode 5 Flow Diagram **b) Mode 5 Pseudocode**

Figure 68: CSR LOI Arrival Mode

6.3.4. CSR ROS Node Software Architecture

In the CSR, a large amount of processes will be performed within ROS nodes running parallel to the main loop. In order to better visualize this, a basic ROS map has been created for the CSR. This may be seen below in Figure 69. This diagram shows the different nodes which will be required to run within the ASUS Tinkerboard. Additionally, it shows the communication that will occur between different nodes, the CSR ROS master, sensors, and the separate processors.

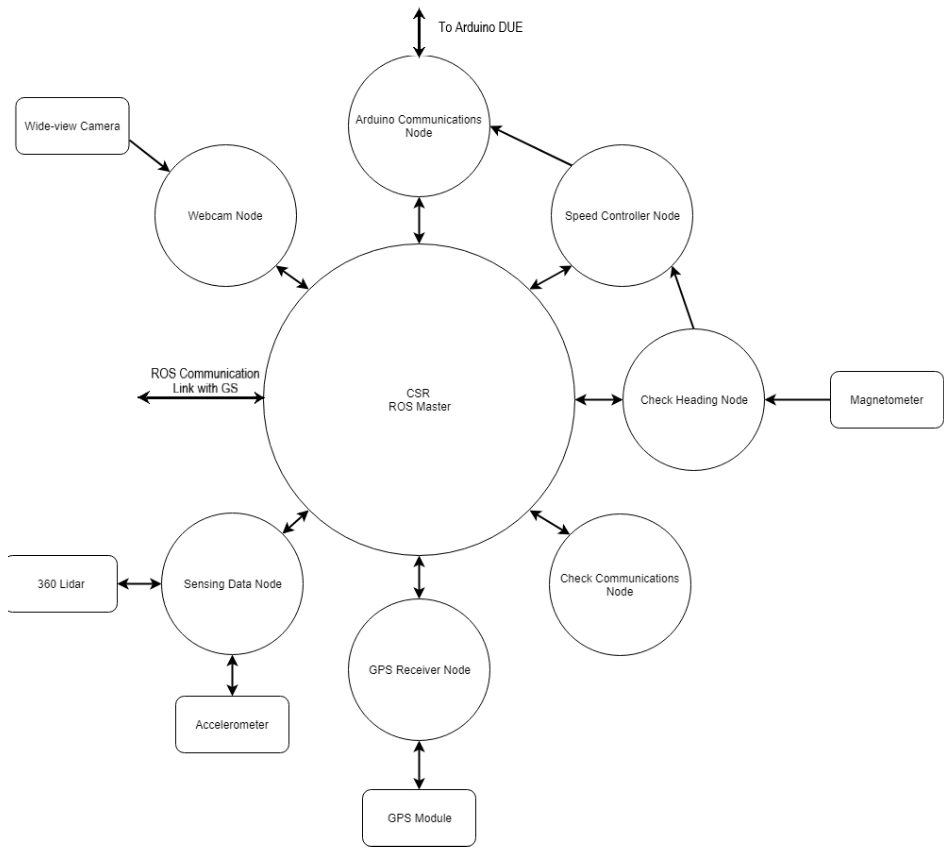

Figure 69: CSR ROS Map

6.4. Environment Sensing Detailed Design

Author: Quinter Nyland, Marcos Mejia, Alexander Sandoval, and Alexis Sotomayor

The CSR must be capable of entering a semi-autonomous mode, during which it must detect non-traversable obstacles and discontinuities that could be preventing it from reaching the LOI. Environment sensing is a critical project element because in a realistic setting, constant, manual intervention is not feasible. Thus, the CSR must be able to accurately sense its environment so that the user is made aware of their required intervention only when necessary. Four main requirements, which are listed below, guided the design of the CSR's Sensing system.

- SENS.3.1: The CSR Sensing sytem shall detect object at least 37.5 inches (3.125 ft, 0.9525 m) from the Sensing system.
- SENS.3.1.1: The CSR Sensing system shall detect objects within a field of view of at least 103.5^o.
- SENS.3.1.2: The CSR Sensing system shall detect object at least 1 inch in width.
- SENS.3.2: The CSR Sensing system shall detect discontinuities at least 2.4 inches deep.

These four requirements, along with software architecture and the trade studies conducted in the Conceptual Design section, revealed three fundamental sensing conditions for which the CSR must have a solution. The first condition, in-plane object detection, refers to the CSR's ability to sense objects in a single plane, parallel to the ground, 2.4 in. above the driving surface. This sensing need was derived from the delineation of traversable versus non-traversable obstacles. The CSR shall be able to overcome any obstacle at or below 2.4 in. in height, and any obstacle defined in the terrain definition should be a uniform shape, so it is only necessary to detect objects that pierce the 2.4 in boundary on that single plane. The second sensing condition is discontinuity detection, requiring the CSR to be be capable of stopping before reaching a discontinuity (defined to be at least 2.4 in. in depth in the terrain definition). This means that the CSR must have the capability to sense the ground ahead of it a short distance away. The final sensing condition is discontinuity sensing, which is slightly different than discontinuity detection. During the discontinuity traversal mode, the CSR must know where it is in relation to the discontinuity it is attempting to cross, so the Sensing system must be able to feed back depth information in the front and back of the CSR. The independence of each sensing condition allowed for the Sensing system to be modular. In other words, one sensor or device did need to be capable of providing a solution for all three conditions; instead, a single, independent solution was designed for each condition. Thus, this section will cover how these three conditions are satisfied be their individual sensing solutions.

6.4.1. In-Plane Object Detection Sensing System

This condition is the most critical sensing condition for which the CSR must provide a solution because it corresponds to the most requirements (SENS.3.1, SENS.3.1.1, and SENS.3.1.2). The design solution developed for this condition was the use of a 360° LiDAR scanner mounted to the bottom of the CSR so that the scanner is 2.4 in. above the ground. The LiDAR Scanner is the Slamtec RPLIDAR A2M8, a rotating scanner that sends laser pulses out at a rate of ≈4000 Hz and spins at a rate of 5 - 15 Hz. This sensor will only detect non-traversable obstacles within a desired area of detection (an area in front of the CSR defined by the field of view necessary from requirement SENS.3.1.1 at a range defined by SENS.3.1). A picture of the sensor istelf, the mounting location of the RPLIDAR, and a visual description of the desired area of detection are shown below in figures 70 and 71.

Figure 70: Slamtec RPLIDAR A2M8

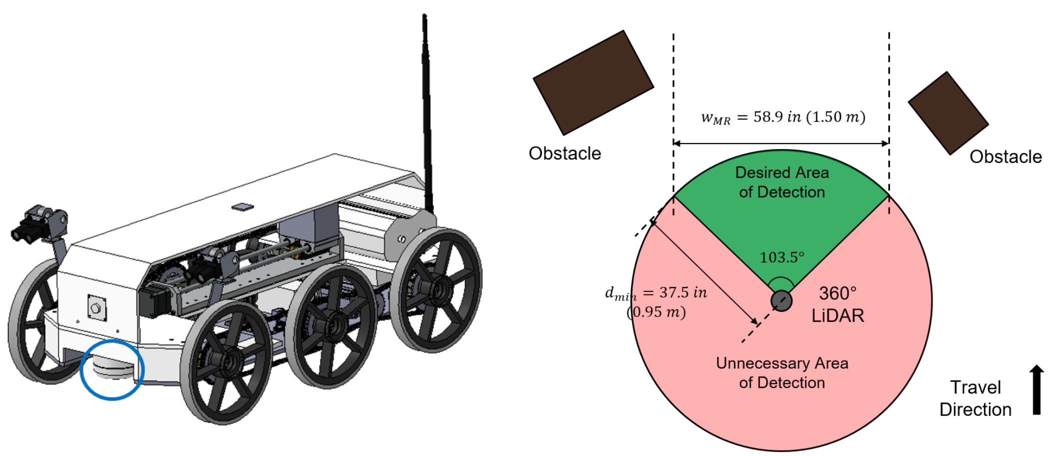

Figure 71: Isometric View of CSR Showing Mounting Location and Diagram of Desired Sensing Area of the RPLIDAR

The area in green in figure 71, or the desired area of detection, which is derived from the requirements above, indicates the area that is used as a trigger for any obstacle detection. If an object enters this area, the Sensing system must be capable of accurately detecting it. d_{min} is represented by the range specification given in requirement SENS.3.1 and dictates a range specification required for RPLIDAR. Based on the specification sheet given by the manufacturer[30], the RPLIDAR A2M8 has a maximum range of 8 m (315 in) which exceeds the required range of 37.5 in.

w_{MR}, the width of the MR, is what defined the field of view necessary for requirement SENS.3.1.1 and dictates a field of view requirement of the RPLIDAR. The RPLIDAR is a 360° scanner, so it therefore provides a field of view of 360°, which exceeds the required field of view of 103.5°. Constraining the field of view is important, however, because the CSR must mimic the size and shape of the MR. So, it is too restrictive to utilize the entirety of the 360° field of view. In addition, the mounting location of the RPLIDAR creates additional problems because the scanner will also scan the CSR's wheels. To avoid this issue, the RPLIDAR records not only a distance measurement per pulse, but also a heading, which indicates where, in a polar coordinate system, that pulse took place. So, within the software architecture, all data from the RPLIDAR outside of the desired area of detection will be discarded. This provides the added capability to accurately define the area of interest pertaining to the requirements.

Within the desired area of detection, the minimum width of any object the CSR will encounter is 1 in. (see Terrain Definition and requirement SENS.3.1.2). This desired capability dictates another required specification of the In-Plane Object Detection system, the angular resolution. Below is a diagram visualizing this angular resolution specification.

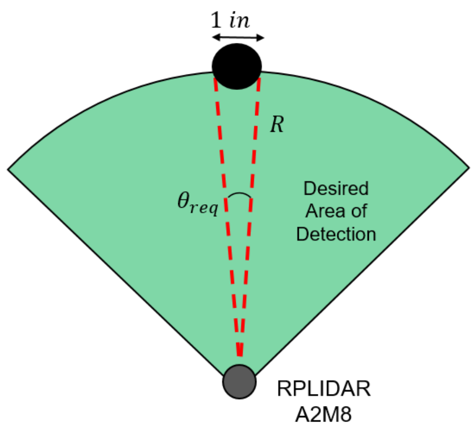

Figure 72: Diagram of the RPLIDAR's Required Ability to Detect 1 in Obstacles

In order to ensure that an obstacle will not be missed during any rotation of the RPLIDAR, 2 adjacent beams of the LiDAR must strike the obstacle on either side. θ_{req}, or the angular resolution required for 2 adjacent beams to connect with the obstacle, is derived using simple trigonometry, and translates into a required angular resolution of 1.54° at a range of 37.5 inches. Of course, this range will be flexible during a mission, so the equation for the required angular resolution at any possible range, R, is shown below.

$$\theta_{req} = sin^{-1}\left(\frac{0.5}{R}\right) \tag{28}$$

Below is a plot of this design constraint versus LIDAR range. The range requirement, SENS.3.1, as well as the RPLIDAR's angular resolution achieved specification are over-plotted on the same graph.

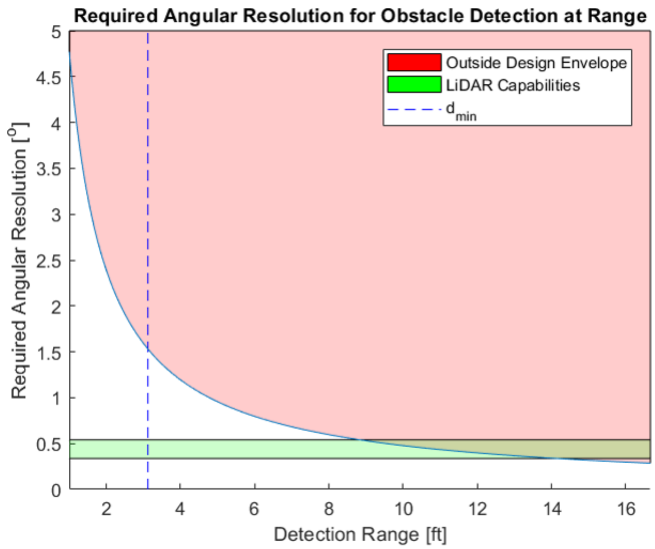

Figure 73: Required Angular Resolution for 1 inch Object Detection at range

This graph shows that even at ranges beyond the required 37.5 inches, the RPLIDAR is still within the design envelope defined by the white space. Thus, it is clear that this design solution satisfies SENS.3.1, SENS3.1.1, and SENS.3.1.2 simultaneously.

If an obstacle enters the green space in figure 71, the CSR's C&DH system will switch the CSR to the manual mode, and the user will be notified the CSR has detected something in that area. It is clear that the RPLIDAR has the physical capability to do this, but part of the requirement involves getting sensing information and converting that into a clear message that an object is detected. Thus, the integration of this sensor with the CSR's C&DH system is critical for requirement satisfaction. Below is an interface diagram for the RPLIDAR A2M8 that shows its connections to the C&DH system on the CSR.

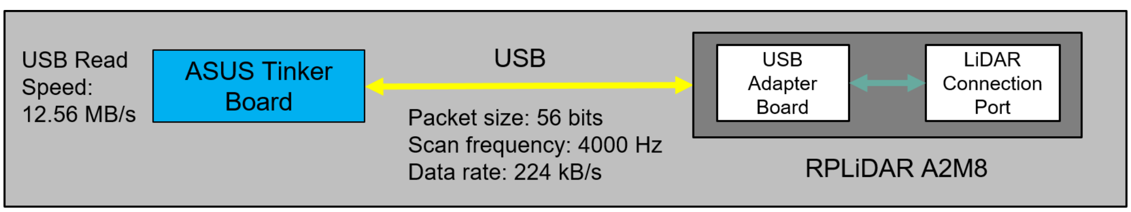

Figure 74: Interface Diagram for RPLIDAR A2M8 and C&DH System

This interface utlines the physical integration needs of the RPLIDAR so that it properly connects and interacts with the Tinker Board and the rest of the CDH system. The RPLIDAR requires a USB Adapter Board that converts its analog signals into USB-readable serial communication data. This adapter board is then directly connected to the Tinker Board through a USB connection. The USB Read Speed on the Tinker Board is 12.56 MB/s and the RPLIDAR sends data at a a rate of 224 KB/s so the Tinker Board has enough bandwidth to accept all data coming from the sensor through this port.

Beyond the physical interface, several software and firmware interfaces must be properly initialized and set up as well. First, the USB communication protocol must be established that makes sure the Tinker Board is attempting to receive the exact data that the RPLIDAR is trying to send through the adapter board. This process is handled by an open source ROS package which does not need to be modified by the team. This package establishes a clear communication link between the data packets the sensor is trying to send and the ROS framework discussed in the previous section of the detailed design. This data then must be passed through an object detection Python sketch, written by the team, that utilizes the data sent by the RPLIDAR. This sketch will analyze each data packet and figure out if the pulse is within the desired area of detection and if it has detected an object that is too close to the CSR. If the sketch determines that the sensor measurements indicate an object is within the area, then a mode change will occur. As discussed previously, this mode change will instantly stop the CSR and all data flowing into the C&DH system that is not pertinent to the current mode will be discarded. If the CSR is in any other mode than the semi-autonomous mode, it will discard the RPLIDAR data. However, there is one final consideration for the integration of this RPLIDAR, which is covered next.

The RPLIDAR sends one data packet per one pulse, and those pulses occur at a frequency of 4000 Hz. This means that, to avoid post-processing, the Tinker Board must accept the data packet, process the data, and be ready to receive the next data packet before the next pulse occurs 250 μs later. Consider the data flow diagram below.

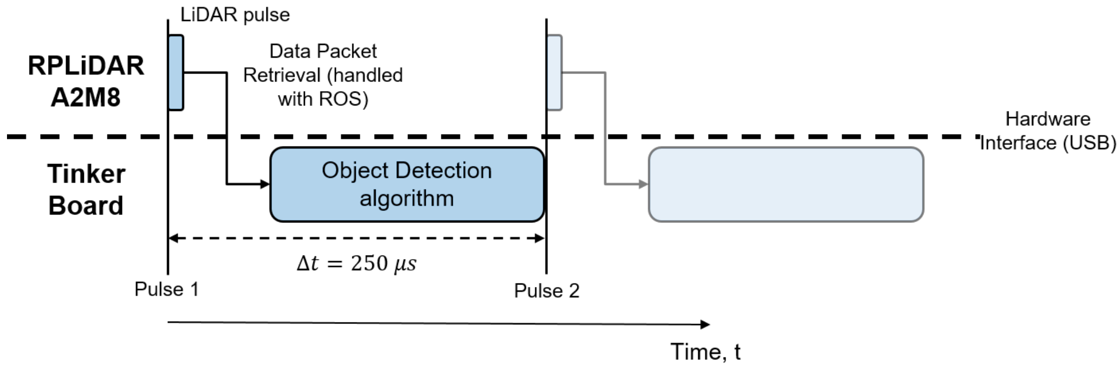

Figure 75: Data Flow Diagram for RPLIDAR A2M8

The two sections of this sequence that take the most time are the data packet retrieval in ROS and the execution of the object detection Python sketch. To check to see if both of these processes could occur within the time allotted between laser pulses, the team conducted a benchmark test using a computer with a similar processor to the Tinker Board. The Tinker Board's processor is a Rockchip Quad-Core RK3288 1.8GHz and the processor in the test computer is an Intel Cor i7-8550U 1.8 GHz. Both have similar clock speeds and core power. A simulated python sketch was used for the object detection sketch and a simple publisher/subscriber model was used to carry a data packet through the sketch. It was determined that the estimated Python execution time was $\approx 10\mu s$ and the ROS data retrieval time was $\approx 50\mu s$, which results in a total processing time of $\approx 60\mu s$. This means that, based on these estimations, the data will process quick enough while the CSR is in semi-autonomous mode without data conditioning.

In the CONOPS, the CSR immediately stops when a non-traversable object is detected, but, given the integration scheme described above, it is not clear that the CSR will stop in time to avoid colliding with the obstacle. If the CSR is travelling at 1 m/s (a high estimate, but used here to show the fastest possible velocity), the sensing system must detect the object, the beam must be sent, returned, data must be sent to the C&DH system, that must transmit a stop command to the mobility system, and the CSR must stop. This process is shown in a flow chart below.

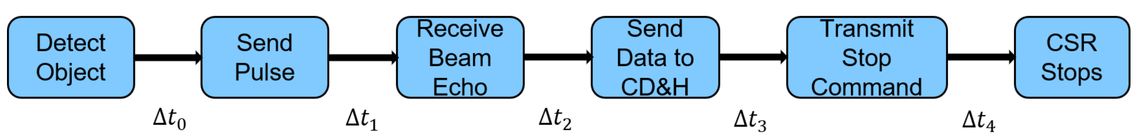

Figure 76: Speed Analysis for RPLIDAR A2M8

Between each stage in the stopping process, there is an associated time value that indicates how long it takes between each block. Ultimately, this time contributes to an additional stopping distance d_{stop}, which must be $< d_{min}$, the horizontal detection distance. In equation form,

$$d_{stop} = v_{max} t_{tot} \qquad where \qquad t_{tot} = \Delta t_0 + \Delta t_1 + \Delta t_2 + \Delta t_3 + \Delta t_4 \tag{29}$$

Δt_0 refers to the time that it takes for the RPLIDAR to detect an object in the worst case scenario when the device must complete a full scan before it detects an object. Based on the scan rate from the manufacturer[30], this time is $0.2s$. Δt_1, the time of the pulse ($\approx 0.0000003s$), Δt_2, the sensor response time ($0.00025s$), and Δt_3, the data processing time estimated above ($0.00006s$) can all be considered negligible since the full scan revolution time, Δt_0, is >> than any of those Δt values. So, the above equation for total time can be reduced to,

$$t_{tot} \approx \Delta t_0 + \Delta t_4 \tag{30}$$

Finally, Δt_4 is the time for the CSR to stop due to skidding, which can be derived using the equation below.

$$\Delta t_4 = \frac{v_{max}}{a} \qquad where \qquad a = \mu g \tag{31}$$

Assuming that the friction coefficient is $\mu = 0.7$, just like in the mobility analysis, Δt_4 can be approximated as 0.15 s. Utilizing the numerical values for Δt_0 and Δt_4 and substituting them into equation 29, the total stopping distance, d_{stop} is ≈ 0.35 m, which is $< d_{min}$ which is = 0.953 m. So, even at a velocity faster than the CSR is expected to produce, this sensor works quick enough for the CSR to stop in time before colliding with the detected obstacle.

In conclusion, the RPLIDAR satisfies requirements SENS.3.1, SENS.3.1.1, and SENS.3.1.2 simultaneously, while integrating into the software framework the team has developed and interfacing physically with the CSR's C&DH system.

6.4.2. *Discontinuity Detection Sensing System*

As mentioned previously, this sensing condition corresponds to the CSR's ability to detect discontinuities before it arrives at one. Thus, this condition related directly to requirements SENS.3.1 and SENS.3.2; this system has to detect discontinuities at least 2.4 in. deep, from a distance of 37.5 in. away. The design solution developed for this condition is two single-beam LiDAR sensors, mounted 11 in. above each wheel, directed at a downward angle of 16.35° in front of the CSR. The sensors are Lidar-Lite v3's, which are well-documented LiDAR devices that can be utilized through I2C protocol or pulse width modulation. For this project, the sensor will read data based on pulse width modulation at a frequency of 40 Hz. It should be noted that two sensors are utilized instead of just one for two reasons. First, two sensors offer the capability of redundant checks from a software side to confirm a discontinuity has actually been detected. The second reason is that it is possible to encounter a discontinuity with a side edge, so the entirety of the CSR will not traverse the discontinuity, but one side will. The wheels are the only interface between the CSR and the ground, so the sensors are mounted over the wheels to determine if the wheels will encounter a discontinuity, not the CSR as a whole. An image of one of the sensors and both sensors' mounting locations are shown below.

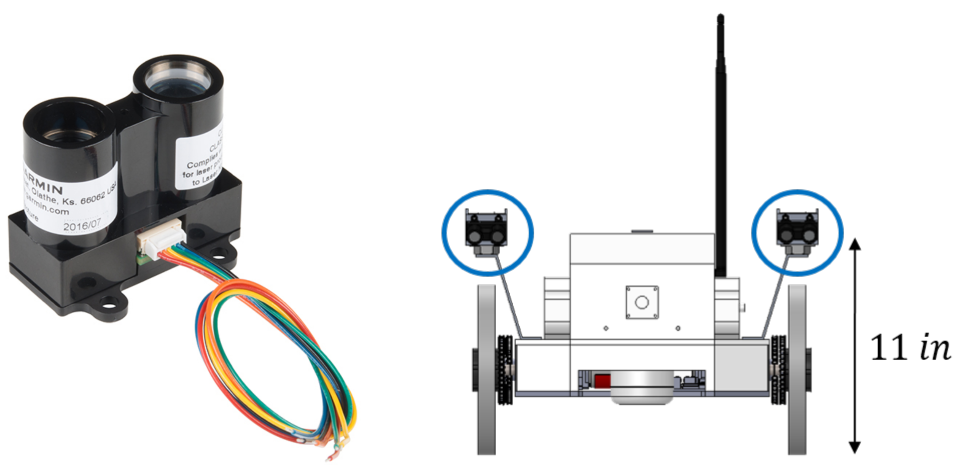

Figure 77: Lidar-Lite v3 and Front View of CSR showing Sensor Mounting Locations

Requirements SENS.3.1 and SENS.3.2 help define a standard situation in which the data from these sensors will be used to determine if a discontinuity is present. When the CSR is 37.5 in. away from a discontinuity, the sensors are mounted at an angle (16.35° down) so that they will be aimed directly at the front edge of the discontinuity. If the CSR moves forward, the sensor will instantly measure a slightly larger distance since it is detecting the bottom of the discontinuity. This slightly larger distance is the required specification for the sensor's range. A diagram of this situation is shown below.

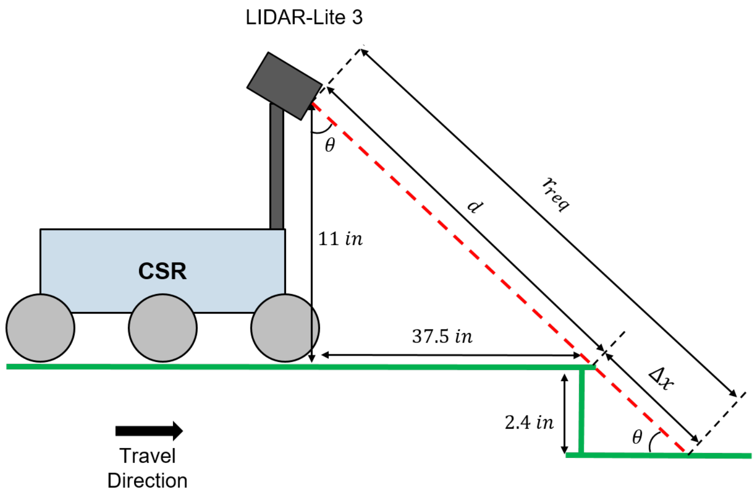

Figure 78: Side View of the Moment of Discontinuity Detection

This diagram shows that the previously detected distance, d, and the distance delta that the sensor detects, Δx, drive the required range specification for the sensor.

$$r_{req} = d + \Delta x \tag{32}$$

d and Δx can both be calculated by utilizing trigonometry and the known values in the diagram which are the sensor mounting height (11 in), the horizontal distance of the CSR from the discontinuity (37.5 in), and the depth of the discontinuity (2.4in.). In fact, θ, the mounting angle from the horizon of the sensor was also derived with these values. d and Δx are calculated to be 39.1 in and 8.39 in respectively, and thus the required range of the sensor, r_{req} = 47.5 in. Based on data from the manufacturer's datasheet[31], the Lidar-Lite v3 has a range of 40 m (1575 in), so this sensor comfortably achieves this range specification.

To accurately detect if a discontinuity is present, however, the sensor must have a high enough resolution so that when it encounters this delta distance, the C&DH system does not mistake this spike as a natural sensor error. So, in other words, the distance accuracy of the sensor must be much smaller than the delta distance value of 8.39 in. The HERMES team was able to acquire a Lidar-Lite v3 early and performed a characterization test on the sensor. The sensor was aimed at a cardboard box 1 m (39.4 in) away (measured with a tape measure), and 120 seconds of data were captured while the sensor was connected to an Arduino Uno through the I2C protocol. The results of the distance measurements, as well as the residuals of expected vs measured data points are shown below.

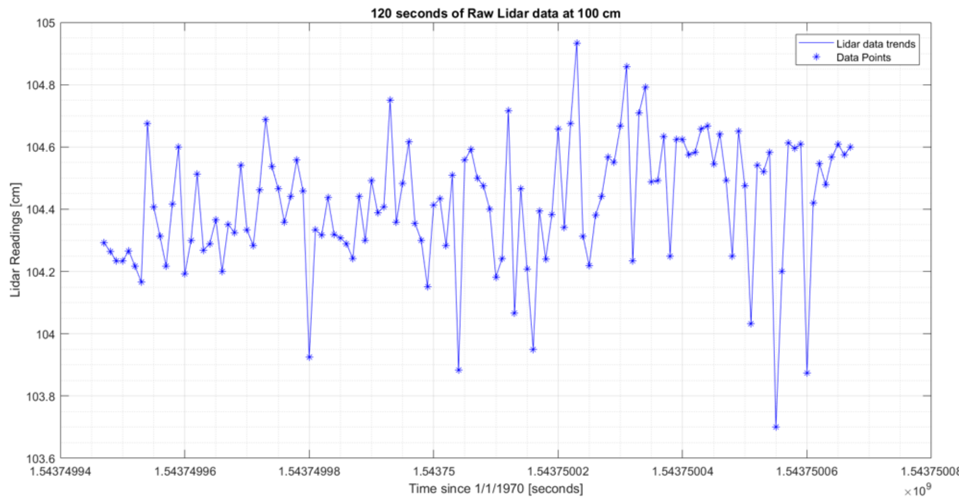

Figure 79: 120 Seconds of Raw Lidar-Lite v3 Data Pointed at Cardboard Box 1 m Away

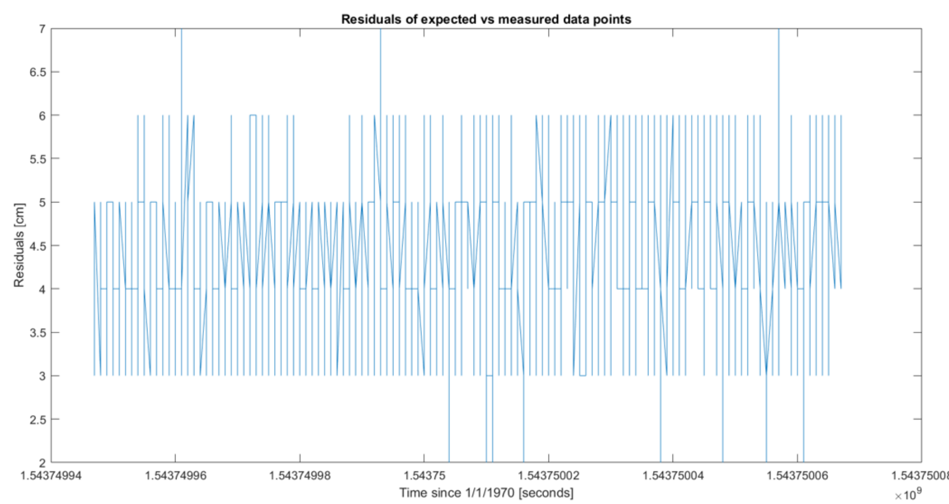

Figure 80: Residiuals of 1 m Cardboard Box Lidar-Lite v3 Test

Figure 79 shows a bias in the data that trends above 100 cm to an average of ≈ 104.4 cm. Multiple tests were conducted, so more than likely, this bias exists naturally in the sensor, but this could also be a result of the test setup. Regardless, this bias is easy to calibrate in software. The more pertinent information is the graph of the residuals in figure 80. On average, the error between the expected value (100 cm) and the measured distance was 4.42 cm, which results in an average error of 4.42% of the expected value. During the standard discontinuity detection situation in figure 78, at the moment that the sensor detects the bottom of the discontinuity, the sensor expects to measure a value of 47.5 in (r_{req}). If the error from the test carries over, the sensor could detect a distance with an error of 4.42% of this measured value, or 2.10 in. Since this error is < the delta distance of 8.39 in, the sensor is capable of detecting the presence of the discontinuity.

Like the RPLIDAR A2M8, the Lidar-Lite v3 must interface with the physical C&DH system and the software architecture in order to fully satisfy both of the aforementioned requirements. An interface diagram for one of these sensors is shown below.

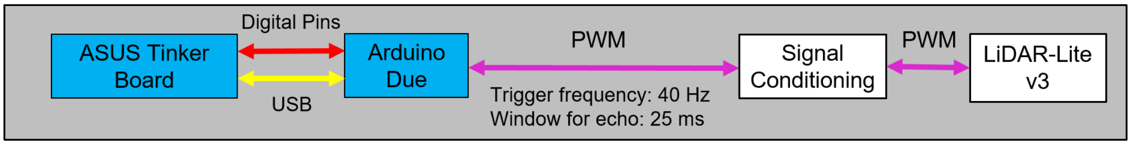

Figure 81: Interface Diagram for Lidar-Lite v3 and C&DH System

Unlike the RPLIDAR A2M8, the Lidar-Lite v3 is not directly connected to the Tinker Board, instead it it passed through a signal conditioning circuit which is connected to 2 PWM ports on the Arduino Due. In PWM mode, the signal conditioning that is absolutely necessary is outlined by the manufacturer to be a single 1 kΩ resistor to eliminate cross-talk between the trigger and echo pins on the Due. Filtering is most likely not necessary since the sensor is producing a digital signal and digital signals are usually resistant to system noise, but a noise characterization test midway through the testing phase will help determine if filtering is required.

Controlling the PWM signal requires some software integration as well. The Lidar-Lite v3 responds to PWM similarly to other comparable sensors, and does so with a trigger/echo signaling scheme utilizing one pin on the sensor. This sensor is triggered by pulling the mode-control pin to the LOW voltage (≈0 V). The sensor then pulses out a laser beam and waits for it to return to the device. Once received, the sensor pushes a HIGH voltage (≈5 V) to the same pin. The time it takes between the trigger and the echo is used to calculate the distance that the sensor measures. This modulation will be completed by software on the Arduino in a time that allows for the complete trigger/echo cycle of the sensor. The manufacturer claims that the sensor's maximum response time (which corresponds to its maximum range) is 20 ms, so to utilize all data that the sensor generates, the Arduino must trigger slow enough to create a large enough window for the sensor to be read accurately. The trigger frequency is ultimately a flexible design choice, since the team can utilize delays and other functions when programming the Arduino. A window of 20 ms requires a frequency ≤ 50 Hz, so the team has determined that a trigger frequency of 40 Hz (which corresponds to an echo window of 25 ms) offers a small safety margin that eliminates the possibility of accidentally discarding data.

Similarly to the in-plane condition, this sensor must also detect a discontinuity in time to allow for the CSR to stop before reaching it. This process is exactly the same as figure 76 because this sensor also utilizes LiDAR. However, Δt_0 can actually be approximated as $0s$ because the Lidar-Lite v3 is not a rotating sensor. Thus, $t_{tot} \approx \Delta t_4$, and therefore, from equation 29, $d_{stop} \approx 0.15m$. This value is $< d_{min}$, 0.95 m, so this sensor also allows for the CSR to stop in time before reaching a discontinuity.

In conclusion, the Lidar-Lite v3 achieves the physical specifications outlined by requirements SENS.3.1 and SENS.3.2, it has enough accuracy to detect a discontinuity at its specific mounting height and angle, and it integrates into the software architecture framework while interfacing physically with the CSR's C&DH system.

6.4.3. Depth Sensing for Discontinuity Traversal Mode System

The only requirement that this sensing condition is related to is SENS.3.2; this system must only detect discontinuity depths as the CSR traverses them. The design solution developed to solve this condition is two ultrasonic sensors, mounted on the underside of the CSR in the front and back, pointed directly at the ground and mounted in line with the front and back wheels. Described briefly in the discontinuity traversal mode subsection of the Guidance, Navigation, and Control section, these sensors are placed in line with the wheels so that the CSR knows if the front and back wheels are on the ground or over the discontinuity at any point during the traversal. These sensors are Itead Studio HC-SR04's and utilize pulse width modulation to measure distance. A picture of one of the sensors and both mounting locations is shown below.

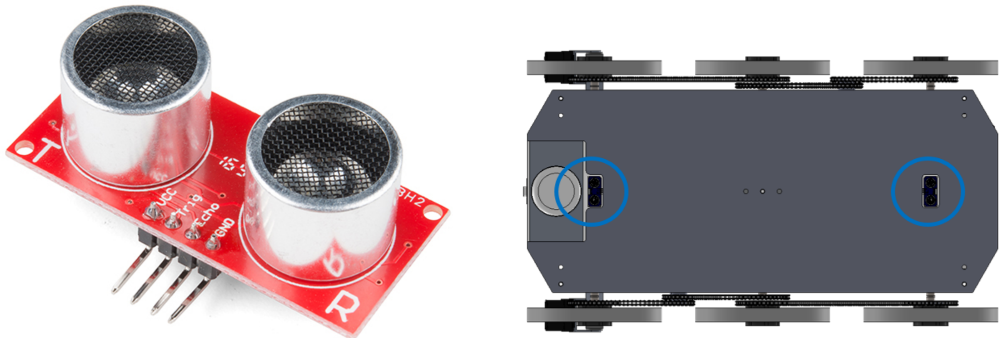

Figure 82: Itead Studio HC-SR04 and Bottom View of CSR showing Sensor Mounting Locations

The requirement SENS.3.2 defines the range specification or this sensor without a derivation. The sensors are mounted 2.4 in. above the ground, like the RPLIDAR A2M8, and the sensors must measure the discontinuity floor from this position. Since the depth of a discontinuity is defined to be at least 2.4 in, the required minimum range of the ultrasonic sensor is the depth plus the mounting height, or 4.8 in. The HC-SR04 has a maximum range of 0.5 m (19.7 in)[32], so the sensor is capable of achieving this range specification. It should be noted that discontinuities can be deeper than 2.4 in, so based on the capability of the sensor, the maximum depth that can be sensed is 17.3 in. Although the capability is limited, it still satisfies the requirement.

Below is the interface diagram showing the connections and specific PWM trigger frequency for the HC-SR04.

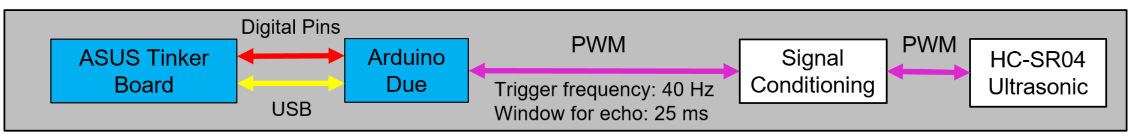

Figure 83: Interface Diagram for HC-SR04 and C&DH System

The connections are exactly the same as the Lidar-Lite v3, but without a resistor within the signal conditioning circuit. This is not needed since the HC-SR04 utilizes two different pins that monitor the trigger and echo signals independently. This circuit is still depicted in the interface diagram because the noise characterization test will help identify if filtering is required for this sensor's signal. Below is a timing diagram of one pulse width modulation cycle, from the manufacturer's datasheet[32].

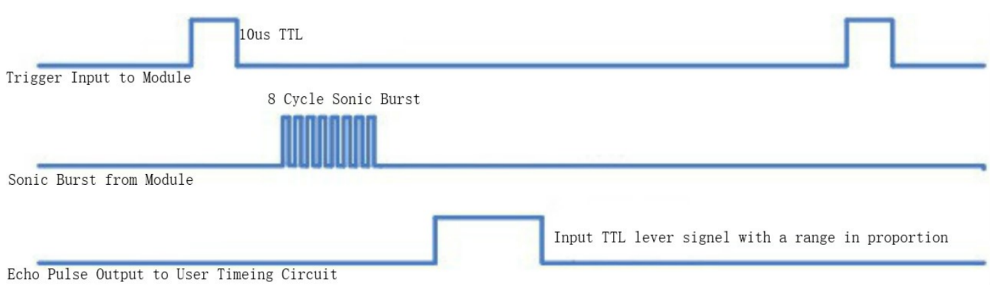

Figure 84: Timing Diagram for PWM Control on the HC-SR04

The sensor is triggered by pulling the voltage HIGH ($\approx$ 5 V) on the trigger pin. It responds by sending out a sonic burst at a particular frequency (40 kHz) and raising the echo pin to HIGH voltage. This pin will remain on a HIGH voltage until the echo, at 40 kHz, is received. The echo pin will then be pulled to a LOW voltage once again. The time that the echo pin is at a HIGH voltage is then used to calculate the distance of the closest obstacle within the ultrasonic sensor's field of view. The Arduino will still trigger this sensor at 40 Hz, so the echo window is the same as when the CSR is in semi-autonomous mode, 25 ms. The HC-SR04's maximum response time, based on the manufacturer's datasheet is 17.4 ms, so the 25 ms window still offers enough time for the C&DH to not discard data from this sensor.

In conclusion, the HC-SR04 achieves the range specification offered by the requirement SENS.3.2, while integrating into the software architecture framework and interfacing physically with the CSR's C&DH system.

6.4.4. Environment Sensing Control

To make the necessary sensors effectively detect an obstacle, discontinuity, and corresponding distance of discontinuity, an efficient approach integrating sensors to the controller is paramount. The single beam LiDARs and ultrasonic sensors are straightforward to control due to the fact of having available software for interfacing with them. The 360 LiDAR on the other hand is more sophisticated. As mentioned above, this requires the use of integrating the data readings using a ROS package across a USB interface. This interface diagram for the entire Sensing system, incorporating the design solutions for all three sensing conditions, is shown in Figure 85.

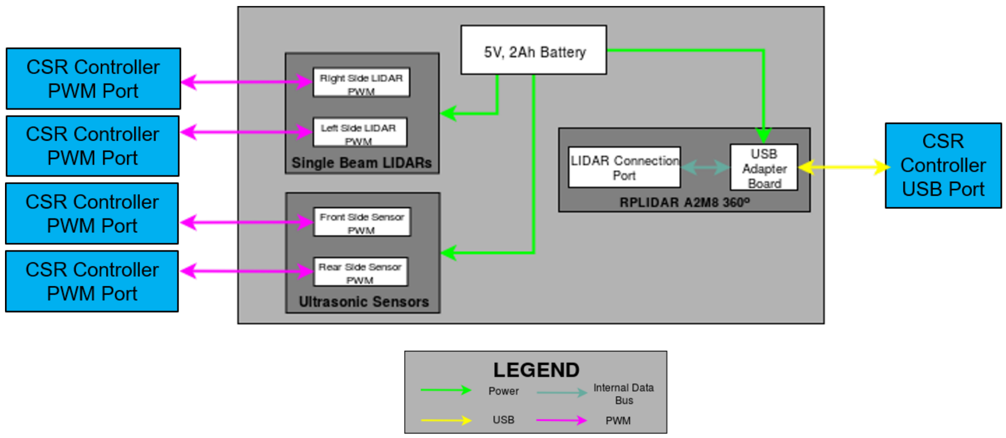

Figure 85: Hardware Interface Diagram for Environment Sensing that Comprises of Ultrasonic Sensors, Single Beam Lidars, and the 360^o Lidar Scanner

Below in figure 86 is a power block diagram for the devices in the Sensing subsystem. Since the two controllers being used will primarily be used for collecting data from the CSR's sensors, a separate power supply is needed for these sensors.

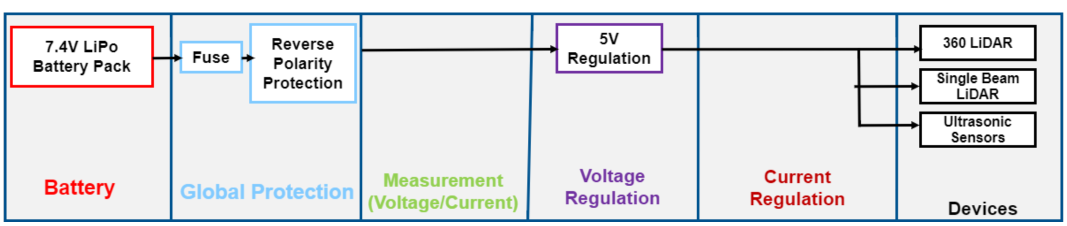

Figure 86: Power Distribution Block Diagram (Sensing).

Two batteries of the following type will be used for the sensing subsystem: Lithium Ion Battery - 3.7 V 2000 mAh, combining for a capacity of 4000 mAh. For a one hour mission, the total capacity required for this subsystem is 1.3 Ah, and the the total capacity is 4.00 Ah, leaving a 68 percent margin capacity for this extended mission.

7. Verification and Validation

Author: Ashley Montalvo

Shown below is a table specifying the main verification and validation phases the team will follow in the Spring. Phases 1-3 are broken up into date ranges in which the underlying tests should be completed.

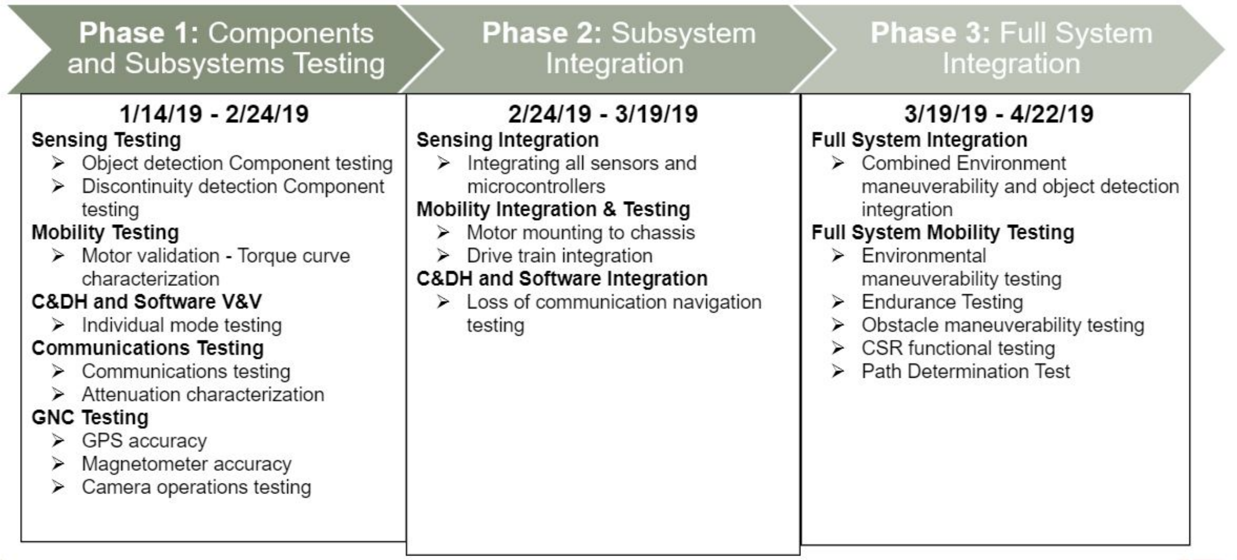

Figure 87: Verification & Validation Phases

All Major tests that verify critical requirements will be covered within this section and likewise are shown within the Main Tests Table. Supplementary tests and verification including smaller components testing, data analysis, and performance tests not directly related to requirements will be conducted in between the main tests listed.

Main Tests				
Test	**Test Date**	**Test Location**	**Subsystem**	**Requirements Verified**
Object Detection Component Testing	1/22	CU Business Field	Sensing	SENS 3.1, SENS 3.1.1, SENS 3.1.2
Camera Operations Testing	2/5	CU Boulder South	Sensing, GNC	SENS 5.1, SENS 5.1.1, SENS 5.1.3
Communications Testing	2/19	CU Boulder South	Communication	COMM 1.1, COMM 2.1, COMM 2.3, COMM 2.4, COMM 2.5
C&DH Testing and Integration	2/24-3/19	ITLL	C&DH	CDH 1.1, CDH 1.2, CDH.2.1
Sensing Integration (Object Detection & Discontinuity Testing)	2/24-3/19	Senior Project Room	Sensing, C&DH	CDH 1.1, SENS 3.1, SENS 3.3
CSR Functional Testing	3/19	Parking lot and gravel areas (flat ground)	Mobility	MOB 3.1
Environmental Maneuverability Testing	3/26	CU Boulder South	Mobility	MOB 3.4, MOB 3.4.1
Obstacle Maneuverability Testing	4/7	Open Field & 20 ° slope next to ITLL	Mobility, Full System Test	MOB 3.2, MOB 3.3
Path Determination Test	4/14	Open Field & 20 ° slope next to ITLL	Full System Test	CSR 1, CSR 2, CSR 3, CSR 5

Table 45: Major Tests

7.1. Object Detection Component Testing

Objective

This testing will determine the FOV, range, and angular resolution of the 360° LiDAR and verify objects within 103.5° and at least 1 inch in width are detected from 1 meter away. This testing will verify requirements SENS 3.1, SENS 3.1.1, and SENS 3.1.2.

Test Plan

Both tests for the 360 ° LiDAR are shown in the figure below and will be conducted on CU's business field to ensure no unwanted in-plane obstacles will be detected. The team will reserve a small section of the business field by talking to the scheduling staff at least 3 weeks in advance. First, for the FOV & range test it should be verified the LiDAR is positioned 2.4 in. above the ground (mounting height on the CSR). Two boxes at least 2.4 in. in height should be placed 1 ft from the LiDAR such that the "box-LiDAR-box" angle is 103.5 °. Once it is verified the LiDAR can detect the boxes within its FOV, the angle between the boxes should be increased until they are at the edge of the LiDAR's FOV. At this point the final FOV should be recorded and confirm this values is greater than 103.5 ° in order to meet requirement SENS 3.1.1.

Next, for the Angular resolution test a pole with a 1 in. diameter should be placed 1 m (3.28 ft) from the LiDAR. To verify the sensor is able to detect this pole and meet requirement SENS 3.1.2, at least 2 data points should be returned with the 1 m distance. The pole will then be moved farther away from the LiDAR and the test repeated until 2 data points are no longer returned with the pole's distance. The angular resolution can be calculated based on the object size and the farthest distance the LiDAR is able to detect the obstacle.

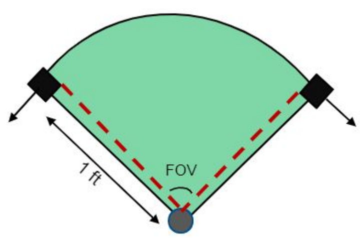

a) FOV & Range Test

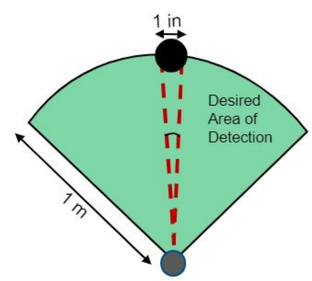

b) Angular Resolution Test

Figure 88: Obstacle Detection Component Test Setup

Required Equipment & Measurements

The equipment required for this test includes one 360 ° LiDAR, one 1 in. diameter pole, and two boxes (taller than 2.4 in). An Arduino Due will be connected to the LiDAR and programmed such that it returns the 25 closest data points (heading and distance). This live data will be utilized to adjust the placement of the obstacles during the test. Testing errors may include both human error (correctly measuring the "true" distance to the obstacle) and sensor measurement error. Mitigation will include using a tape measure to place obstacles at precise distances and comparing the true and measured distances to characterize the average sensor error.

7.2. Camera Operations Testing

Objective

Camera operations testing will be used to verify the camera system's FOV, determine a quality length of time for video/image transmission, and verify Standard Definition resolution. The results will be used to verify requirements SENS 5.1, SENS 5.1.1, and SENS 5.1.3.

Test Plan

A FOV test will be conducted first by taking images and video at CU Boulder's South Campus due to its ideal tree density. The outermost objects in the image will be located and compared to the actual degree measurement/ arc length of the distance between the trees on site. The next test will involve image and video transmission. The user should turn the camera on, take a 10 second video which spans around the forest at the testing location, and sends the data to the ground station at a distance of 250 m. Once the transmission is received by the ground station, the resolution of video will be checked to verify it meets Standard Definition quality, meaning the rate of transmission is less than or equal to 30 fps.

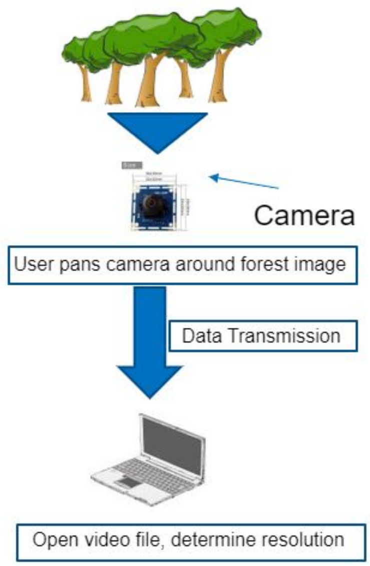

Figure 89: Camera Operations Test Setup

Required Equipment & Measurements

Necessary hardware will include one 180 ° Fisheye Lens camera, one Ubiquiti Radio for data transmission, one ASUS Tinker Board and the Ground Station computer. The largest source of testing error will be the human error in measuring the camera FOV. However, since the SENS 5.1.3 requirement is for the video device to have a FOV of at least 100 ° and the camera being used is commercially rated to have a 180 ° FOV, the error in the FOV measurement will be insignificant unless it exceeds 80 °, which is highly unlikely.

7.3. Communications Testing

Objective

This test will be used to determine the largest tree depth for successful transmission and reception of data and will also ensure video, GPS, and sensor data can be transmitted and received. This testing will verify requirements COMM 1.1, COMM 2.1, COMM 2.3, COMM 2.4, and COMM 2.5.

Test Plan

Communications testing will be conducted on CU South Campus due to its abundance of both trees and open space. To conduct this test, live video and regular intervals of simulated magnetometer and GPS data will be sent at a distance of 250 m from the CSR radio to the Ground Station radio and relayed to the MR radio by using the Linux Ping Command. The tree depth between the CSR and Ground Station and between the MR and Ground Station will be increased so the maximum tree depth can be found. This will be determined by analyzing the signal strength sensitivity of the radio transmissions.

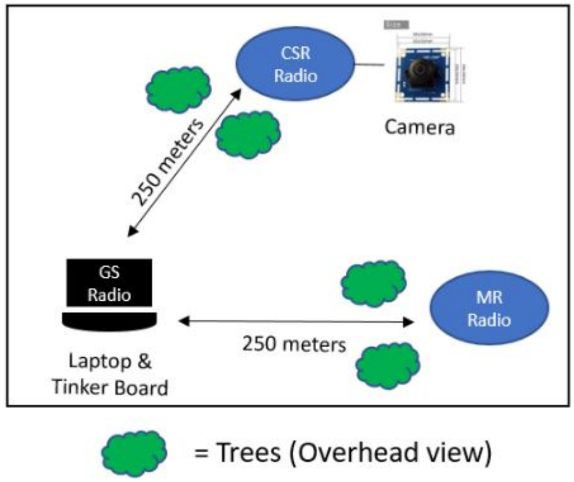

Figure 90: Communications Test Setup

Required Equipment & Measurements

To conduct this testing, the team will need two Ubiquiti Radios, one Laptop, one ASUS Tinker Board, and one USB Camera. As previously mentioned, the signal strength sensitivity of the radio transmissions will be the main test measurement. Testing errors will include the measurement of tree depth and densities and the estimate of the simulated data packet sizes. Once the team's magnetometer component tests are completed and sample data is gathered, however, the data packet size will be known which will mitigate the estimation error.

7.4. C&DH Testing and Integration

Objective

The following tests will verify the C&DH system can process commands by identifying, distributing, and timestamping commands and data as well as ensure the C&DH system handles mode changes as intended. Requirements CDH 1.1, CDH 1.2, and CDH.2.1 will be met through this testing.

Test Plan

This C&DH verification will be used to confirm each mode can accomplish the stated objectives and complete the following functional mode tasks. After ROS software is implemented and main program functions are written the user should determine the following main items by inspection. Note, tests including sensor signals will be simulated for this testing.

Mode 1 Verification (Manual Mode):

- Verify magnetometer correction algorithm returns correct angle between current heading and LOI location
- Verify GPS coordinates are reported when a user command is given (the saveAndSendGPS() command should be called)
- Verify time stamped data is received with returned data
- Verify Mobility commands are published when forward, backward, or turn commands are sent by the user
- Verify when system checks for loss of communications the check returns NULL

Mode 2 Verification (Semi-Autonomous Mode):

- Verify magnetometer correction algorithm returns correct angle between current heading and LOI location
- Verify stop command is sent to Mobility when an "object detected" signal is received from the Arduino

Mode 3 Verification (Discontinuity Traversal Mode):

- Verify stop command is sent to Mobility from the Arduino when the Ultrasonic sensor detects the ground after crossing the discontinuity
- Verify linear mass stage movement command is sent to Mobility to move the moving mass from back to front after the stop command is sent to Mobility
- Verify move command is sent to Mobility after the linear mass stage has been moved
- Verify stop command is sent to Mobility from the Arduino when the second Ultrasonic sensor detects the ground after crossing the discontinuity
- Verify linear mass stage movement command is sent to Mobility to move the moving mass from front to back after the stop command is sent to Mobility

Mode 4 (Loss of Communications Mode):

- Verify the ability to compare the current GPS coordinate to the last known saved GPS coordinate by using the compareGPS() function
- Verify a stop command is sent to Mobility once the current GPS reading is within 5 meters of the last saved GPS point

Required Equipment & Measurements

The equipment and software needed for this test includes the ASUS Tinker Board, Arduino, Ground Station laptop, ROS main program and mode functions. Since these tests will be verified by inspection, required measurements will either not be necessary or will be minimal and test-specific.

7.5. Sensing Integration (Object Detection & Discontinuity Testing)

Objective

The purpose of this testing is to properly integrate the LiDAR and Ultrasonic sensors with the C&DH system. More specifically, it will be determined if an Arduino connected to a single beam LiDAR or Ultrasonic sensor will send a mode change signal when detecting a discontinuity and if an Arduino connected to a 360 ° LiDAR will send a mode change signal when detecting an obstacle when all three sensors are connected to the Arduino. This will verify requirements CDH 1.1, SENS 3.1, and SENS 3.3.

Test Plan

The first test will be conducted for the single beam LiDAR. Note that all tests will be conducted at the ITLL. As shown in Figure 91 the single beam LiDAR should be mounted on a tripod at a height of 13.1 in. above the ground at an angle of 74.8 °. A box the height of a discontinuity (2.4 in.) will be placed 1 m (3.3 ft) from the LiDAR and moved toward it until the LiDAR beam detects the floor. At this point the Arduino should send a ”STOP” signal to the Tinker Board which alters the GNC mode from 2 to (semi-autonomous to manual mode). Thus, a successful test will simulate the signal the Arduino should send to the mobility system to command the CSR to stop 1 m from a discontinuity (LiDAR reading > 3.4 ft +/- threshold).

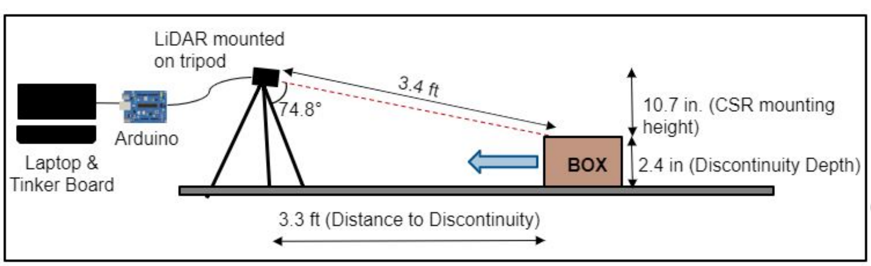

Figure 91: Single Beam LiDAR Test

The Ultrasonic sensor test will be conducted similarly to the LiDAR test, depicted in Figure 92. A piece of plywood will be held 2.4 in. in front of the Ultrasonic sensor to represent the height the sensor will be mounted above the ground. The plywood will be moved 2.4 in. away from the sensor to simulate the CSR traversing over a discontinuity. Once the Ultrasonic reading is 4.8 in. +/- threshold a "MOVE" signal should be sent from the Arduino to the Tinker Board which will alter the GNC mode from 2 to 1. Thus, a successful test will simulate the signal the Arduino should send to the mobility system to command the CSR to stop when the first wheel crosses the discontinuity. Once the CSR is stopped the moving mass will be commanded to move from the back to the front of the CSR so it can successfully cross the discontinuity.

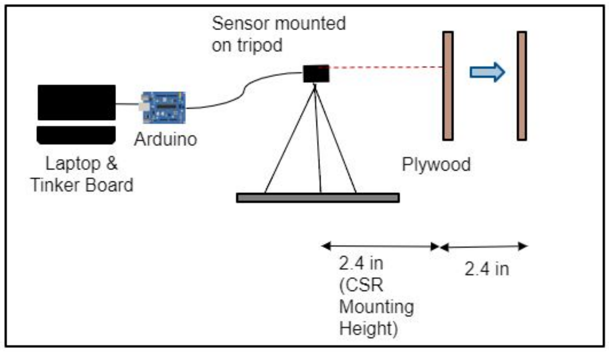

Figure 92: Ultrasonic Sensor Test

Lastly, a test will be conducted to determine if the 360 ° LiDAR is correctly integrated with the C&DH system. A 1 in. wide by 3 in. tall cylinder/pole should be moved towards the LiDAR.When the object is 1 meter (3.3 ft) away from the LiDAR, the Arduino should send a "STOP" signal which will alter the GNC mode from 2 to 1 on the Tinker Board and will ultimately signal the CSR to stop 1 m before encountering an obstacle greater than 2.4 in.

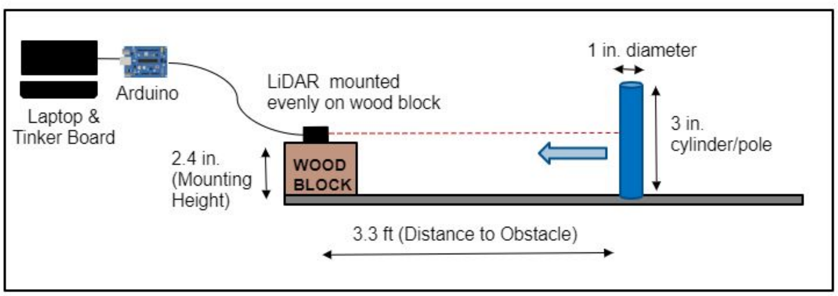

Figure 93: 360 ° LiDAR Test

Required Equipment & Measurements

The required test equipment includes one single beam LiDAR, one 360 ° LiDAR, one Ultrasonic sensor, one Arduino Due, one ASUS Tinker Board, and the Ground Station laptop. The CDH modes should be written in ROS and implemented on the Tinker Board before the test is conducted. Potential test errors include small human error in setting up obstacles at the correct distance from the sensors and sensor error. Similar to the Object Detection Component Testing error mitigation, the sensor error can be characterized by comparing the "true" distance to the measured distance and taking the average over a period of time (at least 1 minute).

7.6. CSR Functional Testing

Objective

This will be a basic test to verify the mobility system is properly functioning and the CSR can drive forward, in reverse, and perform a 360 ° turn. This will verify requirement MOB 3.1 and will indicate the CSR is ready to conduct subsequent mobility tests.

Test Plan

This test will be conducted on flat ground, initially in a parking lot and again on a gravel terrain to observe any slippage or traction issues. The CSR will be controlled with the LabVIEW command interface (Figure 95) and it will be verified the forward, reverse, and 360 ° turn maneuvers are completed successfully.

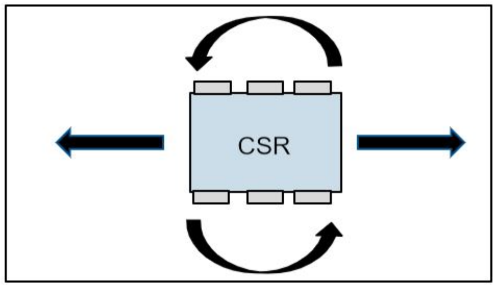

Figure 94: CSR Functional Test Setup

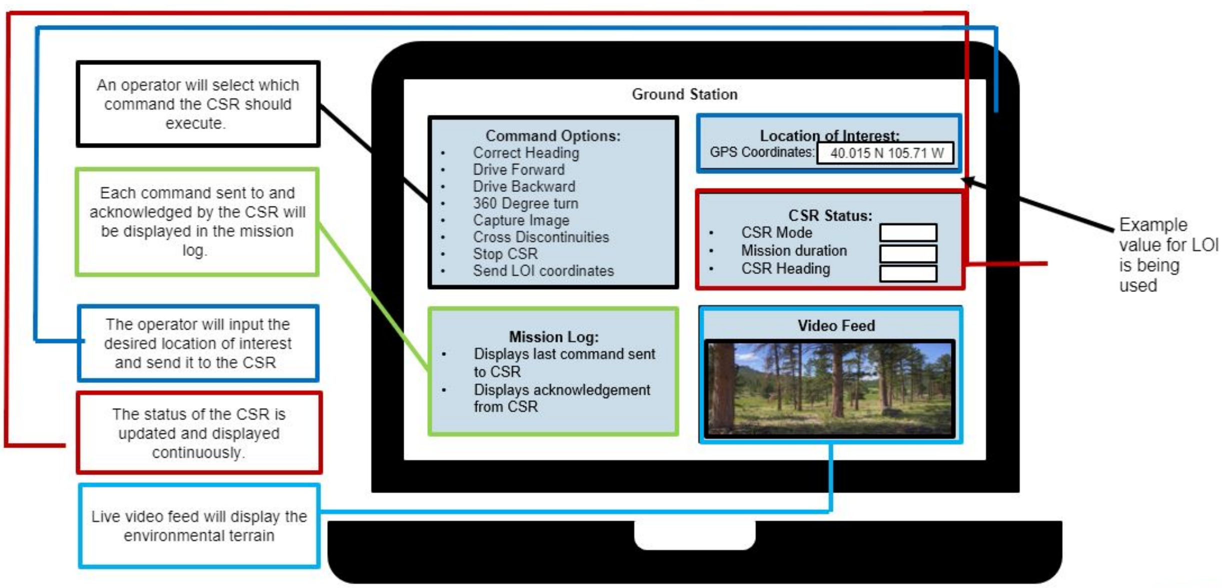

Figure 95: LabVIEW Command Interface

Required Equipment & Measurements

This test will require the full CSR mobility system (motors, motor mounts, and mobility power source) and chassis as well as the Ground Station computer, Ubiquiti radios, Asus Tinker Board (for modes and commands), and LabVIEW interface. All user commands will be made within the LabVIEW interface. In addition to testing the CSR's functionality, the torque and power consumption will be monitored, for performance analysis, to ensure the torques and currents line up with preliminary analyses done in the Fall Semester.

7.7. Environmental Maneuverability Testing

Objective

This test will prove the CSR is able to drive through underbrush (See Terrain Definition) and drive over a 2.4 in. step/obstacle in order to verify requirements MOB 3.4 and MOB 3.4.1.

Test Plan

This testing will take place on CU Boulder's South Campus since it has ideal rocky trail terrain, small slopes, and light grass. To determine if the CSR is able to cross over 2.4 in. obstacles and meet requirement MOB 3.4.1, a test will be conducted where the CSR drives over a wood block 2.4 x 2.4 x 16 in. An L-bracket should be attached to both 2.4 x 2.4 in. sides of the block and secured to the ground with stakes. The test will be successful if the CSR is able to traverse over the block. The second test will involve manually driving the CSR through the terrain on CU South Campus to verify requirement MOB 3.4.

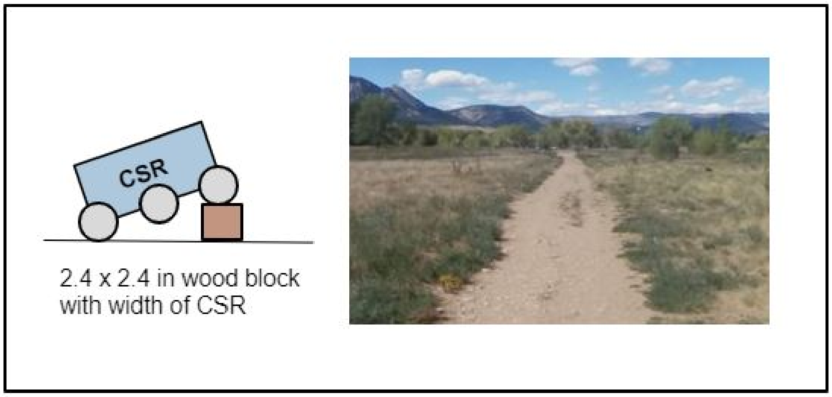

Figure 96: Environmental Maneuverability Test Setup & CU Boulder South Terrain

Required Equipment & Measurements

This test will require the full CSR mobility system (motors, motor mounts, and mobility power source) and chassis as well as the Ground Station computer, Ubiquiti radios, Asus Tinker Board (for modes and commands), and LabVIEW interface. Alike the functional testing, all user commands will be made within the LabVIEW interface. Torque and power consumption will be monitored for performance analysis, but are not required for successful completion of the mobility requirements.

7.8. Obstacle Maneuverability Testing

Objective

The Obstacle Maneuverability testing will involve running full system tests to verify all subsystems can correctly work together. It will be determined if the CSR can traverse over discontinuities, up and down 20 ° slopes, and meet requirements MOB 3.2 and MOB 3.3.

Test Plan

The discontinuity traversal test will be conducted on a self-constructed discontinuity in an open field or backyard. The team will dig a trench 2.4 x 9 x 16 in. and line the interior with plywood for sharp corners as depicted in the project ConOps. The CSR will be placed 1 meter away from the discontinuity, drive until the 1st wheel crosses the discontinuity, stop and transfer the moving mass from back to front, and continue crossing. The goal is for this process to be autonomous while in Mode 3 (discontinuity traversal mode) which will meet our level 3 success for controls. However, if this cannot be accomplished by April 5th, the team will conduct a manually controlled test while still utilizing the ultrasonic sensor data which will still meet our level 2 success.

The 20 ° slope test will be conducted next at the same location DRIFT conducted their 20 ° slope test for the MR. This slope is next to the ITLL and based off of the DRIFT team's measurements the slope varies from 19-24 °. Since it was verified the MR can traverse up and down this slope, if the CSR can traverse this same terrain it will prove the MOB 3.3 requirement will be met and the path is indeed suitable for the MR to travel over. Both test plans are shown in the figure below.

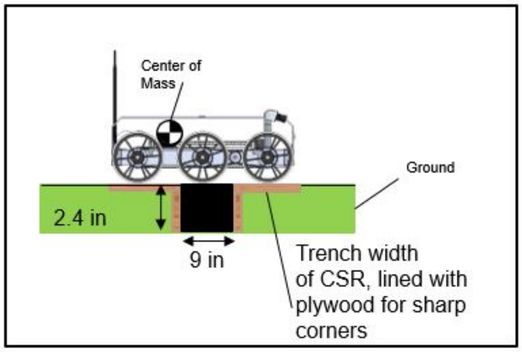

a) Discontinuity Traversal Test

b) 20 ° Slope Test

Figure 97: Obstacle Maneuverability Test Setup

Required Equipment & Measurements

This test will require a fully functional CSR with an integrated mobility system, moving mass, sensing system, communications system, and C&DH functionality. This testing will also require two 2.4 in. x CSR width planks of plywood, one 9 in. x CSR width plank of plywood, Ground Station computer, Ubiquiti radios, Asus Tinker Board (for modes and commands), and LabVIEW interface. All commands will be made with the LabVIEW interface. The tests will be successful if the CSR can cross the discontinuity and drive up and down 20 ° slopes.

7.9. Path Determination Test

Objective

The purpose of this test is to determine if the CSR is able to complete a scaled down end-to-end mission including obstacle detection, operator commanded obstacle traversal or avoidance, and pathpoint communication. This test will also focus on determining the validity of the final path. This test will verify functional requirements CSR 1, CSR 2, CSR 3, and CSR 5.

Test Plan

This test will be a small scale representation of the overall project ConOps. Thus, the CSR will travel only 50 m to a location of interest and will be required to travel around a tree, over a discontinuity (made of plywood pieces 2.4 inches high, and 9 inches long), as well as up and down a 20 ° slope. The viability of this path for the MR will be tested by following the CSR with a 5 ft wide pole (width of MR) as it completes the test. Since the GPS is accurate to 2.5 cm, as long as the 5 ft wide pole is at least 2.5 cm away from any given non-traversable obstacle, it can be verified the path is viable. The accuracy of the GPS will be further verified in the test environment once obtained and if this number differs, the test plan will be modified accordingly.

After the CSR reaches the LOI and returns the path coordinates, the user should now have a list of GPS points in which the MR is able to travel along to reach the LOI. An additional or alternative verification strategy will be to complete a "walk-through" test. The user will plug the GPS coordinate list into a phone, slowly follow this given path so it's as accurate as possible, and determine if the MR can fit on this path by holding the 5 ft wide pole while walking. This process should be repeated a total of at least 5 times to verify this path is accurate enough such that it is viable for the MR traverse and to mitigate human error. A day in the life testing ConOps is shown in the figure below, to show how the CSR will be tested against a discontinuity, a traversable and non-traversable obstacle, a slope, and arriving to the location of interest.

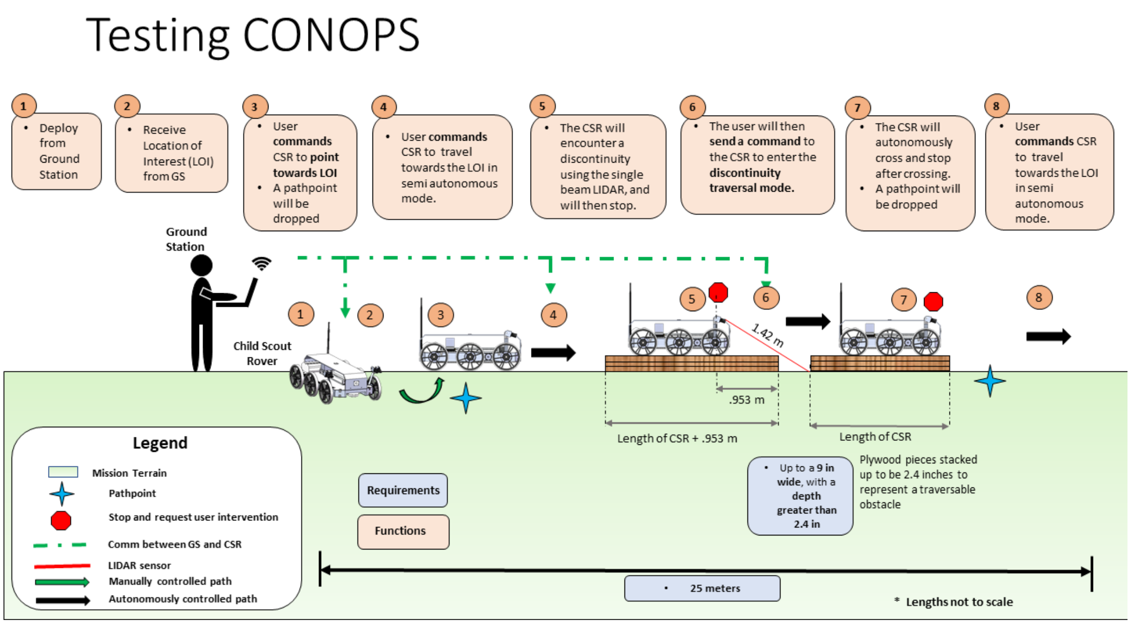

Figure 98: Path Determination Test

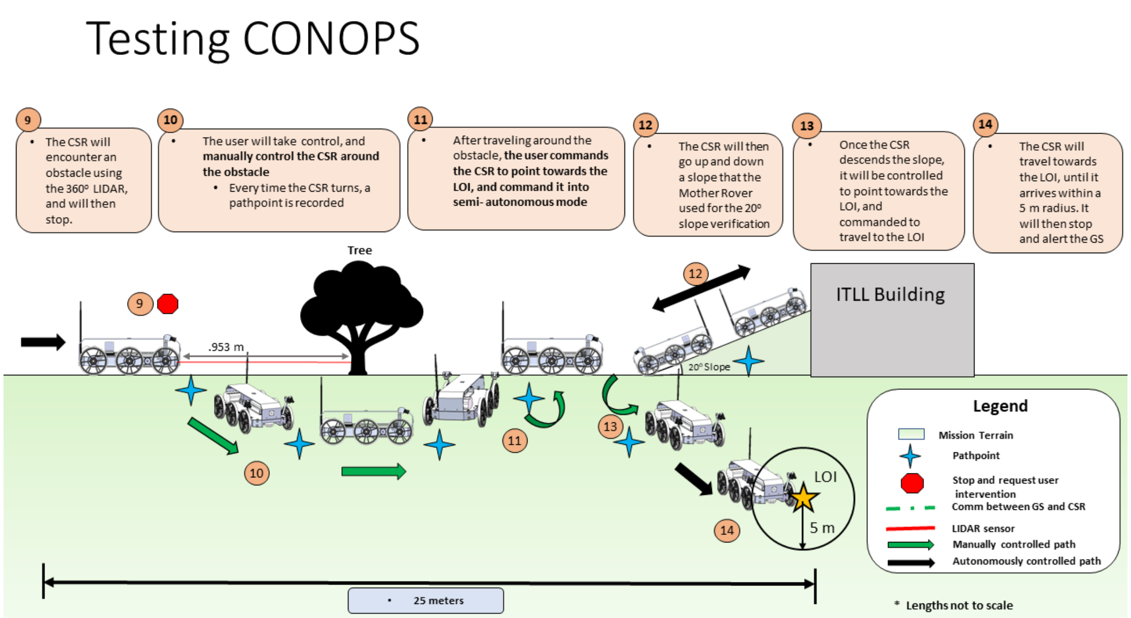

Figure 99: Path Determination Test Continued

Required Equipment & Measurements

This test will require the fully functional CSR with an integrated mobility system, sensing system, communications system, and C&DH functionality. All commands will be made with the LabVIEW interface and the comsumption of torque and power will be monitored throughout the test for performance analysis. As previously stated, GPS error will be characterized through environment testing and human error will be mitigated by repeating multiple“ walk-through” tests.

8. Risk Assessment and Mitigation

Author: Katelyn Griego

A risk assessment was performed on the final design of the CSR. Through this assessment, specific risks were identified in achieving the project objectives. The risks addressed were split into four categories: technical, schedule, safety, and financial. Risks were identified by considering all subsystems throughout the design, fabrication, and testing life cycle, as well as the impacts on the functional requirements. Each risk was evaluated two criteria; likelihood and consequence on a 1-5 scale, with 5 being the most impactful. The two ratings were then multiplied to obtain a final score. The rating criteria is show in Tables 46 and 47. After consideration, two groups of risks prevailed, technical, T, and schedule, S. Table 48 depicts the associated risks and their effects and ratings.

Consequence		
Level	**Technical, T**	**Schedule, S**
1	Minimal or no impact	Minimal or no impact
2	Small reduction in technical performance	Additional activities required; able to meet key dates
3	Some reduction in technical performance	Minor schedule slip; will miss need date
4	Unacceptable; but workarounds available	Program critical path affected
5	Unacceptable; technical goals cannot be achieved	Cannot achieve key program milestone

Table 46: Severity

Likelihood	
Level	**Likelihood**
1	Not Likely
2	Low Likelihood
3	Likely
4	Highly Likely
5	Near Certainty

Table 47: Likelihood

Risks					
Risk	**Description**	**Effect**	**Likelihood**	**Consequence**	**Total**
CDH.1.S	Software development is complex and timely	System integration will not be possible. Functional requirements cannot be verified and validated. Schedule will not be met.	5	5	25
SENS.1.T	Integration of 360° LiDAR is too complex	Solution would require extensivetime and resources, which would affect other critical project elements.	4	4	16
MOB.1.T	Motors and motor controller failure due to overheating stemming from stalling, back current, power cycling	The motor does not function properly and cannot complete mission successfully.	3	5	15
COMM.1.T	Data budget deficit	Unable to send all necessary data back to the GS (video/images, GPS, magnetometer) leading in failure to reach LOI.	3	5	15
SENS.2.T	Noise interference on magnetometer from motors	Data from the magnetometer is incorrect and therefore cannot accurately correct heading.	5	3	15
COMM.2.T	Error uncertainties of GPS and magnetometer data through trees	Error in readings greater than specifications, may result in error greater than 5m at LOI	5	2	10
MOB.3.T	Chain slippage	Tension is not sufficient to drive CSR.	3	3	9
MOB.4.T	Wheel slippage	May not be able to overcome obstacles.	4	2	8

Table 48: Risks

A matrix of the risks is shown in Figure 100. The green regions on the matrix represent acceptable risk where the opposite is true for the red regions. It can be seen that the top 5 risks fall in unacceptable regions. This is where most of our efforts as a team lie in regards to mitigations. This is explain next.

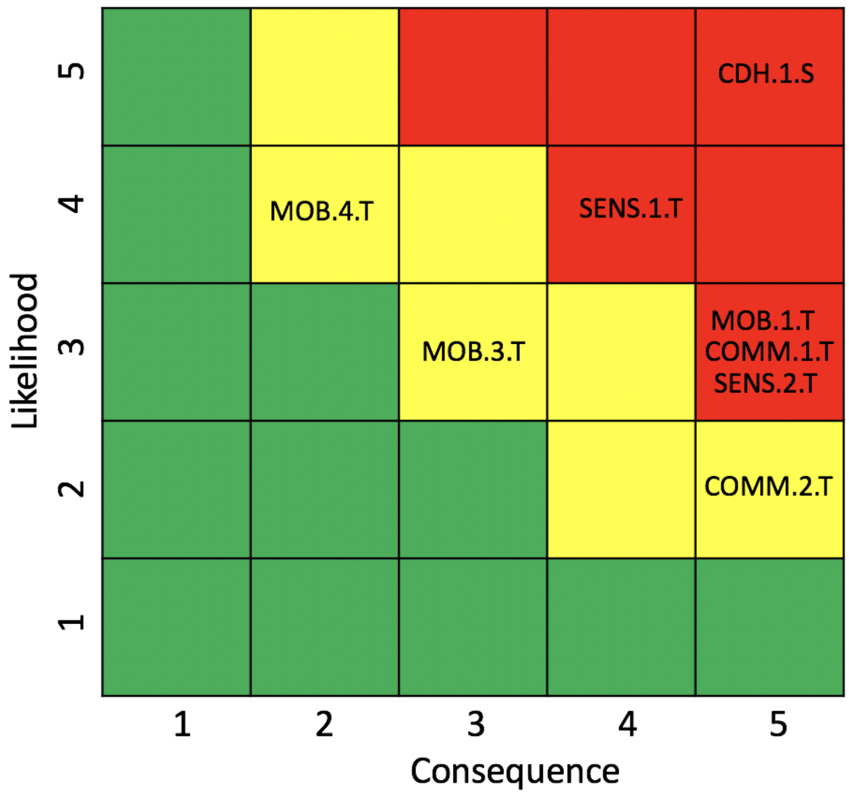

Figure 100: Pre Mitigation Risk Matrix

An analysis was then performed on each risk to mitigate their effects and decrease the scoring of each risk. The purpose of this is to plan for such high risks in that the consequences are not as great to the project. Mitigation plans were determined for each risk and new ratings were assigned. The mitigations relevant to each risk can be seen in Table 49.

A new risk matrix was then created after mitigations as seen in Figure 101. The risks have now all been moved into tolerable and acceptable regions.

Mitigations				
Risk	**Mitigation**	**Likelihood**	**Consequence**	**Total**
CDH.1.S	Allow enough time for software development with sufficient time margin, have an understanding of the complexity of the system through diagrams, begin to prototype with ROS early on, hold frequent code reviews	2	4	8
SENS.1.T	Members increase skill set with ROS early in schedule, members have taken a ROS introduction and have experienced resources, move to off-ramp options by February 4th	3	2	6
MOB.1.T	Ensure sufficient airflow around motors and implement heat sinks; utilize current limiters and monitor current	2	3	6
COMM.1.T	Allocate a sufficient margin in data budgets; start testing components early to validate data budget	1	4	4
SENS.2.T	Place the magnetometer a safe distance away from the motors. Test results show that 15cm should suffice, however if not can utilize mu-metal foil shielding	3	2	6
COMM.2.T	Start early component testing through tress to determine true error. Determine if this error is still within the 5m tolerance or implement feedback	3	2	6
MOB.3.T	Utilize chain tensioners	1	3	3
MOB.4.T	Design for non-slip conditions, research types of wheels used in this environment and preform trade studies, if slipping does occur can try another path	2	2	4

Table 49: Mitigations

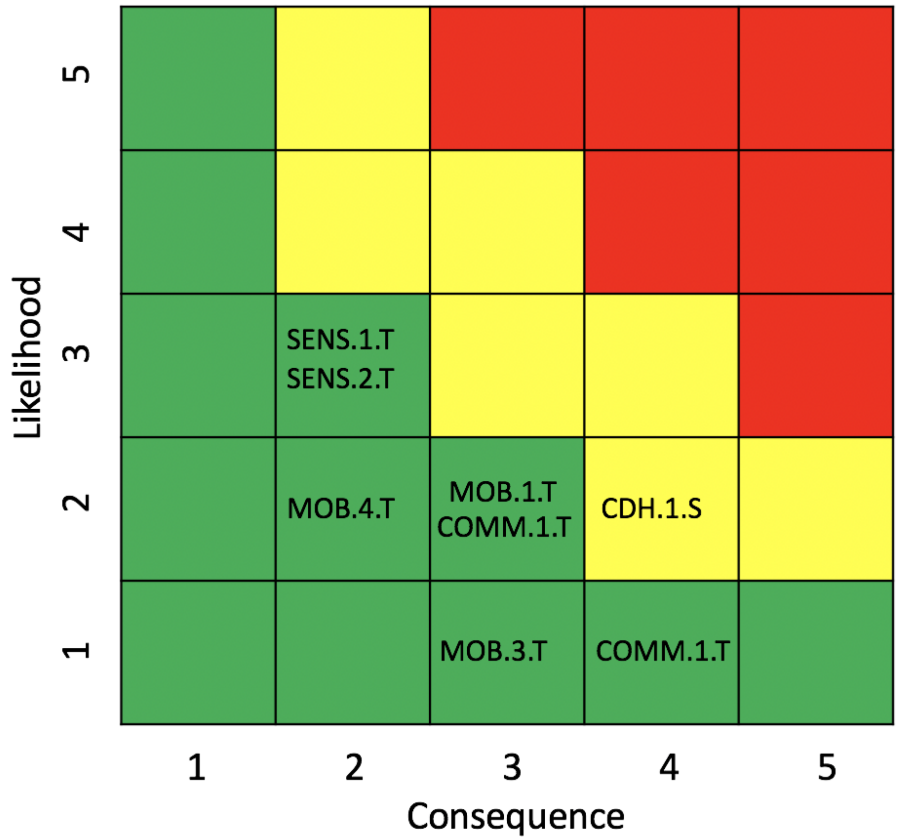

Figure 101: Post Mitigation Risk Matrix

9. Project Planning

Author: Marcos Mejia and Alexis Sotomayor

9.1. Work Breakdown Structure

All of the work products for the project were split into six main deliverable categories. These categories were determined based on critical project elements, and project milestones. Due to these the six main deliverables were determined to be Mobility, Control and Software, Communications and Electronics, Integration and Test, and the deliverables from both semesters. These main deliverables are shown in the figure below in grey. These main deliverables are broken down into sub deliverables that were determined based on project progress. The sub deliverables are listed in order under each main deliverable, so the deliverable before it must be completed in order to move onto the next one. The completed deliverables are shown in green, while the deliverables in progress are shown in yellow, and the future work is shown in white.

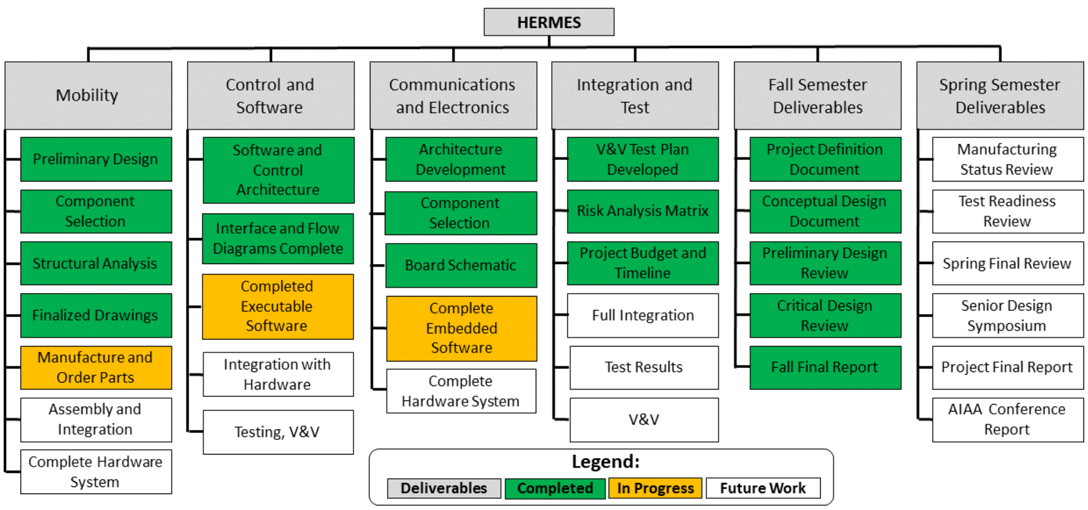

Figure 102: Work Break Down Structure

9.2. Organizational Chart

The organizational chart of the project is shown below, showing the leadership roles of all team members. The grey rounded boxes show main project contributors, while in light blue the system level leads are shown, and in blue the sub system level leads are shown. This structure is shown in the figure below, figure 103.

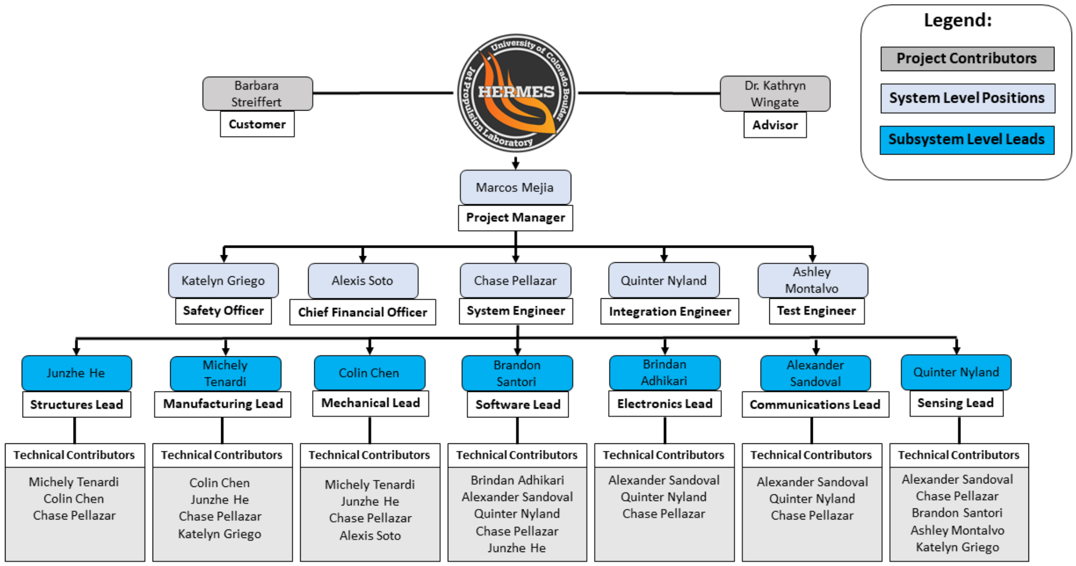

Figure 103: Organizational Chart

The main project contributors were the customer: Barbara Streiffert and Jet Propulsion Laboratory, the project advisor: Dr. Kathryn Wingate, and the course coordinator: Dr. Jeliffe Jackson. The HERMES project is then composed of the team members shown below. The main system level positions are the project manager, the safety officer, the chief financial officer, the systems engineer, the integration engineer, and the test engineer. Then the main subsystem level leads are the structures lead, manufacturing lead, mechanical lead, software lead, electronics lead, communication lead, and sensing lead.

9.3. Work Plan

The work plan showing the main tasks required to accomplish the WBS products and the course milestones are shown in the form of a Gant Chart below. The critical path shows how the project is affected by the milestones and products, and which of these are the most critical to the project and would push back the schedule if not completed on time. The project was divided down into five main phases, two manufacturing phases, and three testing phases. In the first manufacturing phase components will be assembled, constructed, and integrated. Specifically parts would be ordered, ROS background nodes and other main program functions will be written. Once parts arrive the hardware will begin to be manufactured and assembled, so the chassis will be milled in the Aerospace Machine Shop and the drive train will be assembled. Concurrently, the sensors will be integrated with the controllers, and the controllers will be interfaced with eachother (Aruindo Due and ASUS Tinkerboard). The objective of the second manufacturing phase is to integrate all subsystems into a final system by connecting the sensors and controllers into the chassis, the drivetrain with the chassis, and ensuring the system is functional after assembly. As for testing, testing will be completed in three phases. In the first phase, components will be tested individually to ensure they all work as expected. This would include ensuring all sensors provide required measurements, ensuring batteries last as expected, and that motors work with the provided power. These individual component tests will also be tested to begin verifying and validating requirements. The next phase is the subsystem level tests, so these phases will be conducted once all component level tests have been completed, and the objective of these tests is to ensure the system functions on a subsystem level. These would include subsystem level tests such as ensuring the controllers can work with the sensors and software. Lastly, there will be the final system level testing, which would occur after all subsystems have been verified to work in terms of hardware, software, electronics and more. The final system would complete the final verification and validation of requirements, and it would also verify the product is completed and functions as needed.

The margins were developed based on the difficulty and complexity of each of the expected task, as well as how much time in the schedule would be left to complete the rest of the tasks. The manufacturing phases, the component testing, and subsystem level testing phases were given 1 - 1.5 weeks of margin, because they would need to be completed within this timespan, otherwise the project would be pushed back. The margin on the final system testing was a sum of the previous margins.

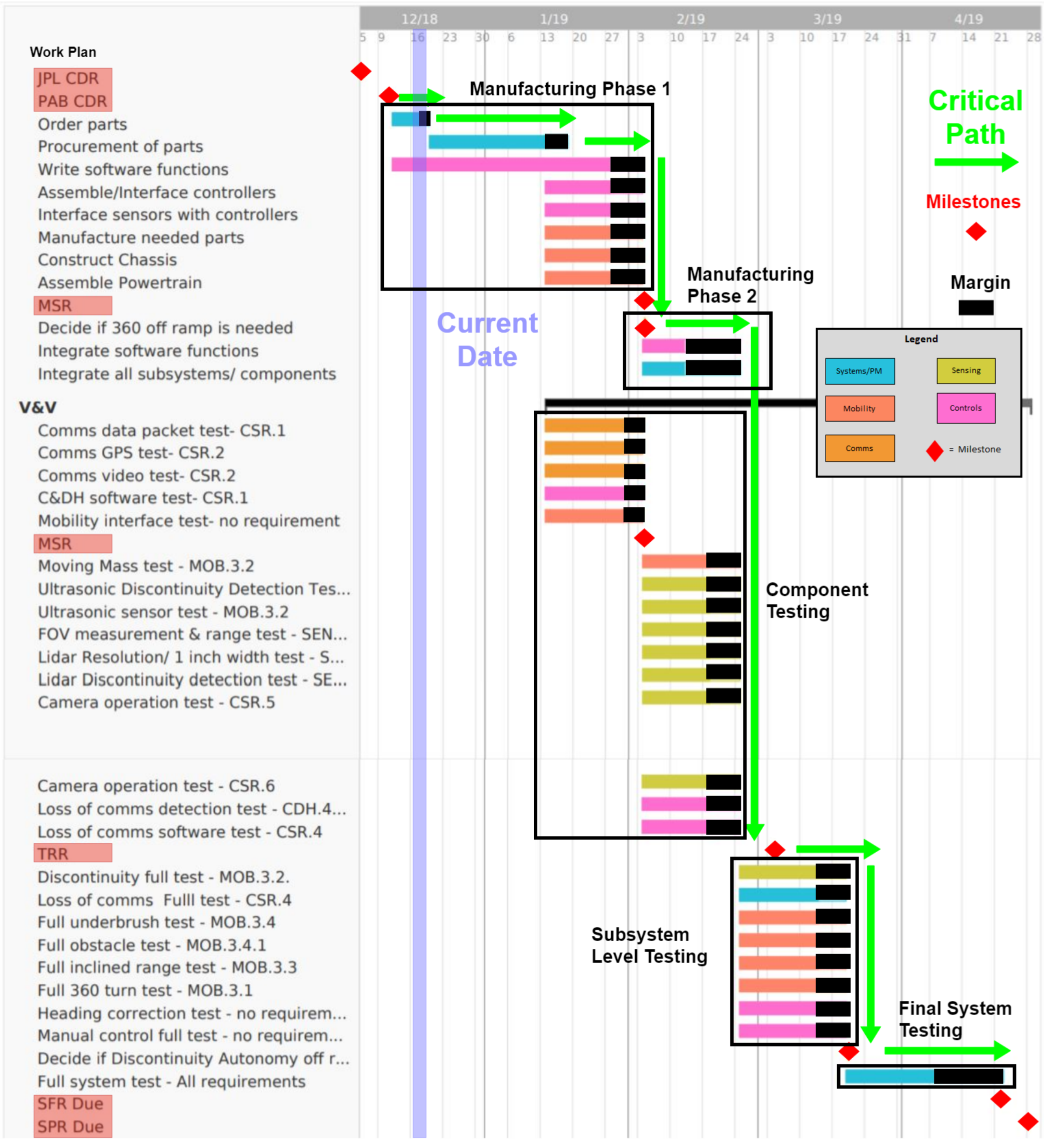

Figure 104: Work Plan

9.4. Cost Plan

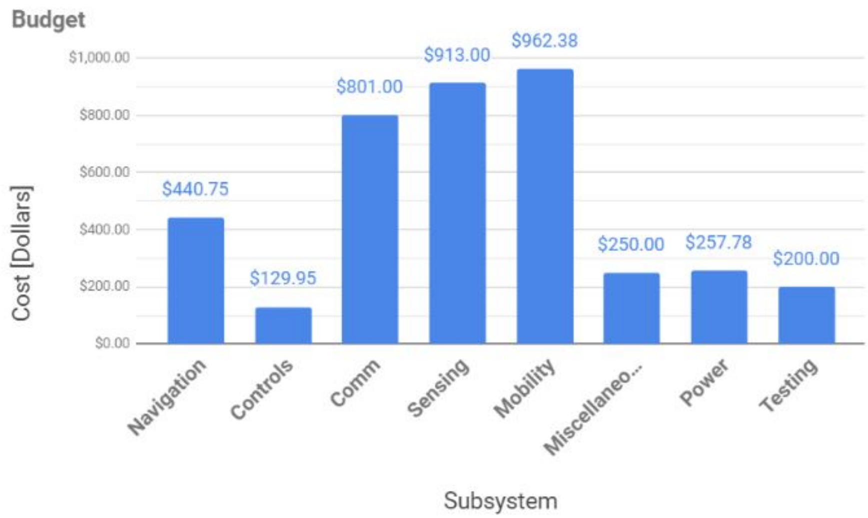

Figure 105: Projected Expenditures by Subsystem

The budget above depicts the projected expenditures by subsystem, with exact costs from a built of materials and a 15 percent margin built in. The most expensive subsystem will be the the mobility subsystem, followed by the sensing subsystem. A detailed Bill of Materials can be found in the appendix.

On December 14th, the HERMES team was notified that we received $1000 in funding from the Engineering Excellence Fund, after presenting a proposal to the committee back in October. The total budget so far, without a margin is $3954.86; with a 15 percent margin, this expected total budget jumps to $4548.09. With a total budget of (including the new EEF Funds) $6000, the expected remaining funds sit at $1451.91, a sufficient amount that will allow us to upgrade a camera or a LiDAR sensor, or buy redundant parts if deemed necessary later in the spring. Moreover, this extra funding can potentially be used to mitigate the challenges of the software in the Spring, by purchasing a more expensive LiDAR that can do more on its own and thereby requires less software development from the team.

10. Individual Report Contributions

- **Brindan Adhikari:**Communication System trade studies and criteria selection, Detailed Design - Communications
- **Colin Chen:** Detailed Design - Mobility
- **Katelyn Griego:** Conceptual Design GNC and Environmental Sensing, Object Detection trade studies, Imaging Trade Studies, Baseline Design - GNC and Environmental Sensing, Risks
- **Junzhe He:** Concept Design - Mobility, Detailed Design - Mobility
- **Marcos Mejia:** Project Information, Project Objectives, Conceptual Design - GNC Baseline Design - GNC, Detailed Design - GPS and Magnetometer, Project Planning, and Revisions and Editing.
- **Ashley Montalvo:** Verification & Validation, Object detection trade studies and criteria selection, grammar and consistency checks
- **Quinter Nyland:** Project Purpose, Conceptual Design - Environment Sensing Trade Studies, Detailed Design - Environment Sensing
- **Chase Pellazar:** Project Objective - Terrain Definition, Project Objective - Functional Block Diagram, Detailed Requirements, Guidance, Navigation and Control Trade Study, Detailed Designs' Power Distribution, Verification & Validation
- **Alexander Sandoval:** Concept Design Studies - Communication, Detailed Design - Communications, Detailed Design - Mobility (Control), Detailed Design - GNC (Pseudo Code, ROS Framework, Hardware Selection), Detailed Design - Environment Sensing (Control)
- **Brandon Santori:** Object Detection trade studies, Detailed Design - Guidance, Navigation, and Control
- **Alexis Sotomayor:** Detailed Design - Mobility, Updated Requirements, Introduction, Cost Plan, Power, Final Revision
- **Michely Tenardi:** Concept Design Studies - Mobility, Detailed Design - Mobility, Revisions

References

[1] Matchar, Emily. This NASA-Developed AI Could Help Save Firefighters' Lives. Smithsonian.com, Smithsonian Institution, 9 Sept. 2016, www.smithsonianmag.com/innovation/nasa-developed-ai-could-help-save-firefighters-lives-180960398/.

[2] Wong, J.Y. "Theory of Ground Vehicles 4th Edition", John Wiley and Sons, Inc.

[3] Friction Coefficients between different wheel/tire materials and concrete http://www2.mae.ufl.edu/designlab/Class%20Projects/Background%20Information/Friction%20coefficients.htm

[4] Skid Steering of Wheeled and Tracked Vehicles" Australian Army Engineering Development Establishment. http://www.dtic.mil/dtic/tr/fulltext/u2/a149826.pdf

[5] Shaft Collars Guide. Misumi, https://us.misumi-ec.com/pdf/fa/2010/p0235.pdf

[6] "How climate is changing", National Aeronautics and Space Administration, Retrieved September 8, 2018, from https://climate.nasa.gov/effects/

[7] "Is Global Warming Fueling Increased Wildfire Risks?", Union of Concerned Scientists, July 24, 2018, Retrieved September 8, 2018, from https://www.ucsusa.org/global-warming/science-and-impacts/impacts/global-warming-and-wildfire.html#.W5k8t-hKiUl

[8] "The Rising Cost of Fire Operations: Effects on the Forest Service's Non-Fire Work", United States Department of Agriculture, August 4, 2015, Retrieved September 8, 2018, from https://www.fs.fed.us/sites/default/files/2015-Fire-Budget-Report.pdf

[9] "Drone-Rover Integrated Fire Tracker (DRIFT)" Retrieved October 2, 2017 from https://www.colorado.edu/aerospace/sites/default/files/attached-files/jpl_fire_tracker_drift_cdd.pdf

[10] "Understanding Tree Basal Area", Thought Co., Retrieved September 26, 2018, from https://www.thoughtco.com/understanding-tree-basal-area-1341712

[11] "Wenthworth (1922) grain size classification", The Lanetary Society, Retreived September 26, 2018, from http://www.planetary.org/multimedia/space-images/charts/wentworth-1922-grain-size.html

[12] "Shrub Plant", The Editors of Encyclopaedia Britannica, Retrieved September 29, 2018 from https://www.britannica.com/plant/shrub#ref144502

[13] Dobson, Martin, and the Arboricultural Advisory and Information Service (1995). "Tree Root Systems" Arboriculture Research and Information Note. Arboricultural Advisory and Information Service, 130/95/ARB.

[14] "GPS Basics", Retreived September 28, 2018, from https://learn.sparkfun.com/tutorials/gps-basics/all

[15] "Inferno Critical Design Review" Retrieved September 28, 2018 from https://www.colorado.edu/aerospace/sites/default/files/attached-files/inferno_cdr.pdf

[16] "Design of Rocker Bogie Mechanism" Retrieved September 26, 2018 from https://www.researchgate.net/publication/313403109_Design_of_Rocker_Bogie_Mechanism

[17] "What is LIDAR?" Retrieved September 26, 2018 from https://oceanservice.noaa.gov/facts/lidar.html

[18] "Ultrasonic Detection Basics Application", El-Pro-Cus, Retrieved September 25, 2018, from https://www.elprocus.com/ultrasonic-detection-basics-application/

[19] Rouse, Margeret. "collision sensor", WhatIs.com, TechTarget, Retrieved September 23, 2018, from https://whatis.techtarget.com/definition/collision-detection

[20] Houston, Pete. ”Capture images in different formats with Raspberry Pi camera module”, Medium, Retrieved September 27, 2018, from https://medium.com/@petehouston/capture-images-in-different-formats-with-raspberry-pi-camera-module-757173386794

[21] Hoiem, D. ”Human Body Recognition and Tracking: How the Kinect RGB-D Camera Works,” University of Wisconsin-Madison, Retrieved September 23, 2018, from http://pages.cs.wisc.edu/~dyer/cs534/slides/17_kinect.pdf

[22] ”Different Wi-Fi Protocols and Data Rates”, Intel, Retrieved September 29, 2018, from https://www.intel.com/content/www/us/en/support/articles/000005725/network-and-i-o/wireless-networking.html#n.

[23] ”Basics of Streaming Video Production”, IBM, Retrieved September 29, 2018, from https://support.video.ibm.com/hc/en-us/articles/207852167-Basics-of-Streaming-Video-Production

[24] ”Zigbee FAQ”, Zigbee Alliance, Retrieved September 29, 2018, from https://www.zigbee.org/non-menu-pages/faq/

[25] ”4G LTE Speeds vs. Your Home Network”, Verizon, Retrieved September 29, 2018, from https://www.verizonwireless.com/articles/4g-lte-speeds-vs-your-home-network/.

[26] ”Detection of Single vs Multiple Antenna Transmission Systems Using Pilot Data”, IEEE Transactions on Signal and Information Processing over Networks, Retrieved September 29, 2018, from https://ieeexplore.ieee.org/document/7544507

[27] ”Radio wave propagation through vegetation: Factors influencing signal attenuation”, Radio Science, Retrieved September 29, 2018, from https://agupubs.onlinelibrary.wiley.com/doi/full/10.1029/2002RS002758

[28] ”Field of View - Rectilinear and Fisheye Lenses” Retrieved September 24, 2018 from http://www.bobatkins.com/photography/technical/field_of_view.html

[29] West, Mick. ”How to Take a Photo of the Curve of the Horizon”, Metabunk, Retrieved September 25, 2018, from https://www.metabunk.org/how-to-take-a-photo-of-the-curve-of-the-horizon.t8859/

[30] Slamtec. ”RPLIDAR A2 Low Cost 360 Degree Laser Range Scanner Introduction and Datasheet”, Slamtec, Retrieved November 13, 2018, from https://cdn.sparkfun.com/assets/e/a/f/9/8/LD208_SLAMTEC_rplidar_datasheet_A2M8_v1.0_en.pdf

[31] Garmin. ”Lidar Lite v3 Operatoin Manual and Technical Specifications”, Garmin, Retrieved November 4, 2018, from https://static.garmin.com/pumac/LIDAR_Lite_v3_Operation_Manual_and_Technical_Specifications.pdf

[32] Sparkfun. ”Ultrasonic Ranging Module HC - SR04”, Retrieved November 6, 2018, from https://cdn.sparkfun.com/assets/b/3/0/b/a/DGCH-RED_datasheet.pdf

[33] Kane, Jack, and EPI Inc. - Power and Torque -. Power and Torque: Understanding the Relationship Between the Two, by EPI Inc., www.epi-eng.com/piston$_{e}$*ngine*$_{t}$*echnology*/*power*$_{a}$*nd*$_{t}$*orque.htm.*

11. Appendix

The Bill of Materials is shown in the following images below. The image has the following information: subsystem, subassembly, part name, description, quantity, unit cost, total cost, component mass, and total mass.

Subsystem	Subassembly	Part Name	Description	Qty	Source	Unit Cost	Total Cost	Component Mass [lbm]	Total Mass [lbm]
Mechanical	Chassis	chassis_bot	Aluminum Chassis Base Plate	1	https://www.mcmaster	$69.02	$69.02	7.4	7.4
Mechanical	Chassis	chassis_top	Acrylic Top Plate (Cut from 0.25"x12"x48" sheet)	1	https://www.mcmaster	$39.86	$39.86	1.99	1.99
Mechanical	Chassis	chassis_housing	Acrylic Housing (Cut from 0.25"x12"x48" sheet)	1	https://www.mcmaster	$39.86	$39.86	2.12	2.12
Mechanical	Chassis	80/20 Framing	Support struts for top plate (Part: 5 struts, 2.2 in height. Component: 2 ft)	1	https://www.mcmaster	$7.79	$7.79	0.21	0.21
Mechanical	Chassis	80/20 Brackets	Support brackets for 80/20 framing and housing (12 for struts).	12	https://www.mcmaster	$5.21	$62.52	0.03	0.36
Mechanical	Chassis	80/20 Fasteners	Fasteners for 80/20 struts (Need 12, Comes in pack of 4)	3	https://www.mcmaster	$2.30	$6.90	0.08	0.24
Mechanical	Chassis	1" 1/4-20 Screws	Plate-Strut Fastener. Need 9, comes in pack of 50	1	https://www.mcmaster	$8.14	$8.14	0.18	0.18
Mechanical	Chassis	14-20 Nuts	Plate-Strut-Bracket Fastener. Need 10, comes in pack of 50	1	https://www.mcmaster	$4.60	$4.60	0.08	0.08
Mechanical	Chassis	1/4" Washer	Washers for 1/4-20 Screws. Need 19, comes in pack of 100	1	https://www.mcmaste	$3.37	$3.37	0.057	0.057
Mechanical	Chassis	0.75" 1/4-20 Screws	Screws for Plate-Strut-Bracket Fastener. Need 10, comes in pack of 50	1	https://www.mcmaste	$7.48	$7.48	0.1	0.1
Mechanical	Chassis	General Purpose Corner Brackets	Corner brackets to support the acrylic housing and walls	12	https://www.mcmaste	$1.00	$12.00	0.034	0.408
Mechanical	Chassis	0.5" 10-32 Screws	Screws to fix corner brackets interfaces. (Need 20, Comes in pack 100)	1	https://www.mcmaster	$9.60	$9.60	0.2	0.2
Mechanical	Chassis	10-32 Nuts	Fastener for corner bracket interfaces. (Need 20, Comes in pack of 100)	1	https://www.mcmaster	$3.77	$3.77	0.06	0.06
Mechanical	Chassis	Shaft Mount	Part: 12 of 2"x0.5"x1.5" aluminum blocks. Stock: 1 of 2"x0.5"x24"	1	https://www.mcmaster	$17.86	$17.86	1.08	1.08
Mechanical	Chassis	1" 1/4-20 Screws	Screws to mount shaft mount to base plate (Need 12, use from line 8).	12	Line 8	$0.00	$0.00	0.24	2.88
Mechanical	Chassis	1/4-20 Helicoils	Helicoil Inserts for shaft mount (Need 24, Comes in pack of 10)	3	https://www.mcmaster	$6.15	$18.45	0.072	0.216
Mechanical	Chassis	0.5" 10-32 Screws	Screws to mount the gearbox to the base plate (Need 8, use from line 13)	8	Line 13	$0.00	$0.00	0.08	0.64
Mechanical	Chassis	#10 Washers	Washers for gearbox screws (Need 8, Comes in pack of 100)	1	https://www.mcmaster	$2.33	$2.33	0	0
Mechanical	Drive Train	AndyMark 775 RedLine Motor	Drive Motor	2	ark.com/RedLine-Motc	$18.00	$36.00	0.9	1.8
Mechanical	Drive Train	57 Sport 64:1 Gearbox	Drive train gearbox	2	http://www.andymark.	$96.00	$192.00	1.27	2.54
Mechanical	Drive Train	AndyMark Motor Vent Spacer	Drive Motor Ventilation Spacer	2	https://www.andymark	$5.00	$10.00	0.002	0.004
Mechanical	Drive Train	Wheel Sprocket (#25-38t)	Sprocket to fix to wheel	8	https://www.vexrobotic	$11.99	$95.92	0.06	0.48
Mechanical	Drive Train	Gearbox Sprocket (#25-22t)	Sprocket to fix to gearbox	4	https://www.vexrobotic	$9.99	$39.96	0.04	0.16
Mechanical	Drive Train	10-24 Wheel Set Screws	Screws fixing sprocket to wheel. Need 36. Comes in set of 50.	1	https://www.andymark	$8.50	$8.50	0.252	0.252
Mechanical	Drive Train	Chains	5 ft, 1/4 in pitch chains for drive train	1	https://www.mcmaster	$25.70	$25.70	0.562	0.562
Mechanical	Drive Train	Shaft	Part: 6 of 3.75", 1/2"OD Shaft. Stock: 1 of 24", 1/2" OD Shaft	1	https://www.mcmaster	$17.21	$17.21	1.25	1.25
Mechanical	Drive Train	Wheels	8" Rubber Treaded Wheels	6	https://www.andymark	$12.00	$72.00	0.62	3.72
Mechanical	Drive Train	Bearings	1/2" ID Wheel Bearings	6	https://www.andymark	$3.00	$18.00	0.038	0.228
Mechanical	Drive Train	Needle Thrust Bearings		12	https://www.mcmaster	$3.23			
Mechanical	Drive Train	Shaft Collars	1/2" ID Shaft collars to ensure wheels stay on shafts	10	https://www.mcmaster	$2.72	$27.20	0.03	0.3
Mechanical	Linear Mass Stage	Linear Stage	Actuated Linear Stage to vary CoM	1	https://www.amazon.c	$98.99	$98.99	7.2	7.2
Mechanical	Linear Mass Stage	Linear Mass	Mass used to vary CoM	1	https://www.mcmaster	$39.49	$39.49	4.58	4.58
SUBTOTAL							$994.52		41.297

Figure 106: Bill of Materials

Subsystem	Subassembly	Part Name	Description	Qty	Source	Unit Cost	Total Cost	Component Mass [lbm]	Total Mass [lbm]
Power	Power	Sensing Battery	Sensing Battery	1	https://www.adafruit.c	$12.50	$12.50	0.115	0.115
Power	Power	Motor Battery	Motor Battery	1	https://www.amainhol	$139.99	$139.99	1.27	1.27
Power	Power	Communication Battery	Communication Battery	1	https://www.amazon.c	$24.79	$24.79	0.4	0.4
Power	Power	Computer Battery	Computer Battery	1	https://www.amazon.c	$34.00	$34.00	0.76	0.76
SUBTOTAL							$211.28		2.545
Subsystem	Subassembly	Part Name	Description	Qty	Source	Unit Cost	Total Cost	Component Mass [lbm]	Total Mass [lbm]
C&DH	C&DH	ASUS Tinker Board	ASUS Tinker Board	1	https://www.asus.com	$80.00	$80.00	0.055	0.055
C&DH	C&DH	Arduino Due	Arduino Due	1	https://www.sparkfun.	$49.95	$49.95	0.08	0.08
SUBTOTAL							$129.95		0.135
Subsystem	Subassembly	Part Name	Description	Qty	Source	Unit Cost	Total Cost	Component Mass [lbm]	Total Mass [lbm]
Comms	Comms	Ubiquiti Radio	Ubiquiti Radio	3	https://www.amazon.c	$184.95	$554.85	1.1	1.1
Comms	Comms	POE Adapter	POE Adapter	3	https://www.amazon.c	$44.90	$134.70	0.35	0.35
Comms	Comms	900 MHz Antenna	900 MHz Antenna	6	http://www.l-com.com	$26.84	$161.04	0.11	0.22
SUBTOTAL							$850.59		1.67
Subsystem	Subassembly	Part Name	Description	Qty	Source	Unit Cost	Total Cost	Component Mass [lbm]	Total Mass [lbm]
GNC	Motor Controls	Drivetrain Motor Controller	Drivetrain Motor Controller	1	www.pololu.com/produc	$49.95	$49.95	0.04	0.04
GNC	Motor Controls	Linear Stage Stepper Controller	Linear Stage Stepper Controller	1	198988&hvpos=1o1&h	$13.99	$13.99	0	0
GNC	Sensing	360 Degree Lidar	360 Degree Lidar	1	w.sparkfun.com/produ	$319.95	$319.95	0.42	0.42
GNC	Sensing	Ultrasonic Range	Ultrasonic Range	2	w.sparkfun.com/produ	$3.95	$7.90	0	0
GNC	Sensing	Single Beam Lidar	Single Beam Lidar	2	1535990000&_gac=1.	$129.99	$259.98	0.049	0.098
GNC	Sensing	180 degree Fisheye Lens	180 degree Fisheye Lens	1	MZJNR1X3E&pd_rd_w	$45.00	$45.00	0	0
GNC	Nav	GPS Module	GPS Module	2	w.sparkfun.com/produ	$199.95	$399.90	0.014	0.028
GNC	Nav	GPS Antenna	GPS Antenna	2	https://www.sparkfun.	$12.95	$25.90	0.165	0.33
GNC	Nav	Magnetometer/Accelerometer	Magnetometer/Accelerometer	1	www.adafruit.com/produ	$14.95	$14.95	0	0
SUBTOTAL							$1,137.52		0.916
	TOTAL						$3,323.86		46.563
	NOTE: Does not include electronics							Total mass, kg =	21.1206043

Figure 107: Bill of Materials